MASTER

A fast trackloss recovery strategy for compact disc

McGee, Philip J.

Award date:
1987

Eindhoven University of Technology.

Faculty of Electrical Engineering.

Department of Measurement and Control Systems.

A Fast
Trackloss Recovery Strategy
for Compact Disc

Philip J. McGee, B.Eng

i

Contents

List of Figures

List of Tables

Abstract

The push-pull radial tracking technique used in Philips' compact disc players generates a sinusoidal radial-tracking-error signal with a restricted quasi-proportional control range. The original solution to this 'problem' resulted in a trackloss-correction system which could only cope with minor external stimuli to a player without introducing audible side-effects. For application in portable and in-car CD players, the performance of this system was less than optimal.

This thesis describes the development of a new trackloss recovery strategy, implemented via an improved servo control system. The system ensures that the scanning laser beam is always returned to the *original* track after a shock, hence precluding the possibility of perceivable rhythm-distortion. This is done *without* the use of the subcode content of the data on the disc, but rather using position information based upon the *periodicity* of the servo error signals. Two different means are used to damp the motion of the arm, and an extended track-capture-and-hold range system is also described.

Samenvatting

Het in Philips CD-spelers gebruikte *push-pull* radiële volgsysteem genereert een sinusoïdaal radieel foutsignaal met een beperkt stabiel regelgebied. De oorspronkelijke oplossing van dit 'probleem' bestond uit een spoorverlies-correctie systeem dat slechts zeer lichte schokken kon verwerken zonder hoorbare neveneffecten. Voor toepassing in draagbare en auto-CD-spelers waren de eigenschappen van dit systeem niet optimaal.

Dit rapport beschrijft de ontwikkeling van een verbeterd spoorverlies-correctie systeem, uitgevoerd met een uitgebreid servosysteem. Het systeem garandeert dat de laserspot na een stoot altijd op het oorspronkelijke spoor terugkomt, waardoor een ritmestoring uitgesloten wordt. Dit wordt gedaan zonder gebruik te maken van de subcode, maar met de positieinformatie die gebaseerd is op de periodiciteit van de servo foutsignalen. Twee verschillende methoden zijn gebruikt om de beweging van de arm te dempen, tevens is een spoorvolgsysteem met een groter stabiliteitsgebied beschreven.

Auszug

Die pendelnde radiale Spurfolgetechnik der Philips Compact disc-Spieler erzeugte ein sinusförmiges Signal der Spurfolgeabweichung mit begrenztem quasi proportionalem Regelbereich. Die verwendete Lösung dieses Problems bestand aus einem Spurabweichungskorrektursystem, das, ohne hörbare Nebeneffekte zu verursachen, nur mit geringen äußeren Anregungen fertig wurde. Für eine Anwendung in tragbaren CD-Spielern oder Auto CD-Spielern war die Leistung dieses Systems nicht optimal.

Diese Dissertation beschreibt die Entwicklung eines optimalen Spurfolgesystems, daß mit einem intelligenten Servocontrol-System ausgeführt ist. Dieses System sichert, daß der Laserstrahl nach einem Stoß immer zur Originalspur zurückkehrt, und auf diese Weise die Möglichkeit von spürbaren Rhytmusstörungen vermeidet. Dieses wird ausgeführt ohne die Zeitinformation des Dateninhaltes der Platte zu verwenden, sondern die Positionsinformationen basierend auf die Zeitkorrelation der Servo control Signale zu benutzen. Es werden zwei verschiedene Mittel zur Dämpfung der Bewegung des Arms genutzt. Außerdem wird ein verbessertes Spurfang-und Spurhalte-System beschrieben.

Condensé

La technique du push-pull radial utilisée dans les lecteurs de disques compacts Philips génère un signal d'erreur radiale sinusoïdal avec une plage de contrôle proportionel limitée. La solution originale à ce 'problème' est un système detecteur de perte de piste (Trackloss correction system), lequel ne peut corriger que de faibles stimuli externes sur la platine sans produire de défaut audible. Pour des applications CD portables et CD automobiles les performances de ce système ne sont pas les meilleures.

Cette thèse décrit le développement d'une nouvelle stratégie de traitement de la perte de piste implantée dans un servosystème intelligent. Après un choc, le système assure le retour du faisceau optique sur la piste en cours éliminant ainsi toute possibilité de rupture de rythme dans la modulation. Ceci est réalisé sans utilisation de l'information contenue sur le disque (subcode), mais grâce à l'information de position basée sur la periodicité du signal d'erreur radiale. Deux moyens différents sont utilisés pour amortir le mouvement du bras, et un système permettant d'obtenir une plage de capture et de maintien étendue est aussi décrit.

Preface

The subject-matter of this thesis, together with examinations in three elective subjects, form the basis for my award of the Dutch degree of *Elektrotechnisch Ingenieur*, or Master of electronic engineering. In August 1985, shortly after being awarded the degree of Bachelor of Engineering in electronic engineering, from the National Institute for Higher Education, Limerick, Ireland, I joined the compact disc development laboratory of the Philips consumer electronics group, Eindhoven, The Netherlands, as a servo systems development engineer. The project presented here represents my first major task at the laboratory.

In the Netherlands, a complete 4-year degree course is normally followed for the Ir. study, but my 4-year B.Eng allowed exemption from many of the components of the coursework. This made it possible to integrate into the last year of *Doctoraal* study, in much the same way as an M.Eng study follows upon the foundation of a B.Eng.

The work covered a wide spectrum of electronic disciplines, ranging from control theory, signal processing, and optical principles, through to CAD simulation and microprocessor programming. I feel that it has been of enormous benefit as a first real-life engineering experience, and the elective subjects have also helped to deepen my understanding of the relevant topics, as well as assisting in the background to the project.

The target readership includes people both from the T.U.E. and from Philips. With a view to completeness, background information on CD has been included for the uninitiated, and some of the main points are repeated at strategic intervals within the report. In the interests of readability, the material is largely presented using qualitative discussion rather than quantitative mathematical deductions. This is combined with the deliberate use of an engineering-article writing style, which should enhance the readability under the circumstances. The completeness will hopefully be of assistance to those less-well informed on the subject of CD, and should render the text suitable as introductory material for newcomers to the CD lab.

The thesis was typeset using the LaTeX document preparation system, running under VAX/VMS, and printed on a DEC LN03 laser printer. Many of the figures and diagrams were also created with this system.

Philip J. McGee, Eindhoven, April 1987.

Chapter 1

Introduction

The Compact Disc (CD) system, introduced by Philips in 1982, opened up the new era of digital audio for the consumer. The acceptance of the system as the *de-facto* world-standard before its launching assured avoidance of any battle-of-the-formats which might otherwise have ensued. The extraordinary sound quality, resistance to wear and tear, and relative ease of handling of the small silver disc, has led the popularity of the format to revive the entire home-audio industry from stagnation in the late seventies.

Initial development plans of the major manufacturers concentrated on reducing costs, so as to increase demand and enable mass-production. Since then, massive strides in component integration have made it possible to greatly reduce the physical *size* of players, so that portable 'Discman' and in-car players have become feasible. The dynamic behaviour of a CD mechanism is highly temperature-dependant, and quite susceptible to the adverse effects of external stimuli. This poses no major problems for players that are intended for home-use, but the step towards portability has created a need for a new generation of shock-tolerant players, capable of functioning over a wide range of temperatures while maintaining high performance levels.

The current trackloss correction system implemented in Philips' compact disc players was developed primarily for correcting mistracking due to disc-scratches and blemishes. Such imperfections can create unreliable or unusable error signals for the player's servo systems. The radial tracking system, limited in its proportional range due to the *periodic* nature of the error signal, could only cope with eccentricity, disc defects, and *minor* external shocks. Intended for a non-portable home-use compact disc player, the system proved ineffective for the requirements of a mobile player.

The initial research efforts of the author concentrated on optimising

the existing electronic servo system for use with the new generation of CD mechanisms designed for portable applications. The results were unfruitful, and it became apparent that an entirely new approach to the correction of stimulus-induced mistracking would be necessary. This report describes the development of an entire new concept in trackloss correction, which has been created with a view to reducing the *audible* consequences of trackloss to a minimum. While it is applicable to all portable players, the emphasis is on a player for use in in-car entertainment systems.

Chapter 2

Compact Disc Basics

The generic term *Compact Disc* refers to a family of 12cm-diameter optically-encoded discs, which store data in digital format. This family currently includes CD-*audio*, [1] *CD-ROM* for data storage, *CD-V* 'video clip', and *CD-I* 'interactive', which includes audio, data, video, and graphics on one single disc. Future possibilities include *CD-PROM* and *CD-EPROM*. While the system described in this report is applicable to all types of compact disc systems, the reference is to the CD *audio* player unless otherwise stated.

The information stored on a compact disc is digitally encoded in a spiral of pits on the surface of a 12cm reflective disc, which is optically scanned by an AlGaAs laser with wavelength $\lambda = 800$nm. The pits show optical contrast with respect to the surrounding mirror surface, and an effective *on-off* modulation of the reflected light results. This is focused on an arrangement of photodiodes, which convert the intensity variations into electrical signals, from which the digital bit-stream and tracking signals for the servos can be derived. Figure 2.1 shows the arrangement of the optical system, and indicates the pit structure. The surface of the disc is protected by a 1.2mm transparent plastic layer, which protects the information sub-layer from dust and surface-damage. It also ensures that dust particles and surface blemishes lie *outside* the focal plane of the scanning laser, where they can have little adverse effect. The optical scanning occurs from *below* the disc and radially *outwards*, at a constant *linear* velocity of 1.25 m/s. During read-out, the angular velocity of the disc thus varies from about 8 rev/s on the inner tracks to 3.5 rev/s at the perimeter of the disc. The diameter of the

---

[1]For an in-depth treatment of audio-CD basics, the reader is referred to [PTR]

a   b
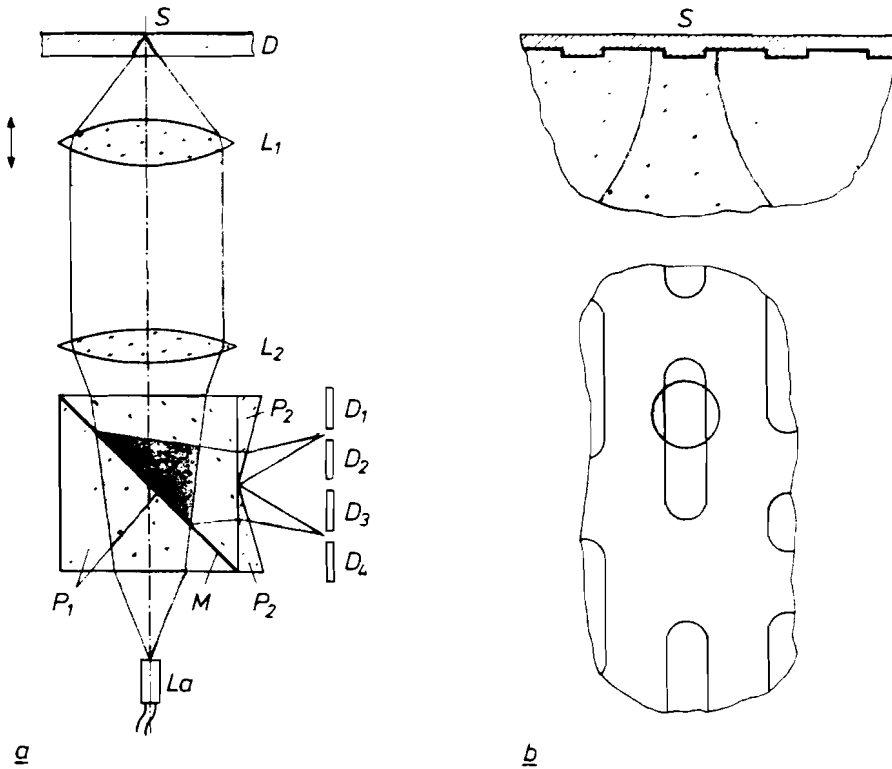
Figure 2.1: (a) Diagram of the optical pick-up. The various components indicated are —
D radial section through the disc. S laser spot, the image on the disc of the light emitted
by the semiconductor laser La. L_1 objective lens, adjustable for focusing. L_2 lens for
making the divergent beam parallel. M half-silvered mirror formed by a film evaporated
on the dividing surface of the prism combination P_1. P_2 beam-splitter prisms. D_1 to D_4
photodiodes whose output currents can be combined in various ways to reconstruct the
bit-stream and to generate error-signals for the focus and radial tracking servo systems.
(In practice, the prisms P_2 and the photodiodes D_1 to D_4 are rotated by 90 degrees and
the reflection at the mirror M does not take place in a radial plane but in a tangential
plane).

(b) A magnified plan-view of the light-spot S and its immediate surroundings. It can
clearly be seen that the diameter of the spot ($\approx 1\mu m$) is larger than the width of the pit
($0.6\mu m$).

4

scanning *light-spot* is $1\mu m$, the pitch of the track $1.6\mu m$, the width $0.6\mu m$, and the depth of the pits is $0.12\mu m$.

2.1 Encoding of the audio and subcode information

In compact disc mastering, the analog audio signal is sampled at a rate of 44.1 kHz, which generously satisfies the Nyquist criterion for reproduction of the maximum audible audio frequency of 20 kHz. The signal is linearly quantised to 16-bits accuracy, which is adequate for a signal-to-noise ratio of >90dB. For one stereo sample, 32 bits are required, leading to a net bit-rate of $(44.1 \times 10^3) \times 32 = 1.4112 \times 10^6$ audio bits/s. These bits are subsequently grouped into *frames*, each containing six of the original samples. Parity bits are then added in accordance with a coding scheme known as the *Cross-Interleave Reed-Solomon code*, or *CIRC*. Next, *control and display* information bits are added in the *subcode* field, which includes such secondary information as the track-number, index-number, playing-time, etc. The bit stream is then modulated in accordance with the *EFM* or *Eight-to-Fourteen Modulation* scheme. This involves the translation of groups of 8 bits into groups of 14 *channel bits*, with a minimum run-length of 3 and a maximum of 11, which results in a minimum of 2 and at most 10 successive zeros in the bit stream. This makes it possible to increase the information packing-density on the disc, and hence a longer playing-time can be achieved. The blocks of fourteen bits are linked by three *merging* bits, and finally, a synchronization pattern of 27 channel bits is added to each frame. The total bit-rate after all these manipulations is 4.3218×10^6 channel bits/s.

2.2 The Swinging-arm mechanism

Two different approaches have been used by various manufacturers in the topology of the read-out mechanism. The *two-stage* approach uses a motor-driven sledge for coarse movements, upon which a secondary fine-positioning actuator is mounted. The sledge is activated to carry the pick-up to a required radial position, and the limited-stroke secondary unit is then used to perform finer small-scale movements, such as tracking eccentricity of the disc. The principle employed in Philips' players uses a single-stage *swinging-arm* mechanism, with one centrally-pivoted arm that enables the pick-up to

5

describe a radial arc across the disc. While this approach is simpler, it does mean that a single radial actuator has to be able to cater for both coarse and very fine movements. In the case of a shock to the mechanism, the entire arm can rotate or translate, making it difficult to hold tracking. With respect to the two-stage mechanism, the relatively rigid sledge on which the fine-positioning actuator is mounted effectively limits any post-shock excursions. The smaller actuator is usually quite a light structure with low inertia, so it is a comparatively easy task to keep it on track.

When the coil in the radial actuator is energized, the pick-up can be directed to any required passage of music on the disc, the locational information being provided by the control & display data contained in the subcode. When a particular track has been found, the pick-up must then follow it accurately — to within $\pm 0.1 \mu$m — without being influenced by reflections from neighbouring tracks. Since the disc may have some slight *eccentricity* due to the non-perfect centering of the spindle hole, and also since the turntable under the disc is not perfectly concentric with its axis of rotation, the track can have a maximum lateral swing of 300μm, at a maximum frequency of some 8 Hz. A tracking servosystem is therefore necessary to ensure that the deviation between pick-up and track is smaller than the permitted $\pm 0.1 \mu$m, and in addition, to absorb the consequences of small internal vibrations of the player. Figure 2.2 shows the pick-up mounted at the end of the *CDM3* arm (*CDM* is an abbreviation for *compact disc mechanism*).

The depth of focus of the optical pick-up at the position of S (see fig. 2.1) is about 4μm. The axial deviation of the disc, owing to various mechanical effects (e.g. warping), can be at maximum $\approx$ 1mm. It is evident that a servosystem is also necessary to maintain correct focusing of the light-spot on the reflecting layer. The objective lens L_1 can therefore be displaced in the direction of its optical axis by a combination of a coil and a permanent magnet, similar to a loudspeaker-cone arrangement. The maximum allowable deviation in focusing is $\pm 1 \mu$m. Figure 2.3 indicates the focus actuator for the *CDM3* mechanism.

2.3 Focus, Radial & Turntable servo systems

Turntable. As mentioned at the beginning of this chapter, the compact disc rotates with a *constant linear velocity* with respect to the pickup, implying that, as readout commences from the centre and progresses towards

6
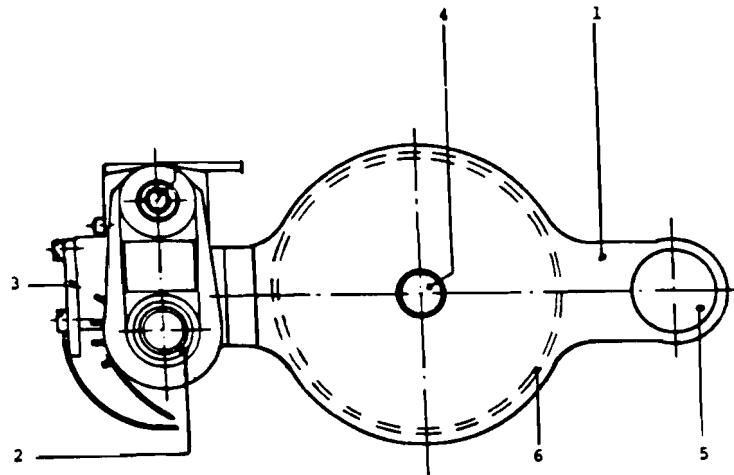
(1) Radial arm (2) Objective lens (3) Photodiodes (4) Ball-bearing
(5) Counterweight (6) Ring-magnet

Figure 2.2: *The CDM-3 pick-up and radial arm, top view*
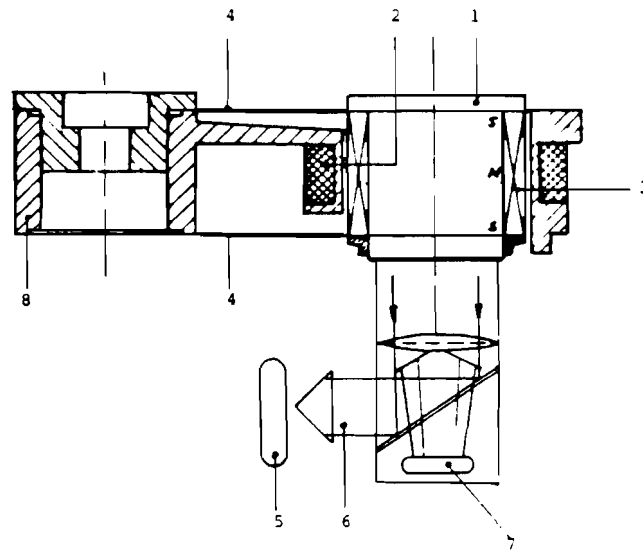
(1) Objective lens (2) Focus coil (3) Ring-magnet (4) Leaf-springs
(5) Photodiodes (6) Reflected light-bundle (7) Laser (8) Radial-arm

Figure 2.3: *Side elevation of CDM-3 focus actuator*

the perimeter of the disc, the *angular* or rotational velocity of the disc has to be adjusted accordingly. A constant linear velocity of 1.25 m/s with a disc diameter of 12cm indicates a rotational speed of 8 rev/s at the inner tracks, which decreases constantly to a value of 3.5 rev/s at the outside of the disc. The correct rotational-speed information at any given moment is supplied to the motor servo by the audio-decoding electronics. Before further processing, and to facilitate the de-interleaving process, the digital data streaming from the disc is first written to a *FIFO* shift-register. It is clocked out of the FIFO referenced to a quartz-crystal frequency, the stability of which ensures elimination of any audible *wow and flutter*. Momentary variations in the rotational-velocity of the disc are effectively absorbed through the fact that the read and write rates of the FIFO are independent. A control-signal for the turntable-motor can be generated on the basis of the difference between the write and read *addresses* of the FIFO, which is analogous to comparing the frequency of incoming and outgoing data. The error is zero when these two frequencies are equal. The signal generated is a *PWM* pulse-width modulated waveform, called the *MCES* motor-control signal.

Focus. Figure 2.4 shows again the optical light-path, and also indicates the basic signal processing by which the error signals are derived from the photodiode currents. If the spot is correctly focused on the disc, two sharp images are precisely located between D_1 and D_2 and between D_3 and D_4. If the disc is out of focus, then the focal point is located either in front of or behind the optimal position, which causes divergence or convergence of the split beams. The result hereof is that the images on the photodiodes are not sharp, and furthermore, that they have moved closer together or further apart compared to the in-focus situation. The signal given by $(D_1 + D_4) - (D_2 + D_3)$ can therefore be used for controlling the focus servosystem, and is called the *focus-error* or *FE* signal. Figure 2.5 indicates the block diagram of the focus servo control loop.

Radial Tracking. The *radial error* signal, *RE*, is generated according to the *push-pull* technique (see next section). The signal is obtained by coupling the photodiodes as $(D_1 + D_2) - (D_3 + D_4)$, as is indicated in figure 2.4.

The radial control servosystem, indicated in block-diagram form in figure 2.6, is more complicated than the focus loop, due to the inclusion of *offset* and *gain* correction circuits. As a result of ageing or soiling of the optics, the reflected beam can acquire a gradually increasing, more or less

9
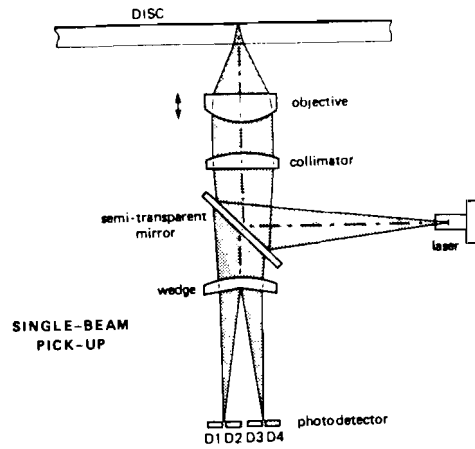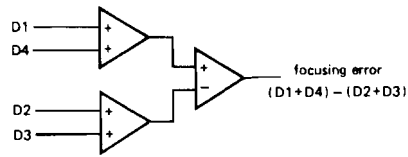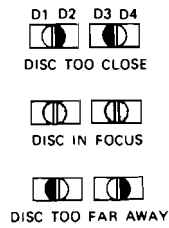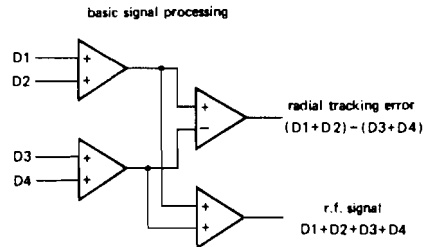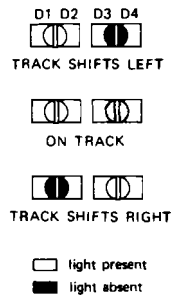
Figure 2.4: *Optical light-path and derivation of error signals*

Optics

X_{disc}

$+$

$-$

X_{act}

| Lpf | k | Lag | Lead | Current control | $\frac{1}{s^2}$ |

Actuator
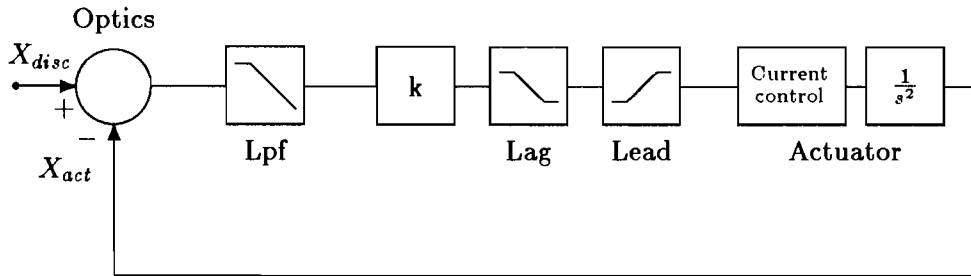
Figure 2.5: *Closed-loop diagram of the focus servo system*

constant asymmetry. Owing to a d.c. component in the tracking-error signal, under such circumstances the spot will always be slightly off-centre of the track. To compensate for this effect, a second tracking-error signal is generated by the injection of a 650 Hz *wobble* signal into the loop. The amplitude of this wobble signal produces a side-to-side displacement of the arm of $\pm 0.05\mu$m. The *SUM* signal obtained from the four photodiodes combined as $(D_1 + D_2 + D_3 + D_4)$ — which is at a maximum when the spot is in the centre of the track — is thus modulated by the 650 Hz signal. The amplitude of the 650 Hz signal increases as the spot moves off-centre, and, in addition, the sign of the signal changes if the spot moves to the other side of the track. This second tracking-signal may thus be used to correct the *RE* signal with a direct voltage. In this way, any offset present is reduced to zero, and the bandwidth of the control loop is kept at a constant pre-determined value.

As with the focus loop, a LEAD network is present to ensure stability, and a LAG network is included to provide greater reduction at lower frequencies. The LAG also acts as a sort of low-frequency memory for the tracking system, which maintains the eccentricity compensation temporarily if the error signals become unreliable due to a disc flaw. The LEAD network also has a differential action, which provides *damping* or velocity feedback in the system.

AGC

Optics

X_{disc}

$+$

$-$

X_{act}

Lpf

k

Lag

Lead

Current control

$\frac{1}{s^2}$

Actuator
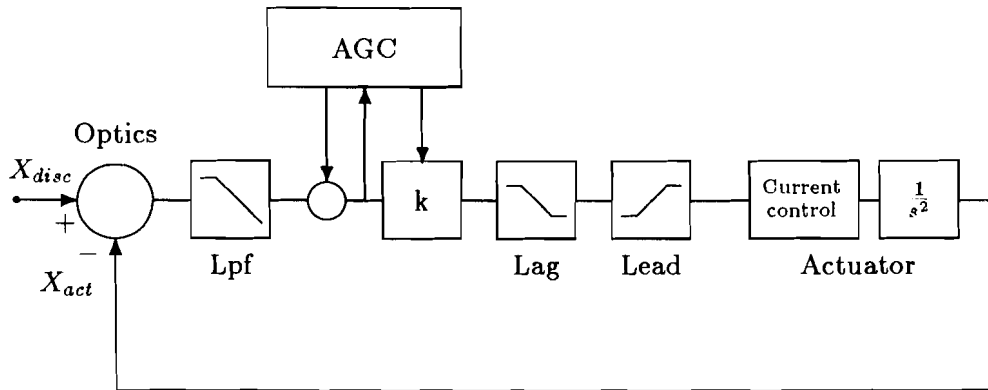
Figure 2.6: *Closed-loop diagram of the radial-tracking servo system*

2.4 The 'Push-Pull' Radial-error signal technique

The *push-pull* method of error-signal generation relies upon detection of interference phenomena produced by diffraction of the reflected light-bundle. It is well-known that a diffraction grating with separation comparable to the wavelength of the light causes an incident spherical wave to split into spherical diffracted waves that partly overlap each other (see fig. 2.7). In a similar manner, the $\frac{1}{4}\lambda$ depth of the pits introduces diffraction interference in the light reflected back from a compact disc (fig. 2.8). This is analogous to the diffraction of a *plane* wave produced by a grating. The spherical beam focused on the disc can be modelled as a set of plane waves with varying angles of incidence. The light diffracted by the disc will consist of three spherical waves according to figure 2.7. The extent of overlap (figure 2.9) is dependant upon the wavelength λ of the light, the numerical aperture NA of the lens, and the track-pitch δ. In theory, an infinite number of diffraction orders is produced, but only the zero and first order bundles have sufficient intensity to be considered in this application. It is important to remember that if the incident beam is laterally shifted towards an adjacent track of pit-structures, only the relative *intensities* of the -1, 0, and $+1$ order bundles varies, and not the area of their overlap regions. This is indicated in figure 2.10, which shows the 'view' through the objective lens
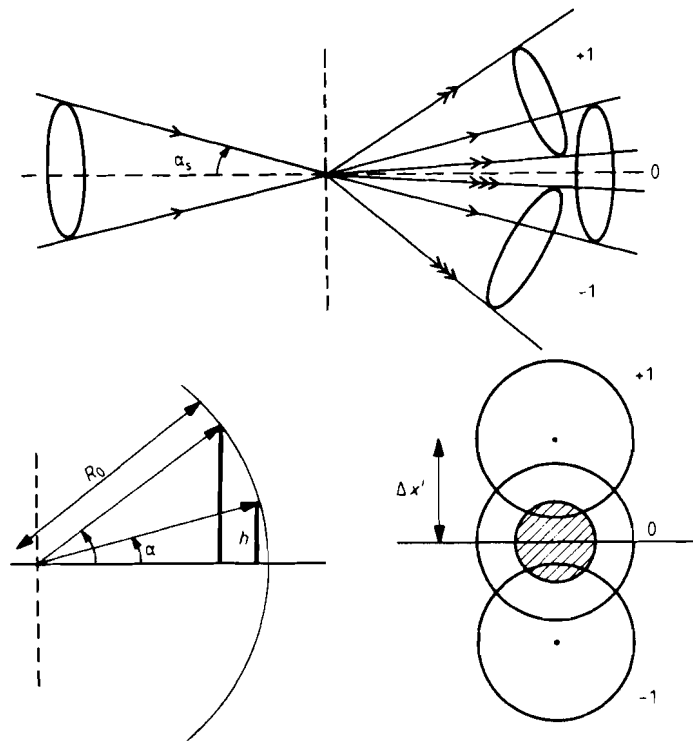
Figure 2.7: *An incident spherical wave is split into spherical diffracted waves that partly overlap. The hatched area indicates that portion of the reflected beam which is picked up by the detector.*

13
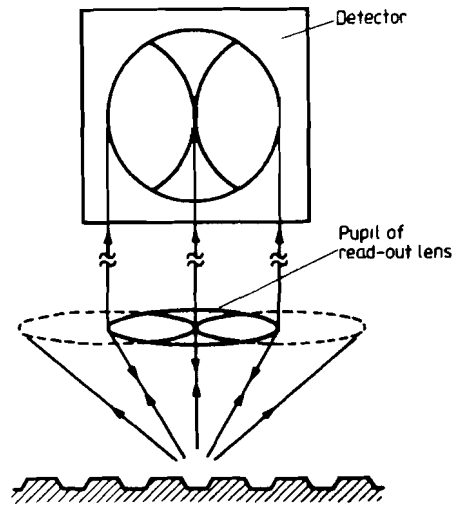
Figure 2.8: *Diffraction pattern in the reflection from the disc*
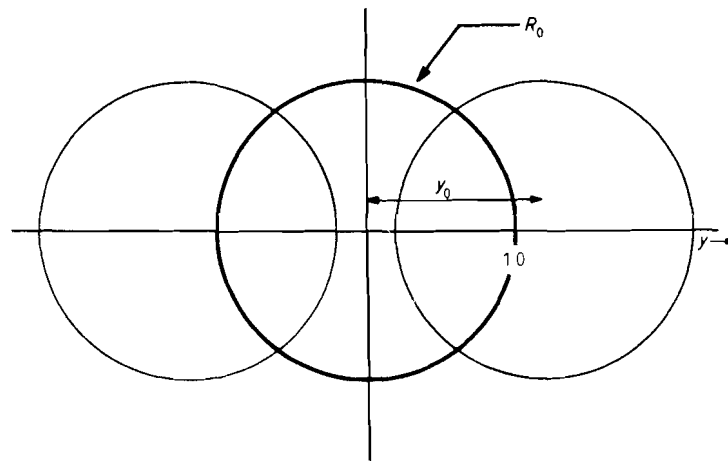
Figure 2.9: *Overlap of the 0 and ±1 diffracted orders*

14

of the intensity-differences at four sample points between two tracks.
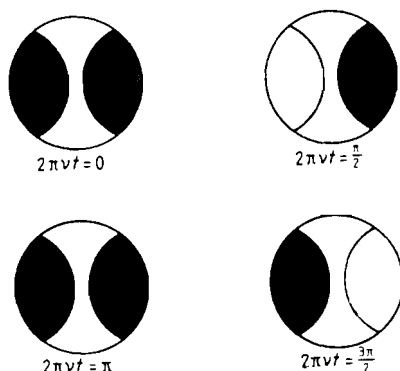
Figure 2.10: *Positional-dependance of the relative intensities of the three main diffraction orders*

If the spot lies precisely in the middle of a track, then the first-order light bundles are in inverse-phase with the zero-order bundles, and the reflected light is a minimum. Off-track movements of the scanning spot produce intensity fluctuations in the overlapping areas of the zeroth and first orders. The *push-pull* method of generating a radial tracking signal purposely detects these variations by separating the light flux through the pupil of the objective into two halves, each directed to a photodiode pair. Precisely how this is done was indicated in figure 2.4. The signal thus produced is called the *radial error* signal RE, which is approximated by

$$RE = a \sin\left(\frac{2\pi x}{\delta}\right) \tag{2.1}$$

where δ is the *track-pitch*, x the error displacement, and a is a constant of proportionality related to the depth of the pits. RE can thus be seen to be a *periodic* signal, with a *period of one track-pitch*. The fact that it assumes a sinusoidal form is largely coincidental, and stems from the $1.6\mu m$ track-pitch inherent to CD (for track-pitches $> 2\mu m$, the sinusoidal character becomes significantly distorted). Figure 2.11 shows the push-pull PP signal as a function of displacement in a radial direction over the tracks.

With respect to radial tracking, a very important fact which is worth remembering is that
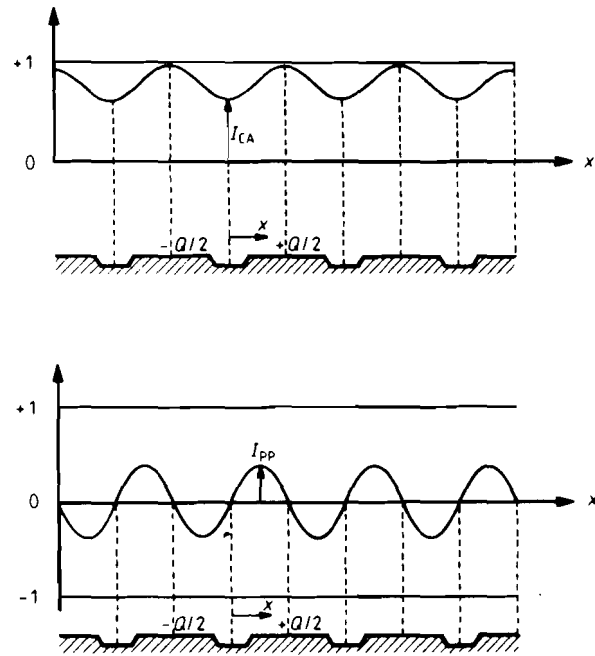
Figure 2.11: *CA* and *PP* read-out signals as a function of the radial position x of the spot. The track pitch is indicated by Q.

16

Loss of focus also implies loss of radial tracking information, since this implies that the push-pull interference pattern either disappears entirely, or becomes so highly distorted that derivation of reliable error signals becomes impossible.

Because the sine function is odd, the initial *polarity* of the RE signal for an off-track displacement x is an indication of the *direction* of movement — radially inward or outward. To enable digital processing of this radial direction information, RE is digitised with the help of a comparator, to produce the so-called *radial polarity* or RP signal.

The *envelope* of the SUM signal (the sum of detector-photodiode currents $D_1 + D_2 + D_3 + D_4$), is also sinusoidal, approximated in this case by

$$SUM = b \cos(\frac{2\pi x}{\delta})$$ (2.2)

where δ is the *track-pitch*, x the error displacement, and b a constant of proportionality. SUM is thus also a *periodic* signal, again with a period of one track-pitch. Optically, the SUM signal is referred to as the *central aperture* signal, CA. This is also shown in figure 2.11. Because the cosine function is even, the polarity of the SUM signal for displacement of the light-spot around a track is independent of the direction of radial motion. Due to the cosine factor, however, SUM is $\pm\frac{\pi}{2}$ radians phase shifted with respect to RE. This 90 deg phase difference will be either positive or negative, depending on the direction of radial movement. An important property of this 90 deg shift is that the SUM signal is negative [2] if the spot lies within a region of $\pm\frac{1}{4}\delta$ from track-centre, and is positive where $\frac{1}{4}\delta < |x| < \frac{3}{4}\delta$. The relevance of a radial positional error greater that $\pm\frac{1}{4}\delta$ is that it marks a region where the amplitude of the CA signal is at a level which makes decoding of the audio information content impossible. A digitised version of the SUM signal can therefore act as a *trackloss* signal (TL), which goes low to indicate that the displacement of the light-spot is greater than $\pm\frac{1}{4}\delta$ from centre-track. Another important significance of this will become evident in the next chapter.

---

[2]To be strictly correct, this signal is always positive, but it has a minimum when the read-out spot is centred on-track. The term 'negative' as used here means that the amplitude is less than the average value of the function.

Chapter 3

Shock-sensitivity, trackloss correction, and the human interface

In the tiny sub-micron world of the information pattern on a compact disc, even quantities which are normally considered as small or negligible acquire comparative significance. The expansion of a metal or plastic mechanism due to a temperature change of, say, 20 degrees, would be undetectable to a human being, yet it represents quite a large deformation in the μm region. In fact, the permanent inelastic deformation of a plastic CD mechanism caused by extremes of temperature can significantly change its dynamic properties. Even the weakest vibrations of the radial-arm translate to tens of microns (hence several tracks of information) of movement of the light-spot if uncontrolled. These excitations can be produced by the footsteps of somebody walking in the room where the player is located. A compact disc mechanism is nothing short of a super-accurate three-dimensional positioning robot, which can locate and position accurately to within $\pm 0.05 \mu$m. This chapter will attempt to explain the 'hazards' which a player typically has to cope with during disc playback, with emphasis on trackloss and its implications.

3.1 Radial tracking during 'normal' playing

One of the great advantages of the compact disc system is its ability to cope with scratched discs. While the advanced error-correction system was originally developed in order to ease the unrealistic manufacturing tolerances

which would be involved in producing discs completely free of errors, a very welcome side-effect is immunity from *most* surface scratches and blemishes on the disc. The interleaving of the data means that error bursts due to scratches and the like are much more likely to occur in the form of several slightly-damaged frames rather than the absence of entire frames. This sort of disc-error poses little problem to the decoding electronics, but it does make life more difficult for the *servo* electronics, which must maintain focus and tracking in the presence of distorted or unreliable error signals. Scratches on the surface are supposed to lie outside the focal plane of the underlying data, but there remains one very important fact which must not be overlooked —

> *The disc itself is as much a part of the optics as the other constituents of the light-path, and must be of optical quality.*

Remember that the incident light-beam must go through the protective layer, be focused on the information sub-layer, and return back through the body of the disc before the reflected light-beam can be 'read'. The mechanical properties and resonances of the disc are also of great importance, and can play a role in the crosstalk between the mechanical and electrical systems in the player.

Figure 3.1 gives an indication of the sub-microscopic appearance of a tiny blemish in the information layer. The rounded corners are produced by the objective lens of the microscope, and must not be confused with the roundness of the disc or the CD-player optics. Because the pit-geometry is so small in comparison with the radius to the tracks, the adjacent tracks appear to be linear, running at an angle of approximately 60 degrees from top to bottom. The track-damage is evident in the centre and to the right in the photograph. Such scratches in the layer material are called *pickelschrammen*. [1] The extent of damage to the tracks is severe, and while the beam is traversing such damaged areas, the optical signals become totally unreliable because the regular periodic pit-structures upon which they are based cease to exist. Other forms of disc-aberrations are also possible. Bubbles in the protective surface layer can cause localised lens-effects which *refract* the light beam, and distort the perceived shape of the underlying track. The so-called 'white' drop-out represents an area on the disc where no pits have been impressed, whereby full reflection of the incident beam occurs, and the overlapping areas merge to form a single entity. Trackloss detection (see

---

[1] The word 'pickelschramm' comes from the German for 'Pimple-like scratch'

Figure 3.1: *Pickelschramm* — *localised track-destruction caused by even a tiny imperfection in the disc*

subsections 3.3.1 and 3.3.2) and drop-out detection have many factors in common, and it can be problematic to distinguish between the two. The conditions for trackloss are that $12\% < HF < 62\%$ and that the low frequency component $LF > 120\%$. It can happen that a drop-out can occur shortly after a trackloss detection, whereby the condition $HF > 12\%$ becomes false, so that end of trackloss is momentarily signalled. This spike on TL occurs at the rather unfortunate moment where a transition on RP is likely, and must thus be suppressed. The DODS (drop-out detector suppression) line from the μp can be used for this purpose. Some of the CD's produced for test-purposes have a deliberate *wedge* shaped engraving on the disc-surface, which varies tangentially in width from 200μm to 1 mm. During read-out under the extremest circumstances, the servo must guide the light-spot, with its diameter of 1μm, through the one-millimeter section of the wedge, bringing it out on the other side within $\pm 0.1\mu$m of a 0.6μm wide track. This feat is the equivalent of throwing a bowling-ball along an alley 10 Km long, and striking the center pin, while wearing a blindfold ! The

20

eccentricity of the disc and its out-of-roundness is analogous to the pin's swinging on a pendulum with simple-harmonic motion, at a frequency of 10 Hz and with a maximum stroke of 100m.

3.2 Bandwidth tradeoffs — Playability & Trackability

The term *playability* is used to refer to a CD player's ability to play damaged discs without generating perceivable abnormalities in the audio output. *Trackability*, in reality a subset of playability, is a measure of the capability of the servo electronics to 'hold' the correct track during a disc flaw or external-shock. Unfortunately, there are conflicting requirements for the bandwidths of the control loops. During normal read-out, a high bandwidth is desired, to enable a quick reaction to maintain tracking of displacements induced by vibration and external shocks. On the other hand, read-out during traversal of pickelschrammen and the wedge can best be handled by a low-bandwidth system, so that the controller does not act too nervously upon the high-frequency content of the garbled error signals. Luckily enough, the eccentricity of the disc is very low frequency (10 Hz), and the 1.25 m/s linear velocity of the disc means that the journey through a disc-flaw such as the wedge takes at most about 1 ms.

In practice, consideration of the mechanical properties of the system will also play a role in the choice of the control loop bandwidths. Various mechanical resonances, which begin to creep in at frequencies lower than 1 KHz, require restriction of the bandwidths to guarantee adequate phase and gain margins to avoid instability problems. Unfortunately, these mechanical 'problems' vary significantly as a function of temperature. Theoretically, the H-curve of the radial loop crosses the 0 dB line in the bode plot of amplitude versus frequency with a slope of -20dB/decade, which increases to a value of -40dB/decade above the bandwidth. This is the net result of the +1 slope of the LEAD network and the -2 of the mechanical mass of the arm (double-integrator). In reality, due to various resonance peaks occurring at the mechanical system's natural frequencies, the mechanical slope can differ quite significantly from the theoretical value of -2, and several peaks can be present in the H-curve above the bandwidth of the system. So long as these peaks do not cross the 0 dB line, the system will remain stable. The problem lies in the fact that the amplitude of these resonance peaks varies strongly as a function of temperature, meaning that the system

may be sufficiently stable at room-emperature, but only marginally stable or even unstable at the extremes of the temperature range. The synthetic O-rings used in the mechanical construction as de-coupling devices have the function of shifting the peaks in the frequency domain. This always represents a compromise, however, and the relationship between the stiffness of the O-rings and temperature influences the overall performance. Bearing in mind that a player intended for in-car applications must operate over a temperature range from -30 to $+85$ degrees, these temperature dependances can play a very important role in the entire system performance. Designing to meet the requirements of stability over a wide range of possible temperatures will require a low-bandwidth controller ($\leq$ 500Hz). The above discussion on this subject should make it clear that this represents a compromise on shock-sensitivity performance. This is unfortunate, because it is the in-car environment which exacts perhaps the most stringent demands upon shock-insensitivity.

3.3 Shock-sensitivity and Trackloss correction

The CD mechanism is mounted on its supporting chassis via vibration-and-shock-damping rubbers, which ensure that frequencies above about 25 Hz are filtered out of the error spectrum. This is necessary because the reduction provided by the servo systems decreases as a function of frequency. Although frequencies higher than 25 Hz are mechanically filtered, they can still pass through to the mechanism with enough force to excite resonant frequencies in the system. Apart from whatever resonances lie in the mechanical construction itself (which will vary from one CDM type to another, and lie to a great extent *outside* the bandwidth of the controller), one very important in-band resonance is that of the CD *disc* itself — 110 Hz. The disc is clamped at its centre to the supporting turntable, but not at its edges, which are therefore more free to vibrate. The error-spectrum is thus a function of the *radius* to the light-spot. Figures 3.2 and 3.3 show error-spectra measured during a controlled driving test in a car with a CD player on board. The error-spectra of both the focus and radial systems are indicated, as measured during read-out of tracks [2] 1–2 and 23–24, respectively, of the same disc. Notice that the 110 Hz peak is much higher in the case of readout from track 24, which is on the *outer* radius of the test disc.

---

[2]The word *track* is used here in a broader sense to refer to the music-programme number, and not to the spiral of information-tracks.
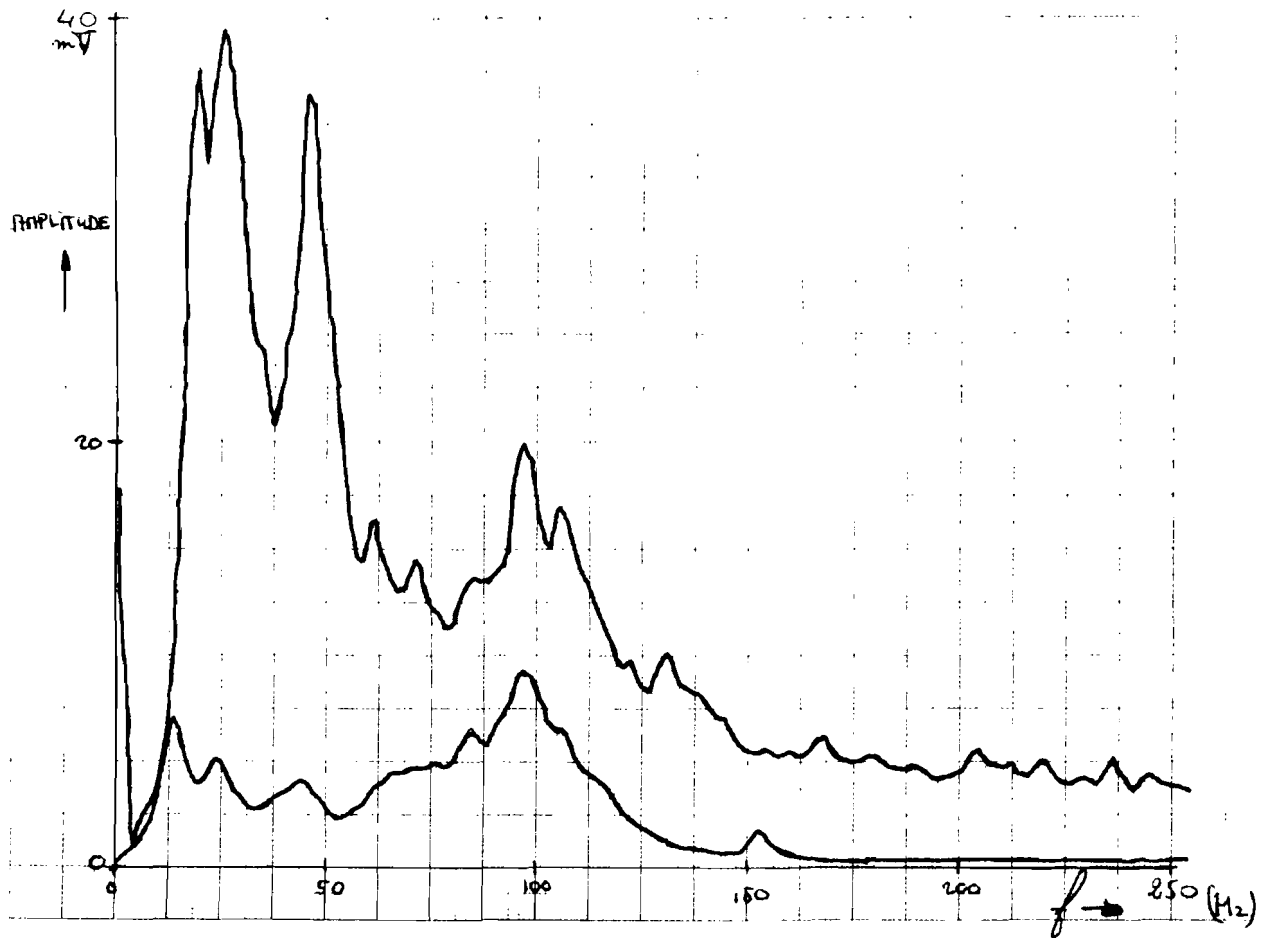
Figure 3.2: Dependance of Focus and Radial error-spectra upon radius to the point of read-out. See also figure 3.3 on following page. The plots were made during a driving-test in a VW Golf car on the DAF test tracks in Nijnsel. The driving conditions were identical in both cases — 40 Km/h, with both tests carried out on the same driving surface and for the same direction. The upper curve shows the spectrum for *radial* movements, and the lower for *focus*. This example was plotted for the case of a *small* radius to the light-spot (tracks 1-2).
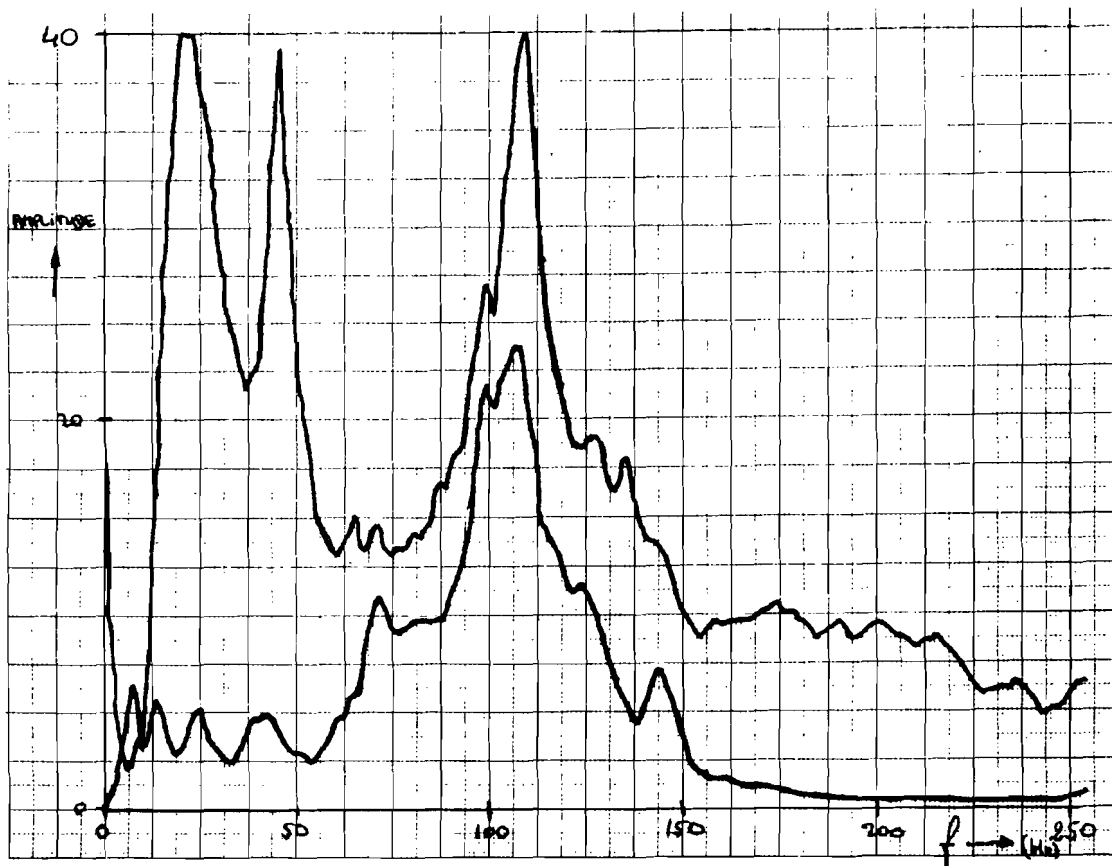
Figure 3.3: Similar plot to that shown on the preceding page in figure 3.2, showing the case for read-out at the *outer* radius of the disc — track 23-24. The peak at 110 Hz represents the resonant-frequency of the disc. This is more evident at larger radii, since here the disc is 'freer' to vibrate than in the centre, where it is supported by the turntable and clamped by the loading mechanics. Vertical movement of the disc due to non-flatness of the turntable is also a maximum at the perimeter of the disc.

24

We may conclude that the mechanical damping of shocks and other external stimuli is not completely effective, so that any shock or vibration to the CD mechanism can excite translation and rotation of the mechanical components. This builds up to a complex series of *relative* movements between the light-spot and the track it was reading from. Furthermore, this is dependant upon the mechanical properties of the disc as well as the mechanism. It therefore rests with the electronic servo systems to provide increased shock-insensitivity.

3.3.1 Limitations of a periodic RE signal

Figure 3.4 again shows the form of the RE signal as the light-spot moves laterally over the tracks. The sinusoidal form $(RE = \sin(\frac{2\pi x}{\delta}))$ indicates
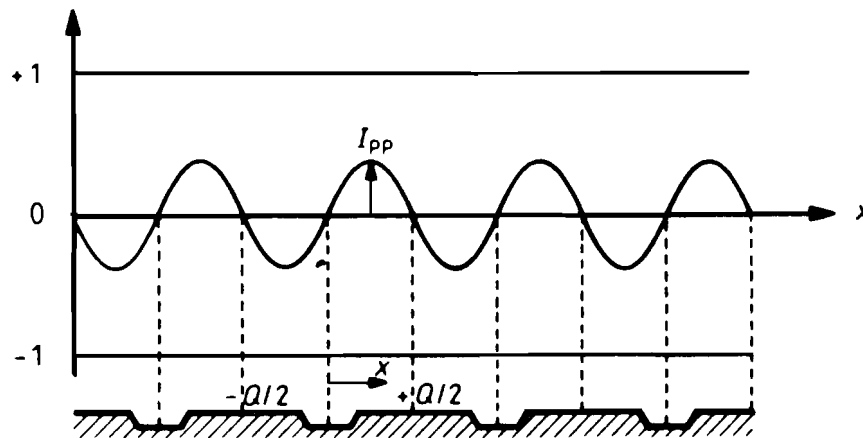
Figure 3.4: *Sinusoidal form of* RE, *showing stable and unstable control slopes. The track-pitch is here represented by Q.*

that the signal *increases* as a function of increasing x for an error x such that $|x| < \frac{1}{4}\delta$. It *decreases* as a function of increasing x in the region where $\frac{1}{4}\delta < |x| < \frac{3}{4}\delta$. The conclusion from this is that

> The slope of the RE signal in the region where $\frac{1}{4}\delta < |x| < \frac{1}{2}\delta$ is a stable control slope, but is only quasi-proportional in the region where $|x| < \frac{1}{4}\delta$. For this reason, RE is only suitable for feedback as a positional-error signal within a distance of $\pm$ one-quarter of the track-pitch from centre-track.

At the point where $x = \pm\frac{1}{4}\delta$, the corresponding angle $\theta = \pm\frac{\pi}{2}$. The *SUM* signal $(SUM = b\cos(\frac{2\pi x}{\delta}))$, will therefore go through zero at this point $(\cos\pm\frac{\pi}{2} = 0)$. The *TL* signal is simply a digitised *SUM* signal, which therefore is at a logic high during the usable slope of *RE*, and at a logic low during the unstable [3] slope.

After a shock to a playing CD-player, the radial control servo will apply a counter-force on the arm to restrict its resultant radial displacement. If the acceleration is so large that it cannot be braked by the feedback of *RE* within its usable slope, then the trackloss procedure will have to take effect.

> *A trackloss is said to occur if the radial positional error x is such that the light-spot is situated further than a distance of one-quarter of the track-pitch from the centre of any track, i.e.,*
>
> $$\tfrac{1}{4}\delta < |x| < \tfrac{3}{4}\delta$$

As mentioned in the previous chapter, this not only marks the unstable/non-proportional working-region of the controller, but also a point where the amplitude of the HF signal has pinched-off to a value which makes reliable detection of the bit-stream impossible. It thus has a double significance.

For the purposes of the following discussions, let it be assumed that the focus-servo bandwidth is high enough to ensure that sharpness of focus is not lost after a shock, so that only an explanation of the *radial* behaviour of the system is necessary. This assumption is made to guarantee the presence of an *RE* signal, and not to neglect the coupling of forces from the focus to the radial plane.

3.3.2   The old trackloss correction scheme explained

The strategy behind the old trackloss-recovery scheme is quite simple. In the regions where *RE* is not the preferred control signal, the actuator is controlled instead by non-linear impulses. Figure 3.5 indicates that two parallel control paths to the radial actuator exist. The *loop-switch*, which selects between the *RE* signal and the DAC correction-pulses, is controlled by the *RCO* (radial control on/off) signal from the servo microprocessor (μp). The functioning of the software routine is quite simple. At the moment that *TL* goes low, the microprocessor is interrupted via its $\overline{INT}$ line and goes into its trackloss procedure. The low on *TL* indicates that the *unstable* slope of *RE* has been reached, so the *RCO* signal is made low to open the radial loop.

---

[3] While the working slope of *RE* does not become unstable until $|x| > \frac{\delta}{2}$ the terminology used in this report will refer to the signal as being unstable for $|x| > \frac{\delta}{4}$.
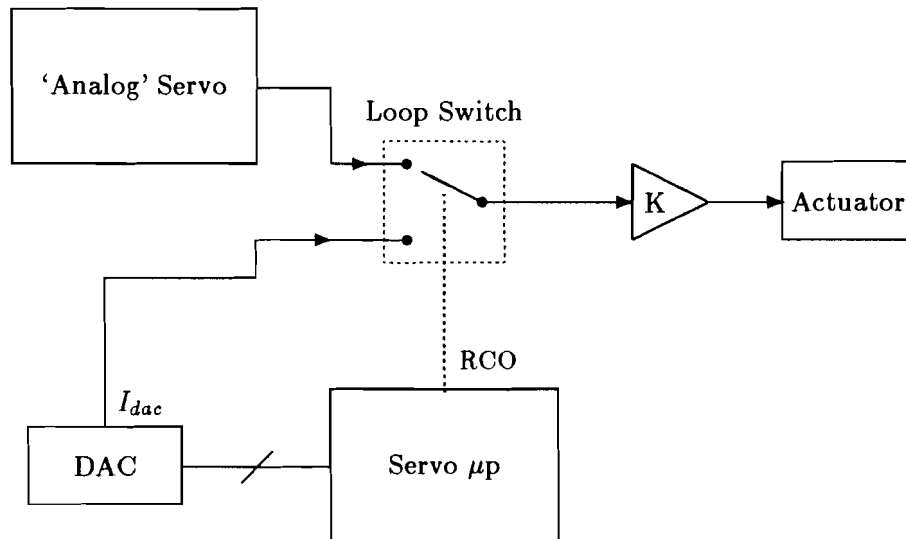
Figure 3.5: *The loop-switch for selecting between* RE *or* μp *control of the radial actuator*

The μp then looks at the polarity of the RP signal, to determine the direction of movement of the wayward arm (i.e. radially inward or outward). Based on this information, the μp 'knows' what polarity of correction-pulse to apply to the radial actuator. This pulse attempts to 'kick' the arm back within the quarter-track boundary where the RE signal regains its usefulness. When this border is reached (whether it be the quarter-track boundary of the *original* track, or the three-quarters-from-original boundary which represents a quarter-track border for the *adjacent* track), the TL signal goes high, and RCO is returned high to re-close the loop, handing radial control back to RE. No attempt is made to ensure that the arm returns to the *original* track. Variants on this scheme use two different levels of steering-current, the first being used as a braking action, with subsequent switching to the lower level to continue the pushing in a more gentle fashion.

The photos in figures 3.6–3.9 give some examples showing the operation of the system. In each case, the uppermost signal is RE, the middlemost RP, and the bottom waveform is TL. The time scale on the oscilloscope is 1 ms/div. The behaviour in each situation, together with an interpretation of the system performance, is explained individually in the caption under the photograph.

3.3.3 Faults inherent in the scheme

The greatest disadvantage of this trackloss correction scheme is that it works blindly with an *open* control-loop. The only 'measurement' which it performs before applying the correction-pulse is to look at the *sign* (= direction) of the relative-error between the light-spot and the track, and to adjust the *polarity* of the applied pulse accordingly. The μp makes no attempt to scale the pulse according to information over the acceleration or velocity of the arm, only to the displacement error x. What this means is that the applied pulse will be too short for serious shocks, too heavy-handed for small shocks, and optimal only for a very small range of excitations. The system was mainly developed to correct mistracking due to the unreliable error signals produced by a disc flaw.

The limited processing-rate of the μp means that its corrective actions can be out of phase with the system behaviour for large shocks. In the first few milliseconds after a shock to the CD mechanism, the entire mechanical system vibrates with a multi-faceted spectrum, with the result that the *relative* motion between the arm and disc can continuously change *sign and magnitude* until the immediate effects of the shock have died down somewhat. In these early moments when the disc and arm are swinging back and forward relative to each other, the μp is bombarding the arm with impulses, trying to get it back into the linear control region within $\frac{1}{4}\delta$ of track-centre. The result of an over-enthusiastic out-of-phase action is that it can impart such force to the arm that it *overshoots* the linear control region, resulting in another trackloss on the *other* side of the track. The net result of such hammering of the arm inwards and outwards is zero, just as for example, the average value of a sine function is zero. In this way, the arm is free to make translational movements over the tracks without much resistance from the trackloss correction system. It will come to rest *on the track where the resultant velocity-error within the quasi-linear control-region can be braked by the RE signal*. The outcome of this is that, more often than not (for a large shock), *the light-spot recommences read-out from a track*

28

RE

RE

RP

RP

TL

TL
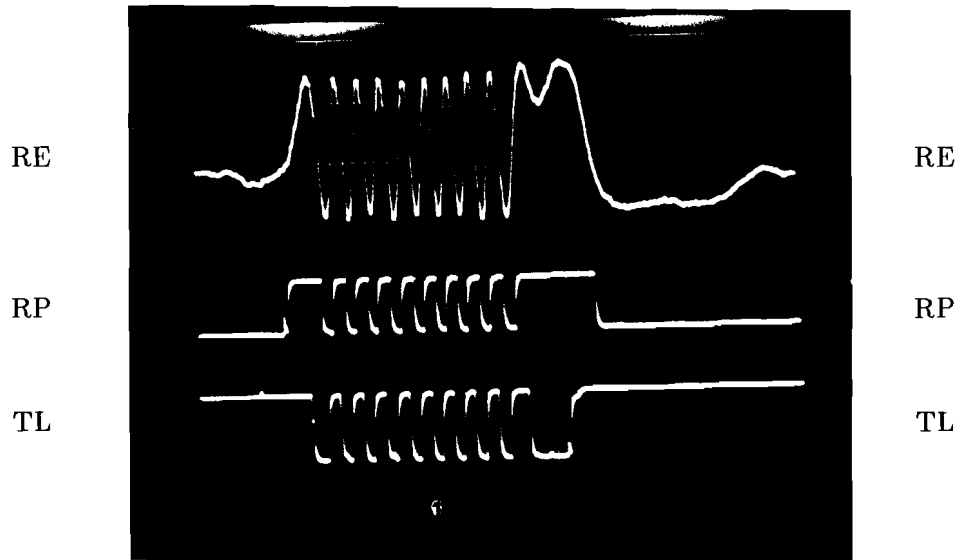
Figure 3.7: Existing trackloss recovery scheme — As a result of a small shock, the arm sweeps over several tracks (10) before 'catching-in' again. The forward journey was totally uninterrupted, indicating the non-desirability of an incoherent strategy. When the 10th track was overshot, the system was able to 'kick' the arm back in the opposite direction to return it to the 10th track. The pulse-width here indicates that the velocity was greatly reduced before final track capture.

RE

RP

TL

RE

RP

TL
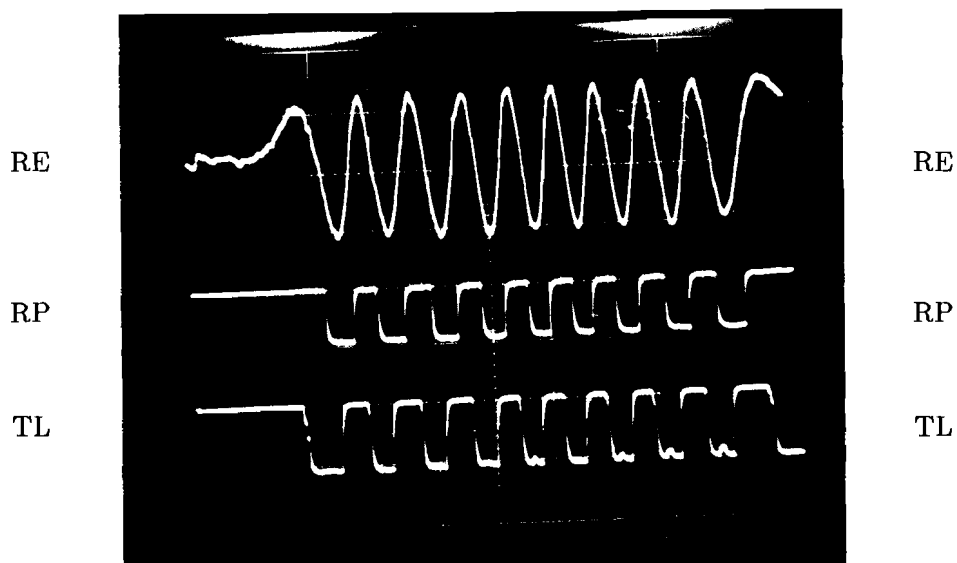
Figure 3.8: Existing trackloss recovery scheme — Expanded view of a skip over a total of 9 tracks. The fact that the period of all 3 signals remains fairly constant shows just what little net braking action is held over from the μp action. The out-of-phase functioning of the μp can actually help the motion of the arm to continue rather than hinder it.

RE   RE

RP   RP

TL   TL
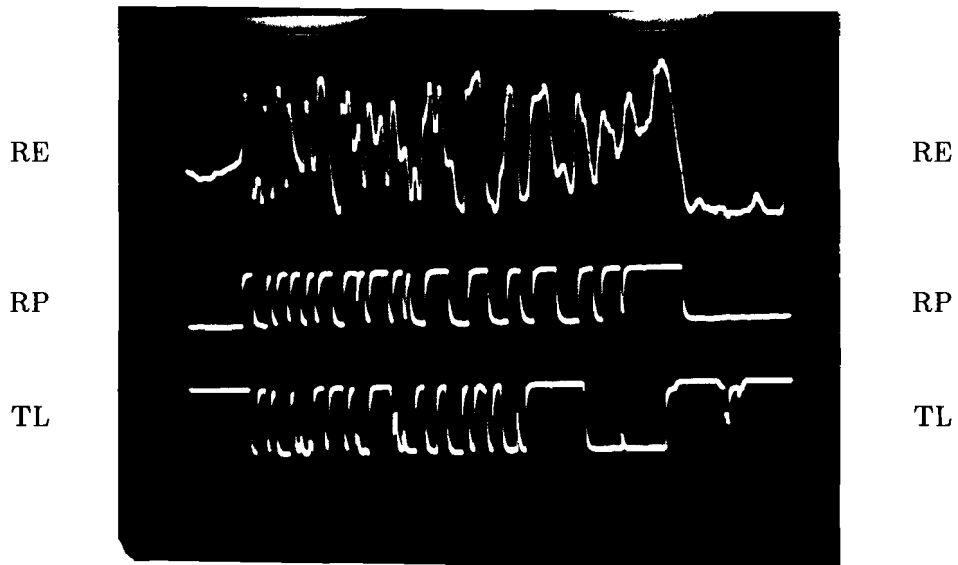
Figure 3.9: Existing trackloss recovery scheme — The behaviour here is chaotic, involving alternate swings inwards and outwards over several tracks. This is the result of the 'nervousness' of the controller in the moments directly after a heavy shock, before the mechanical resonances have subsided. The several-to-the-left then several-to-the-right track-skipping favours the model of the propagation of a shock suggesting a damped sinusoidal phenomenon. The behaviour depicted here can result in 'breakup' of the sound, which is also a disturbing phenomenon.

RE   RE

RP   RP

TL   TL
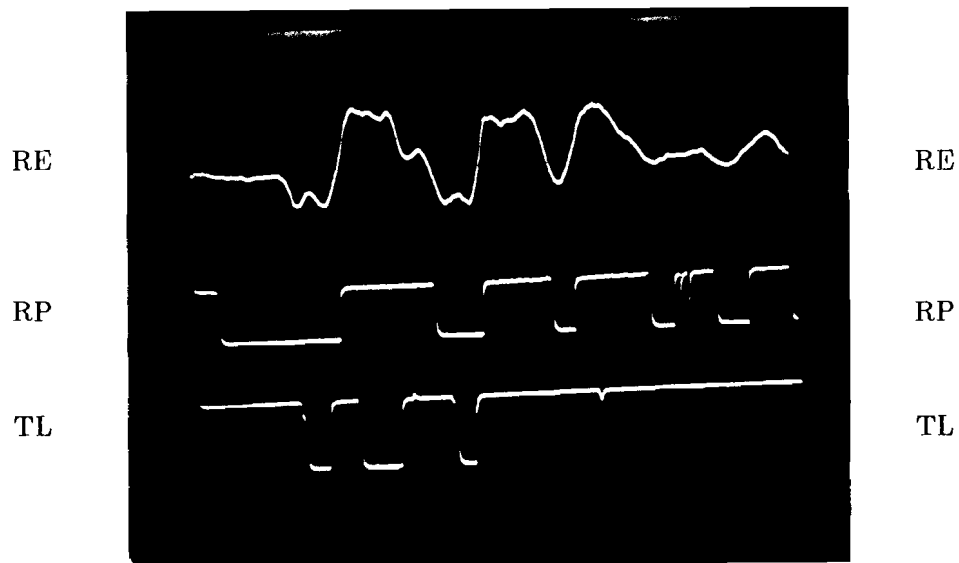
Figure 3.10: Existing trackloss recovery scheme — Example showing typical overshoot resulting from even a very light shock. The arm leaves the track on one side, and gets 'thumped' back in so hard that it overshoots. Here, it is *again* treated over-enthusiastically, causing yet *another* overshoot to the other side of the same track. It is finally safely returned on the *third* attempt to the original track. It takes a very precisely applied shock to excite this behaviour, verifying the totally non-adaptive nature of the strategy to the varying degrees of mechanical stimulation that are possible.

other than the original track which it 'lost'.

Initial experimentation to improve this scheme attempted varying the height and width of the applied correction pulses, and even trailing them with short-duration pulses of the opposite polarity, in an effort to tame acceleration and so avoid overshoot. This was done with the aid of a combinational logic circuit, so that the speed limitations of the μp were eliminated. Restructuring (block transformation) of the radial control loop to achieve the best possible step response in the path from the controlling-pulses to the actuator also had little effect. The most serious limitation to the impulse-control system is the self-inductance of the coil used in the radial actuator, which impedes rapid changes in the current flowing in the coil. This also plays an important role in the out-of-phase behaviour of the system. All of these experiments were seen to have little real effect on shock-sensitivity performance, as the non-adaptive nature of the underlying *strategy* means that system performance can only be optimised for specific magnitudes and types of shocks.

3.4 Human perception of the effects of trackloss

In order to develop an optimal trackloss correction scheme, it is necessary to determine the degree of *audibility* of different 'types' of trackloss. Losing track for an amount of time means that no HF signal can be read from the disc, which in turn means an absence of audio information to decode and send to the player's output. The decoding circuitry in a CD player can use redundant bit information in the *CIRC* coding to reconstruct missing data. If absolute correction is not possible, then if the 'gap' is not too large, it may be feasible to interpolate between the audio samples occurring before and after the missing information. If this is not possible, then the only option is to *mute* the audio output to prevent disturbing noises such as 'ticks' or 'pops' from appearing in the music.

A mute may be defined as a short period of deliberately-induced silence in the audio output of the player.

It is a well known fact that the threshold of audibility of a mute is dependant on six basic *objective* factors. These are

1. The duration of the mute.

2. The average sound pressure level (SPL) in the time before and after the mute.

33

3. Whether the audio level is gradually or abruptly switched to zero (Hard or Soft mute).

4. If the audio-level is switched abruptly to zero, whether or not this occurs close to a zero-crossing.

5. The amplitude of other 'background' sounds or noises which may help to mask the gap left by the mute.

6. The repetition rate of a multiple-burst of mutes.

It would appear that mutes longer in duration than 20–30 ms would be audible with 'normal' background noise levels. This figure rises to 50–60 ms for car CD applications, with engine and road noise as masking factors. Figure 3.10 is an oscilloscope photograph of a 25 ms mute in a 1 KHz sinewave. The logic signal at the bottom of the photo went low when the mute-duration passed a 20 ms threshold, to indicate impending audibility. This signal was part of a specially-developed 'mute and spike' counter, which was designed to assist in objective shock-sensitivity evaluation. A separate report [McGee] has been produced on this subject.

It is obvious, if one imparts a hard shock to a CD player and listens to the outcome, that mutes are not the only audible consequences. If the arm re-captures a track other than the original, then not only is there a period with no HF signal, but also the restart of the HF signal will have a discontinuity in the time-domain. In this case, we speak of a *rhythm distortion*.

> A rhythm-distortion *may be defined as the distortion of the musical rhythm produced by a discontinuity of the audio signal in the time domain. This involves a skip forward (or backwards) from the current moment of music to another piece slightly further on (or back) in the passage, without reproducing the audio in between.*

In order to assess the audibility of such rhythm-distortions compared to mutes, some experiments were carried out. A disc with a continuous 1 KHz sinewave and a music disc were used for this purpose. In each case, a pulse was applied to the radial arm while the disc was playing, which caused skipping over a certain pre-defined number of tracks. In the case of the sinewave disc, this jump introduces a discontinuity in the form of a small mute (no HF signal between the tracks), and a *phase* distortion — when the arm catches in again on the new track, the re-commencement of the sinewave
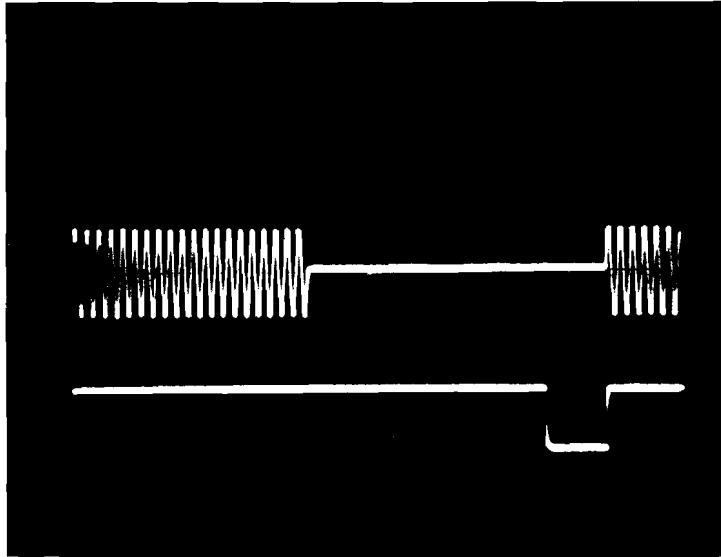
Figure 3.10: *Example of a 25ms-duration mute in a 1 KHz audio sinewave*

can occur from a different point in its period. The important point is that we can only speak of a *phase* distortion, and not a true *rhythm* distortion. This disturbance was only barely audible. In the case of the disc with normal music on it, the track-jump produced the same short mute, together with a rhythm discontinuity of about a half-second, which was definitely *very* audible indeed. The point is that the sinewave has no rhythm, whereas the music has. The inaudibility of the phase distortion would seem to indicate that *skipping over the tracks (if short enough) is inaudible if the rhythm is unaffected.*

If no interruption of the rhythm occurs, then the music segment reproduced directly after the short silence of the mute is the same segment that would appear at that instant if the mute had not occurred. A human being is much less sensitive to this mute-with-preserved-rhythm phenomenon. The results of this experiment are clear —

If a shock to a playing CD player must have some consequences
at the audio output, then this can better be in the form of a
mute than a rhythm-distortion.

3.5 Proposed features of an improved trackloss-correction system

Based on the discussion up to this point, it should now be possible to state
the requirements of a new trackloss-recovery strategy.

Coherence A shortcoming of the old system is that, due to the speed-
limitations of the servo μp, the corrective action can be out of phase with
the behaviour of the system. If, as the result of a shock, the arm achieves
a high enough velocity to enable it to sweep over several tracks, the servo
switches alternately between linear and impulsive control action as the stable
and unstable slopes of RE are traversed in succession. This results in a *non-
coherent* strategy, which retains little *net* effect in getting the light-spot back
on track.

- An improvement can be effected by using an all-out braking effort
  to stop the motion of the runaway arm as quickly as possible. This
  action should be independent of the slope of RE, and should only cease
  when the relative-velocity between the light-spot and the tracks goes
  through zero.

Damping The lack of continuous damping in the old control system re-
sults from differentiation of the sinusoidal RE signal, which yields a cosine
function that provides alternate positive and negative damping. The μp
opens the loop during the negative damping, which is correct of course,
but it acts blindly itself, and does not attempt to scale its action to the
magnitude of the relative velocity between the arm and the disc.

- The new control system must be damped by the use of relative-velocity
  information feedback.

Return to original track The periodic sinusoidal nature of RE means
that the error-signal is zero while the light-spot is centred over *every and
any* track on the disc. A consequence hereof is that, after a disturbance,

36

there is no easily-determined reference track to return to (as would be the case for a *proportional* error signal), so the arm will 'catch-in' to *any* track it can. For a comparatively large shock, this is more often than not a track other than the original. The result of this is, as explained, a rhythm-discontinuity in the music. How serious this will be may be calculated as follows. Assume that, as the result of a shock, the light-spot jumps to a track directly alongside the original. In the time that it takes to cross over between the tracks and re-capture the adjacent track, the disc will have rotated through a *small* angle α. The inter-track spacing is so small compared to the radius of the disc, that a segment of the spiral may be considered as a closed circle. The information on the disc which is 'unseen' as a result of the jump lies in the circle of circumference $(\alpha + 2\pi)r$, where r is the radius from the centre of the disc to that track. The factor of 2π must be included to take the skipped track into consideration. If we consider the more general case where n tracks may be skipped, then the angle becomes $\alpha + n2\pi$. The amount of bits missing from the information stream is then given by $(\alpha + n2\pi)r/l$, where l is the pit-length. Since r will be in cm, and l is in μm, it is obvious that such a track-jump results in the decoder's missing an enormous number of bits (upwards of 1 million). The equivalent duration of the missed passage can be calculated by dividing the calculated length of the skipped tracks by the read-out velocity of 1.25 m/s. On the outer tracks of the disc, for example, the rotational-frequency of the disc is approximately 4 Hz, so that each complete segment of the spiral of tracks represents $\frac{1}{4}$ second of music information. A skip over four tracks would thus mean that the readout process skips over one whole second of music information (or alternatively, that it is read *twice*). *CIRC* simply was not designed to correct such gigantic data errors, and that is why the effect is always audible.

If a scheme were devised to ensure that the light-spot was always returned to the *original* track after a disturbance, then the extra time that this would take would increase α somewhat, but the multiples of 2π would disappear, since n would be *zero*. The result would be a much smaller data error, which would be in the range of the error-correction capabilities of the decoder. Even if this were not the case, the return to the original moment in the music would alleviate the possibility of a perceivable rhythm-distortion. There would almost certainly be a mute, but this would be inaudible if α was kept small by a quick return to track. This should mean that the

consequences of even a heavy shock would be inaudible.

- The new system should ensure that the light-spot always returns to the *original* track after a disturbance, so as to avoid rhythm-distortions. In order to curtail the duration of the accompanying mute, this comeback should take place *as quickly as possible*.

The return-to-track action can be supervised by the use of a *velocity-loop*, which automatically restricts the velocity of the arm to the value which closely corresponds with the ideal trajectory in the phase-plane, and which ensures the easiest possible re-capture of the track without overshoot. In this respect, the original track represents a stable node in the phase-plane.

Playability It stands to reason that the new system should not, if possible, adversely effect the playability performance in any way. As has been stated, the old trackloss correction scheme was developed primarily with a view to correcting disc-flaw induced mistracking. There is no simple clear-cut relation between this and shock-induced trackloss, and it is quite possible to create a system which improves shock-insensitivity but compromises the playability performance. If the return-to-original-track strategy is implemented, this should actually *improve* playability in a broader sense of the word, by drastically improving the effective trackability.

- Any means chosen to implement the new strategy should *not* have an adverse effect on the playability.

If these points are adhered to in a new trackloss correction system, then the improvements achieved in shock-insensitivity of a bandwidth-limited CD player should be quite significant. The imposed limitations make it impossible to completely *avoid* trackloss, but the proposed features of the new strategy should provide *subjective* elimination thereof. Indeed, any compromises which may be necessary in the practical implementation of the system should be made with regard for the possible effects upon the subjective perception of trackloss which may result. Depending upon the final application, it may be possible to attach different weighting-factors to the individual points to be considered. This may also be applicable in any possible tradeoffs of playability performance against shock-insensitivity.

The central theme of the entire strategy may be summarised simply in these words —

- *The goal of an optimal trackloss-recovery strategy/system should be to create a radial-controller with one, and only one, stable point of equilibrium — The original track which was being scanned at the instant before the shock occurred.*

Chapter 4

Implementation of the Return-to-original-track strategy

The previous chapter explained the problems associated with the old track-loss recovery system, and listed the properties of an optimal strategy that should greatly improve overall shock-sensitivity performance. This chapter deals with the theoretical aspects of the chosen means of implementation of the new system. It deals with, among other things, a relative-position and direction detector, *two* principles which can be used to damp the arm's velocity, a system which widens the capture-range in the immediate vicinity of the original track, and the precautions necessary to ensure reliability in measurements and judgements made by the system.

4.1 Determination of Radial-position information

The proposed *RTZ* [1] strategy involves two basic operational phases — braking the motion of the arm which results from the shock, and then guiding the arm back to the point on the disc where read-out was taking place before the displacement. Finding the correct track from the 20,000 or so on the disc will therefore require some sort of radial-position 'co-ordinate' information.

---

[1] This abbreviation for return-to-zero will be used throughout the rest of the report in place of *return-to-original-track*

For example, if as the result of a shock the arm skips over 6 tracks before the controller can stop it, the system must somehow 'know' that it has to jump back over those 6 tracks before restarting playback.

4.1.1   Track-number field of control & display subcode

Perhaps the most obvious way to acquire this information is to make use of the positional content of the *subcode* on the disc. This is already done in the software for the *music-search* routines, which guide the arm to the beginning of the music-programme number chosen by the listener. This is done in much the same way as the *catalog* information is used by a floppy-disk drive to load a particular portion of a computer program. In these music-search procedures, the frame-number of the desired passage is first read from the *TOC* (table of contents) information in the lead-in tracks. The μp then sets the arm in motion towards the target track, reading new subcode information now and again along the way to estimate the size of the remaining jump necessary. In a similar manner, the μp could 'save' the current track-number at the moment of a trackloss, catch the nearest track after successfully braking, read the new subcode, subtract the two to find the difference, and then initiate a jump routine to return to the original track. When it arrived, a simple re-check of the subcode would verify if it was indeed at the correct position.

The greatest disadvantage of this method is that it is too time-consuming. It also provides *absolute* rather than *relative* position-information, which requires further processing to determine relative distances. Capturing and holding a track costs time, as does reading in a section of subcode. This is especially true if read-out does not begin at the start of a frame, as the μp would then have to wait until the disc had rotated to the start of a new frame before it could read the subcode content. Even though the subcode is available at regular intervals ($\approx$ 70 times/sec), such a delay would add to the mute-duration, and must be avoided. A rather unfortunate situation arises if the subcode happens to be damaged by an imperfection in the disc. The *music* bits are clocked through the FIFO and on to the error-correction circuits, but the subcode information is only subjected to a CRC-check. If damaged, it is only *flagged* as erroneous — it is not corrected as such. This is of little consequence for the normal use of the subcode, but does mean in this application that the μp might have to wait for several subcode frames before finding one that is flagged as non-erroneous. As explained, such a delay would be disastrous in this application.

To acquire positional 'updates' so as to effectively close the control loop with the (time-discrete) use of feedback would require constant reading of the subcode from intervening tracks. The task of making even a small jump *accurately* would thus require several tens or even hundreds of milliseconds. Such a delay would not only produce clearly-audible mutes, but the rotation of the disc in that time would ensure that the angle α mentioned in section 3.5 would reach the threshold of perceptible rhythm-distortion. We may thus conclude that —

> In the interests of speed of the *RTZ* principle, subcode data from the disc should *not* be used for determining radial position.

4.1.2 Periodicity of the RE and SUM error signals

It is also possible to turn one of the inherent limitations of the control system — the generation of a *periodic* rather than *proportional* error signal — into a rather useful advantage. The periodicity of the signal means that it goes through zero at, and half-way between, every track. Counting zero-crossings is thus an effective method of counting the passage of a half-track. This can be made even more accurate by also counting the zero-crossings of the *SUM* signal, which is simply a sinusoid that is $\frac{\pi}{2}$ phase-shifted with respect to *RE*. Alternate zero-crossings thus occur on *RE* or *SUM* every quarter-track. If the digitised versions *RP* and *TL* are used instead of the analog waveforms, then the task of counting zero-crossings is reduced to one of counting *transition-edges* on the two TTL-compatible signals. Figure 4.1 is a plot of all four signals during constant-velocity motion of the light-spot over the tracks. It indicates that a transition occurs on *RP* or *TL* each time that the radial positional error x increments by a multiple of one quarter of the track-pitch δ, i.e., $|x| = n\frac{\delta}{4}$.

4.2 Processing of Radial-Direction information

The last section explained the need for *positional* information in correct placement of the radial-arm. It is also necessary, however, to have *directional* information, so that the polarity of the steering-current for the actuator can be determined. In the old trackloss procedure, it was only necessary to use this information *once* (after a high-to-low transition on *TL*) to determine the polarity of a single pulse. This application, however, requires updated information on a regular basis, necessitated by the attempted *coherence* of the strategy. Full braking force is used to stop the arm, which is
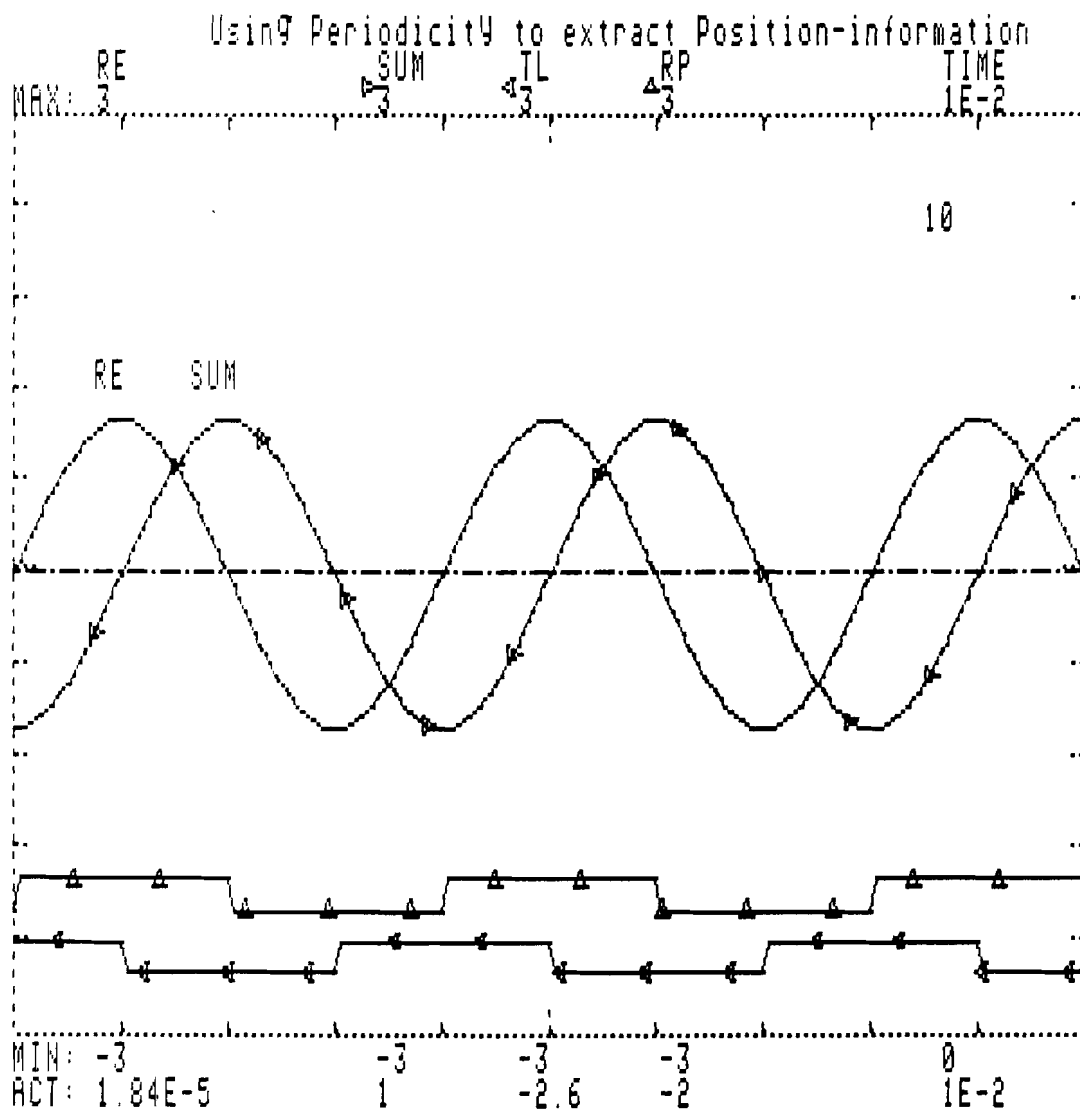
Figure 4.1: *Radial-position information to δ/4 accuracy contained in the edge-transitions of RP and TL (bottom two signals).*

subsequently guided in a controlled manner back on-track. The point which marks the change from full to controlled power will be the *turn-around* point of the arm, where the relative velocity between the light-spot and the correct track changes sign. Updates are necessary because of the possibility of repeated shocks and continuous vibration, both of which may necessitate extra corrective action during one single trackloss recovery. For example, the controlled comeback sequence may have to temporarily switch back to full-power if a second shock manages to overpower the force applied by the control-current.

Direction information is also necessary to determine whether an *up* or *down* count is made on the basis of the $\frac{\delta}{4}$-transitions on RP and TL.

4.2.1 Phase relationship between RP and TL

Just as with position information, it would be possible to determine the direction of motion from the subcode track-number, based on last-state–present-state comparisons. This would require that the arm [2] pauses to read subcode from every track, resulting in a very low average velocity over the tracks. Also, the objections raised earlier in connection with damaged subcode apply. It is thus clear that the subcode is equally unsuitable for providing radial direction information.

A possible alternative is to use the *phase* relationship between the RE and SUM error signals. As explained in the section on the push-pull technique, the mathematical formulas for the signals are

$$RE = a \sin(\tfrac{2\pi x}{\delta}) \qquad\qquad SUM = b \cos(\tfrac{2\pi x}{\delta})$$

There exists an inherent $\frac{\pi}{2}$ phase-shift between the sine and cosine functions. However, the fact that the sine function is odd and the cosine function is even means that this phase-difference will be positive or negative depending on the direction of radial movement, changing by a factor of π if the direction reverses. In other words, the *sign* of the phase-difference (i.e. $+\frac{\pi}{2}$ or $-\frac{\pi}{2}$) will be an indication of the sign of the relative-error x, and thus provides the required directional information.

The phase relationship between RE and SUM is, of course, also reflected in the digital signals RP and TL. The relative phase information can be extracted based upon a knowledge of the polarity of one signal during a transition-edge on the other. This subsequently implies that

---

[2]The reference to 'arm' is used loosely in place of the term 'light-spot'

44

Information as to the relative direction of radial movement is contained in the logic-level of one of either RP or TL during a transition-edge on the other.

Figure 4.2 is a plot from a simulation of constant-velocity motion of the arm over the tracks, showing what changes occur during a direction-reversal. The phase relationships between RE and SUM, evident also in RP and TL, show the π-radians shift after a reversal of direction. A last-state–next-state comparison between the *levels* of RP and TL yields a consistent pattern for each direction of motion. Referring first to the level on RP and then to that on TL, these patterns are —

$$\mathbf{A} \,\dots\quad 1\,1 \longrightarrow 1\,0 \longrightarrow 0\,0 \longrightarrow 0\,1 \,\dots$$

$$\mathbf{B} \,\dots\quad 0\,1 \longrightarrow 0\,0 \longrightarrow 1\,0 \longrightarrow 1\,1 \,\dots$$

The 'A' pattern occurs for radially-*outward* motion; the 'B' pattern for motion radially-*inwards* towards the centre of the disc. At the turning-point in figure 4.2, it is evident that the bit-pattern changes from A to B. The change would have been from B to A if the initial direction had been otherwise. Each progression within a particular pattern is marked by the occurence of a $\downarrow$ or $\uparrow$ transition-edge on one of the two signals, whereby either $1 \to 0$, or $0 \to 1$. Recognition of the pattern is thus simply a matter of comparing the present-state with the last-state, and flagging a direction-change if an element from the other pattern suddenly crops up in the current one. Such a change is, in fact, quite easy to detect, because

A direction bit-pattern change is indicated if both a rising ($\uparrow$) and falling ($\downarrow$) transition edge occur on one of either RP or TL, without any change in the level of the other signal.

4.3 Increasing the capture-range in the vicinity of a track

The last two sections have described fast and efficient means of determining radial position and direction information. Using this knowledge, it should be possible to return the light-spot to its correct position after a shock-induced displacement. The fact remains, however, that the 'intelligent' control system must return control to the range-limited RE signal when the quarter-from-original track boundary is reached. The velocity of the arm
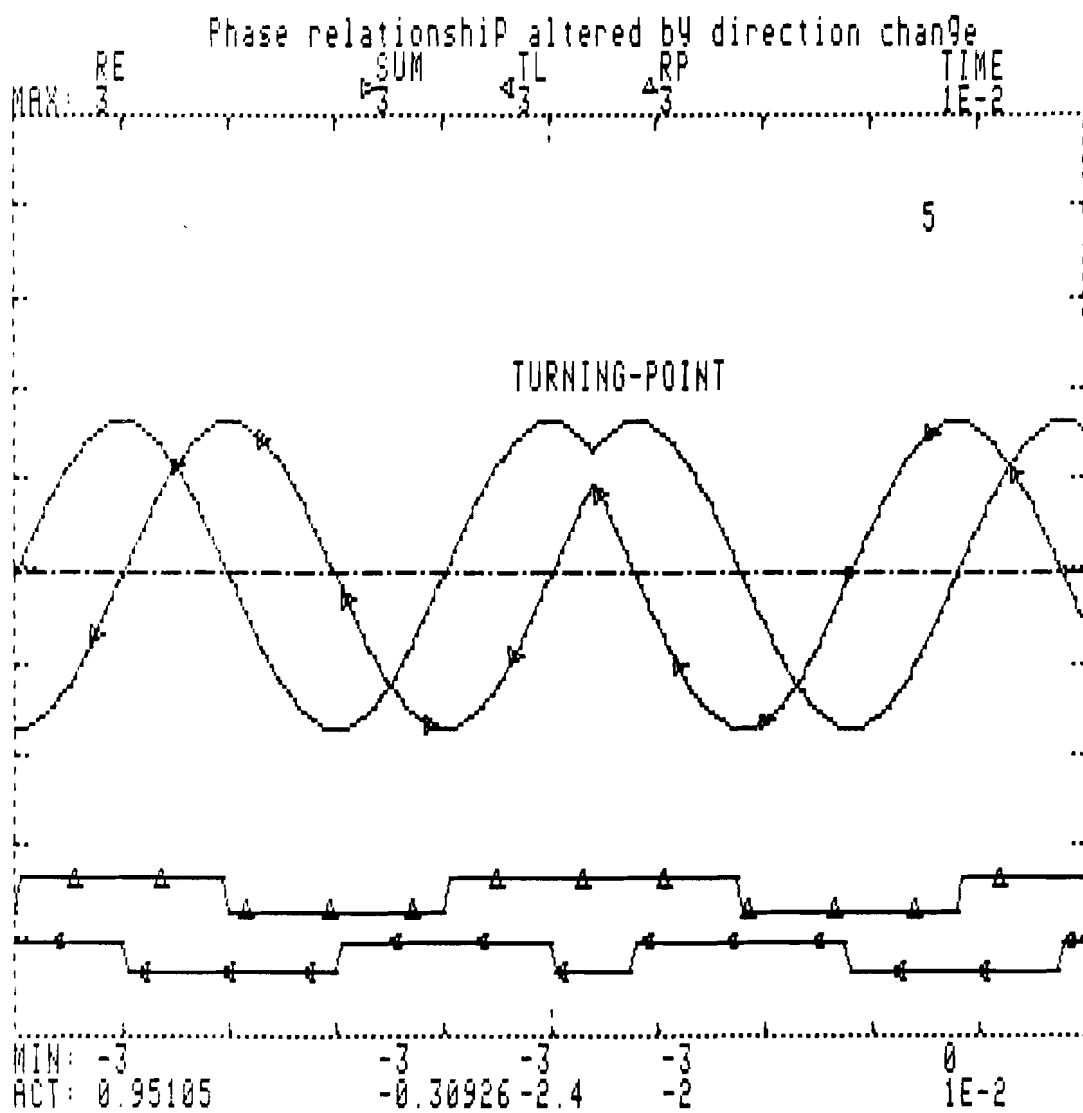
Figure 4.2: *Phase change of* π *radians occurs due to reversal of motion of the light-spot over the tracks. The absolute direction can be read from the sign of the* $\pm\frac{\pi}{2}$ *phase-shift between* RP *and* TL.

46

at this point must be low enough to ensure no overshoot of the $\frac{1}{2}\delta$-wide capture-range. This represents quite a stringent demand, which would be difficult to meet in practice. If satisfied, such a velocity restriction would limit the speed of the system. For this reason, it was decided to process RE to increase its useful quasi-proportional control slope, and thereby increase the length of the track-capture trajectory in the phase-plane.

4.3.1 Extended proportional-range control signal — RE_x

Figure 4.3 indicates the signal generated by operating upon RE so as to mirror the unstable slope around the peak value ($\hat{RE}$). This signal is referred to as RE_x, or alternatively, the extended S-curve. It represents a quasi-proportional control-signal with a slope that implies a stable control region within $\pm\frac{3\delta}{4}$, instead of $\pm\frac{\delta}{4}$, of the on-track position. This makes both the capture and hold range within the immediate vicinity of a track some three times wider. It is, of course, theoretically possible to continue such operations on RE to beyond $\pm\frac{3\delta}{4}$, but this would increase the amplitude of the resultant error-signal to a level which would cause power-supply-saturation limiting. The mathematical operation performed on RE to produce RE_x is

$$RE_x = 2\,\hat{RE}\,\big|_{x=\frac{\delta}{4}} \;-\; RE\,\big|_{\frac{\delta}{4}<|x|<\frac{3\delta}{4}} \tag{4.1}$$

This implies 'following' RE normally until the $x = \pm\frac{\delta}{4}$ boundary is reached. The amplitude ($\hat{RE}$) at that position is sampled and 'held', and then multiplied by two. The slope of RE in the next two quarter-track quadrants is inverted and added to the offset, producing the desired RE_x form.

The use of this RE_x signal in place of the 'normal' RE has many inherent advantages —

- The 'target' area for handover from μp-supervised to normal tracking control is increased, reducing the accuracy-requirements for the track counter, and making small miscalculations tolerable.

- The maximum tolerable velocity of the arm at switchover is increased by a factor of $\sqrt{3}$. A phase-plane plot, showing velocity $\dot{x}$ versus distance x, is indicated in figure 4.4. The asymptotes of the maximum allowable re-capture velocities are drawn for the cases of both the normal RE and the RE_x signals. The rectangles created by joining the asymptote-segments with vertical lines through $\pm\frac{\delta}{4}$ and $\pm\frac{3\delta}{4}$ indicate the capture-ranges with and without RE_x. If the maximum tolerable
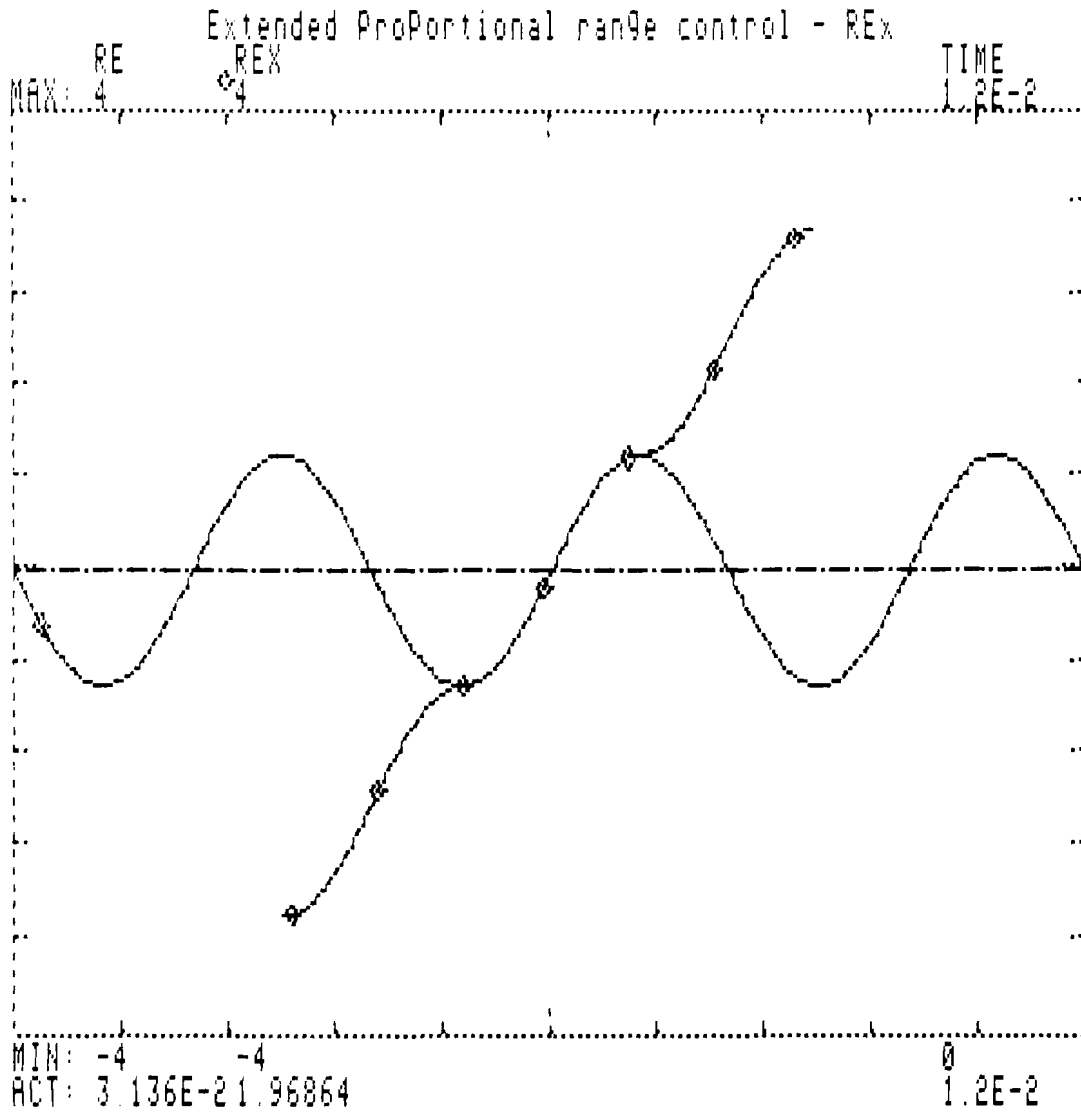
Figure 4.3: *Three-times wider quasi-linear capture-and-hold range in the vicinity of a track — the RE_x signal (extended S-curve)*.

velocity to avoid overshoot is $\hat{x}$ when RE is used, then this is increased to $\sqrt{3}\,\hat{x}$ if RE_x is substituted. If this is considered together with the increase from $\hat{x} = \pm\frac{\delta}{4}$ to $\hat{x} = \pm\frac{3\delta}{4}$ allowable on the distance axis, then it is seen that the area of the target 'footprint' in the phase-plane is increased by a factor of $3\sqrt{3}$.
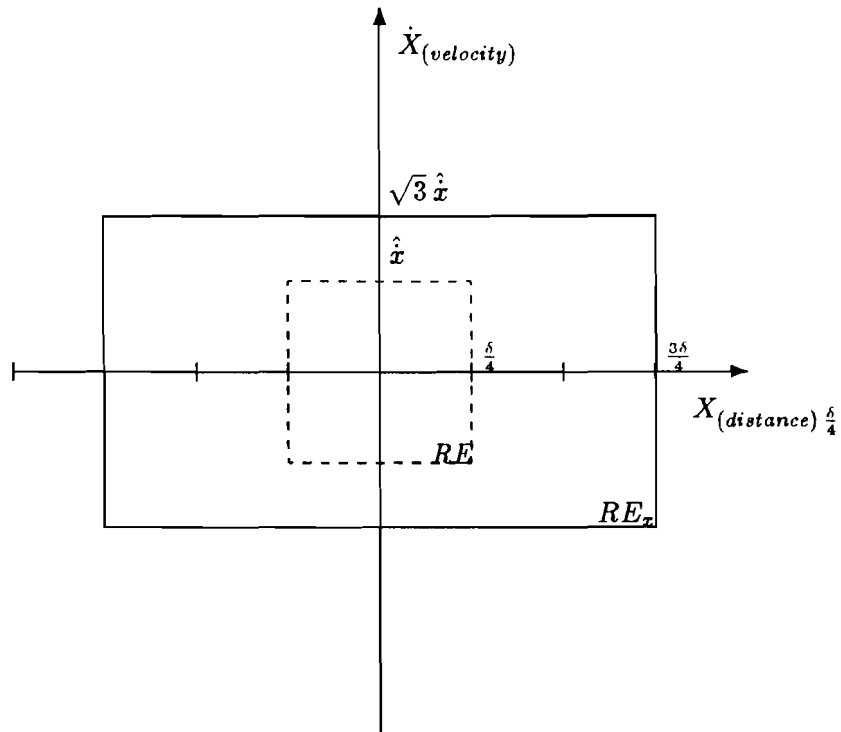
Figure 4.4: $3\sqrt{3}$-times increased area of the track-capture-range 'footprint' in the phase-plane achieved by substituting RE_x for RE

- An increased hold-range means that shock-induced excursions outside the capture-range of the original track are less likely to occur, meaning less-frequent use of the extended features of the trackloss-recovery

49

system.

- RE_x is a continuous-time, continuous-position error signal, which does not have the sampling-frequency limitations of the corrective action of the servo μp. The problem of an out-of-phase controller is thus to a large extent eliminated.

- RE_x should be an excellent signal for coping with the simulated track-bending produced by the presence of disc-imperfections such as 'bubbles' in the layer material.

4.4 Damping of the controller

As explained in section 2.3 describing the radial control loop, damping of the controller is provided by the differential-action of the LEAD network (see figure 2.6, page 12). Control of the velocity of the arm by the use of feedback is desirable to ensure that the RTZ system follows the optimal trajectory in the phase-plane. The LEAD damping is, however, only *partly* useful. Differentiation of the sinusoidal RE function produces a cosine function $\dot{RE}$, which by nature is *bipolar*. The damping provided by the use of this signal is *positive* within a region of $|x| \leq \pm\frac{\delta}{4}$ (increasing slope), but negative within the intervals where $\frac{\delta}{4} < |x| < \frac{3\delta}{4}$ (decreasing slope). Negative damping implies positive-feedback of the velocity-error, which means that the controller will infinitely accelerate or brake the arm rather than hold its velocity at a constant value. The damping provided by the LEAD network is therefore only useful at discrete intervals along the distance (and hence time) axis. Two possible means have been proposed for artificially generating useful velocity-damping.

4.4.1 Velocity damping by means of analog differentiation

Figure 4.5 is a simulation-plot showing the alternative positive and negative damping provided by straight differentiation of the positional-error signal RE. The differentiated sine produces a cosine $(\dot{RE})$, which therefore has the same phase as the SUM and TL signals with respect to RE. It is evident from the plot that a transition-edge ↑ occurs on TL each time that the damping changes from positive to negative or vice versa. It is also obvious that TL is *high* while the damping is positive, and *low* when it is negative. It is therefore possible to multiply $\dot{RE}$ with ± 1 (depending on the logic-level of TL) to invert the polarity of $\dot{RE}$ when it would otherwise produce

negative damping. This is the principle of the *switched differential-action*, *SDA*, which is an 'analog' means of providing damping for the controller. The switched signal is shown in figure 4.6. While it would appear that this is simply a form of full-wave rectification, the latter is not an applicable substitute. The aim of the *SDA* circuit is to create a unipolar signal, just as would be achieved by rectification, but this unipolar signal may be either uniformly positive or negative (depending upon direction). A rectifier would always operate upon the differential signal so as to produce an invariant unipolarity.

The figure also indicates the extended S-curve signal RE_x, which can be used *outside* the normal $\pm\frac{3\delta}{4}$ boundaries simply by holding its deliberately-induced mirroring-offset $\hat{RE}$. The d.c. component added to the a.c. signal in this way effectively compensates for the otherwise-zero average-value of the sine function, and provides a net steering-current for the actuator. The combination of this steering signal and the *SDA* feedback creates a velocity loop, which regulates the movement of the arm so as to provide a constant sweeping-velocity over the tracks. A mathematical treatment of this is provided in Appendix A.

4.4.2 Velocity feedback by digital sampling and calculation

A second possible means of acquiring velocity information uses the servo-μp to mathematically calculate the speed of the arm. As explained in the section describing the processing of position-information from the transition-edges on both RP and TL, such edges represent the passing of a quarter-track-pitch 'milestone'. If a timer-counter in the μp is started and stopped on successive edges, then the velocity of the arm over the tracks can be calculated from simple algebra on the basis of knowing the time taken to cover a specified distance $x = \frac{\delta}{4}$. This simple relationship is

$$velocity = \frac{distance}{time}$$

For this purpose, the radial control loop is open, and the steering-current for the arm is provided by a $3\frac{1}{2}$-bit digital-to-analog converter (DAC), which is currently used to supply the trackloss-correction impulses and during music-search routines. Based upon the calculated velocity, the μp can vary the code to the DAC to adjust the current so as to maintain a constant velocity.

DIFFERENTIATED RE

RE
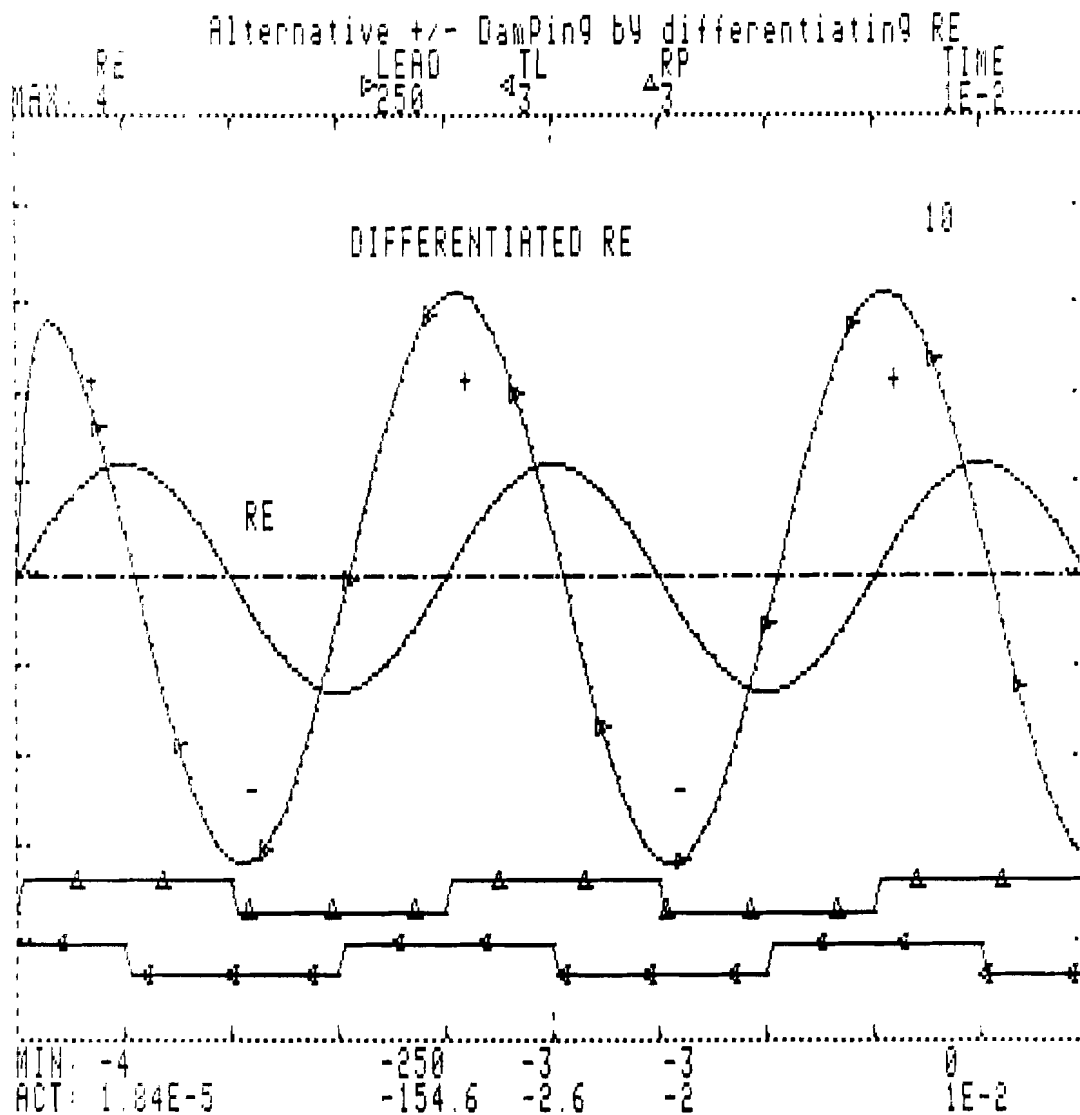
Figure 4.5: *Alternative positive and negative damping produced by* $\dot{R}E$
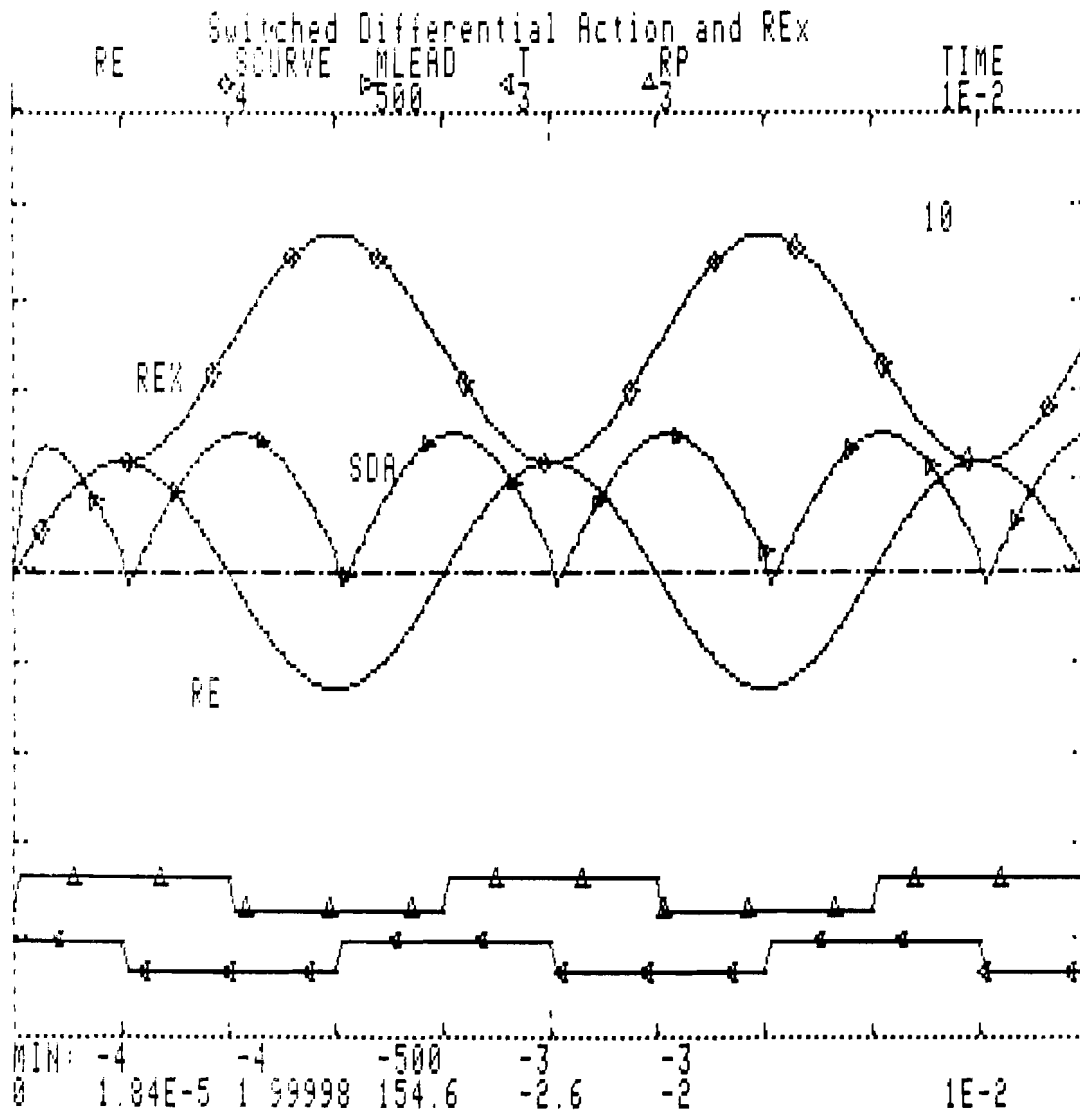
Figure 4.6: *Using the logic-level of* TL *to selectively multiply* RE *alternatively by* ± 1, *thereby converting the quadrants with negative-damping into ones of positive-damping*

53

4.5 Circuit diagrams and the microprocessor algorithm

The report up to this point has attempted to explain the theoretical aspects of the means chosen to implement the improved trackloss-recovery system. The following sections deal with various points concerning the physical implementation of the ideas. The circuitry was developed with a minimum component-count in mind, and is thus in certain ways not as elegant as might be possible with more extravagant signal-processing. The initial emphasis was upon ease of experimentation, and after feasibility of the ideas had been proved, the circuitry was reduced to the minimum possible.

4.5.1 Producing the RE_x signal

The hardware necessary to perform the mathematical operations indicated in equation 4.1 is very simple indeed, and is shown in figure 4.7. It consists of an opamp connected as a differential amplifier, with the inclusion of a sample-and-hold S/H switch and capacitor in the non-inverting (+) input. The gain at the + input is +2, whereas it is −1 at the inverting (−) input. When the switch S_1 is closed (TL high) the S/H tracks the input, resulting in an overall gain of the circuit of $(2-1) = 1$. If S_1 is *open* ($TL \downarrow$ low), then the charging-path to the capacitor is broken, and it 'holds' the value of $\hat{RE}$ at the (+) input. The ×2 amplification supplies the necessary offset for the mirroring operation. If S_1 is closed again, then the output tracks the input normally, and RE_x becomes RE.

4.5.2 Generating the SDA signal

Figure 4.8 depicts the circuitry used to implement the *SDA* action. The selector switch for connecting the signal to the inverting or non-inverting input of the opamp is controlled by TL. When the input is connected to the upper branch, the gain is $-R/R = -1$. This is thus the × − 1 operation. If the switch is connected to the lower branch, the opamp is effectively a voltage follower, with a gain of +1.

4.5.3 Digital hardware and the microprocessor-interfacing

The initial experiments were carried out using a modified CD204 player, equipped with the RE_x circuit, but without the *SDA*. It was otherwise un-
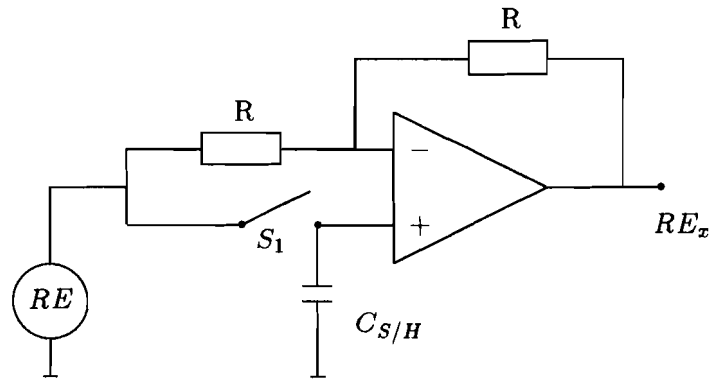
Figure 4.7: *Circuit to generate RE_x from RE. The switch S_1 should be opened when $x = \frac{\delta}{4}$. It may be closed momentarily at $x = n\frac{\delta}{4}$, $n = 1, 5, 9, \ldots$, to refresh the hold capacitor.*
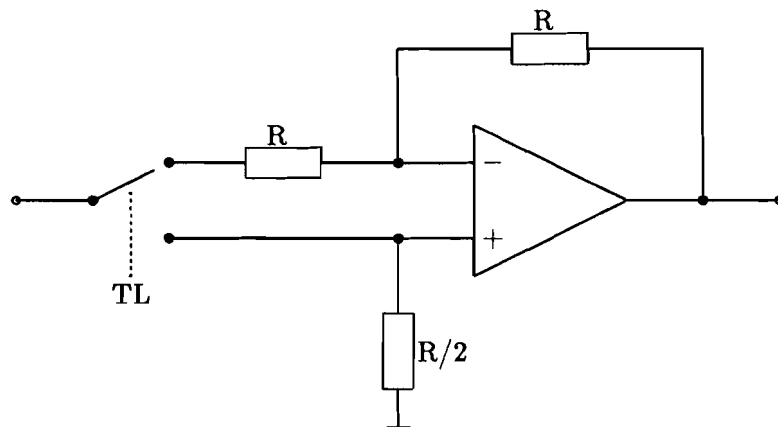
Figure 4.8: *Circuit used to generate the switched-differential action*

modified except for software alterations to the *servo* [3] trackloss-correction software routine. The results of this test were rather disappointing, as the action of the controller was just as much out-of-phase with the required function as was the case with the old strategy. The slow $5\mu s$ machine cycle-time of the MAB8400-series μp and its lack of timer/counters were the obvious relevant factors. After a heavy shock to the mechanism, the velocity of the arm can result in transitions on RP and TL occurring at a rate of over 10 KHz. Looping through software-routines to calculate velocity and direction at that rate requires a fast μp, which meant that the 8400 was unsuitable. The 8051 was chosen to take its place, due to its 12 MHz clock ($1\ \mu s$ cycle-time), *two* counter-timers, *two* interrupt lines, and the possibility to drive the counter/timers directly via a count-input without software assistance. It was also decided to do the track-counting and direction detection externally in hardware, simplifying greatly the initial software routines.

4.5.4   Protection against noise on TL and RP

Due to such phenomena as optical-crosstalk between the focus and radial control systems, mistracking- and flaw-induced HF-noise on RE and SUM, and lack of hysteresis in the digitising-comparators, RP and TL are plagued with noise-spikes. This happens mostly during a level-transition, when the corresponding analog waveform is making a zero-crossing. Such unreliability is absolutely unacceptable in a system which relies upon sampling these two signals to provide distance, direction, and velocity information. A spike between two legitimate transitions makes it look to the μp as if *two* quarter-tracks have been traversed instead of one, and also the arm's velocity appears to be much higher than it is in reality. In order to prevent such spikes interfering with the reliability of the system, the hardware shown in figure 4.9 was developed to clean up the signals. It was used only in the initial stages of experimentation, to simplify the software routines and generally make it easier to interpret the action of the controller.

The circuit functions by creating a pulse-width threshold in the system. One of the one-shot multivibrators is triggered each time that a positive or negative-going edge occurs on the input signal. The resultant ⊔ pulse is applied to one input of the and-gate, forcing its output low. The output of the and-gate will only return high when *both* one-shots have timed-out, and

---

[3]In this context, *servo* refers to the microprocessor used for, among other things, trackloss correction. The μp controlling the programmable features of a player is likewise called the *user*.
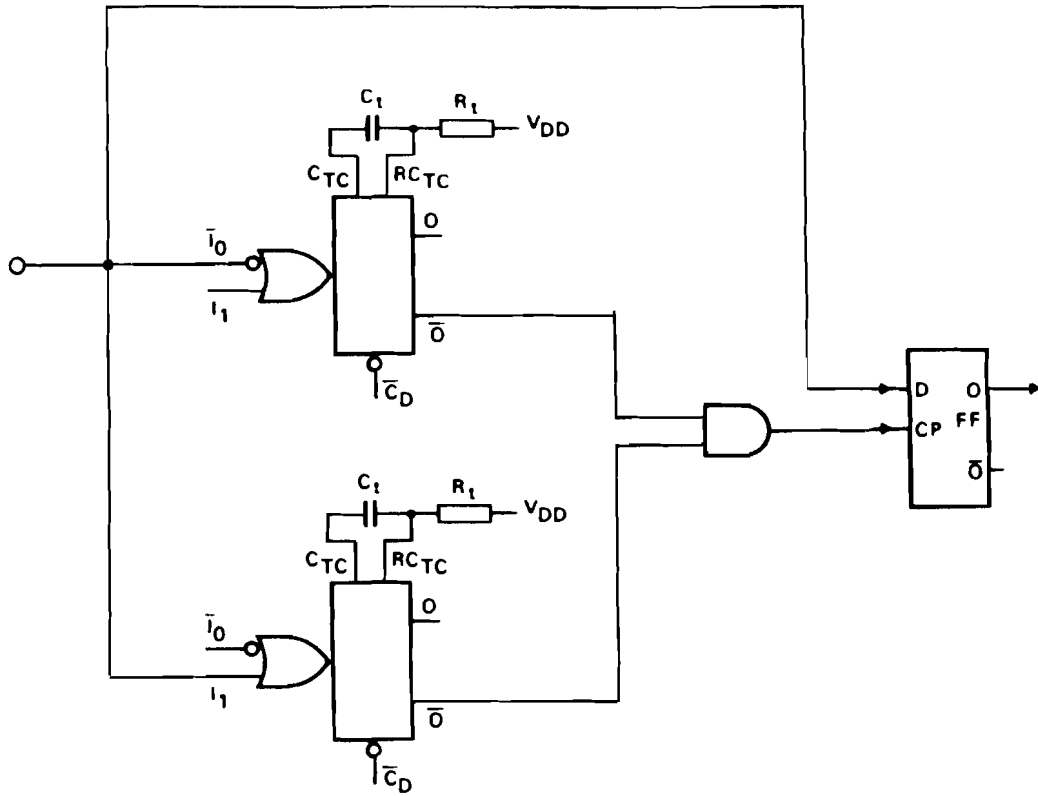
Figure 4.9: *Spike-remover circuit for* RP *and* TL

the positive-going ↑ edge produced hereby clocks the level on the input signal into the D flip-flop. If the one-shot triggering was produced by a spike, then the spike will have disappeared again by the time that the signal is clocked through, so it will not appear on the output. A genuine transition will be transferred, however. It has been experimentally found that an empirical value of ≈ 20μs represents a suitable value for the time constant of the one-shots. Figure 4.10 shows the effect of the circuit upon both the *RP* and *TL* signals.

4.5.5 Hardware track-counter driver and reversal-interrupt generator

Figure 4.11 shows the *RPDIP* circuit, an acronym for *Radial Position and Direction Information-Processor*. Together with the spike-removers, the basic function of the circuit is to —

1. Improve the reliability of *RP* and *TL* by introducing a pulse-width threshold to effectively block spikes and speed-up edges.

2. Produce a short-duration ⊔ pulse each time that a quarter-track transition edge occurs on *RP* or *TL*. This pulse is used to drive the 8051's internal event counter.

3. Measure the sign of the phase shift between *RP* and *TL* to indicate the direction of relative-motion between the arm and the original track. This information is also read by the *μp* to select either up or down count mode for the track-counter.

4. Generate a short ⊔ interrupt pulse to tell the 8051 that a direction-reversal of the arm has occurred (i.e. *sign* of relative-velocity has changed).

The circuit effectively detects the unique repetitive bit-pattern indicated by *RP* and *TL* for movement in each of the two possible radial directions. The polarity of some of the bits in the pattern is inverted, to simplify recognition of a direction-change. As the D flip-flops can only be clocked by a positive-going ↑ edge, two inverted signals $\overline{RP}$ and $\overline{TL}$ are also used to provide clocking on negative-going edges. The main arrangement of four flip-flops ensures that any *edge* on one signal clocks through the *level* on the other. Table 4.1 shows how *absolute* direction of motion can thus be determined.
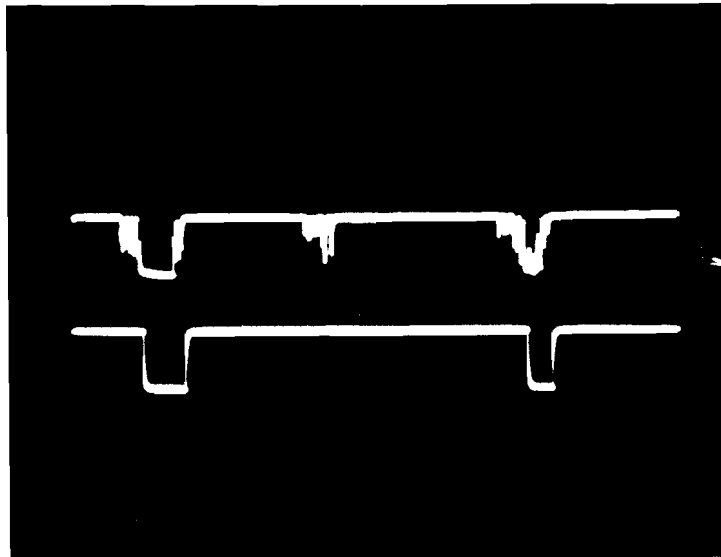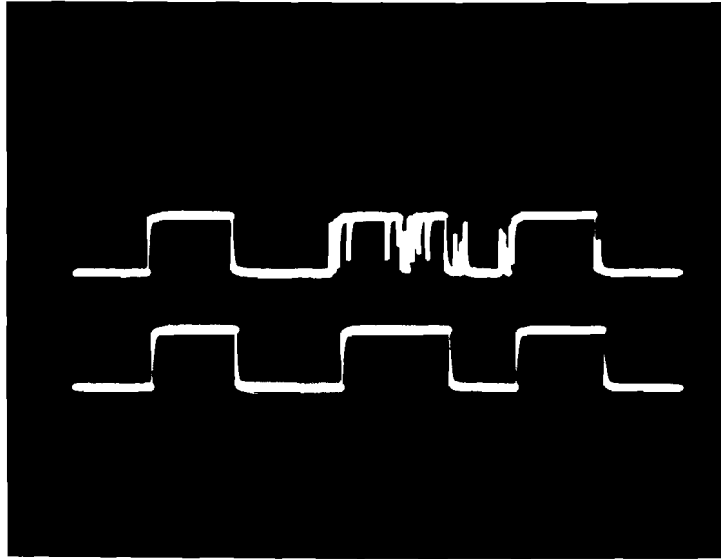
Figure 4.10: *Effect of the pulse-width threshold circuit on* RP *and* TL. RP *is shown in the upper photograph,* TL *in the lower one. In both cases the top waveform indicates the signal before de-spiking, and the lower one is the processed signal.*
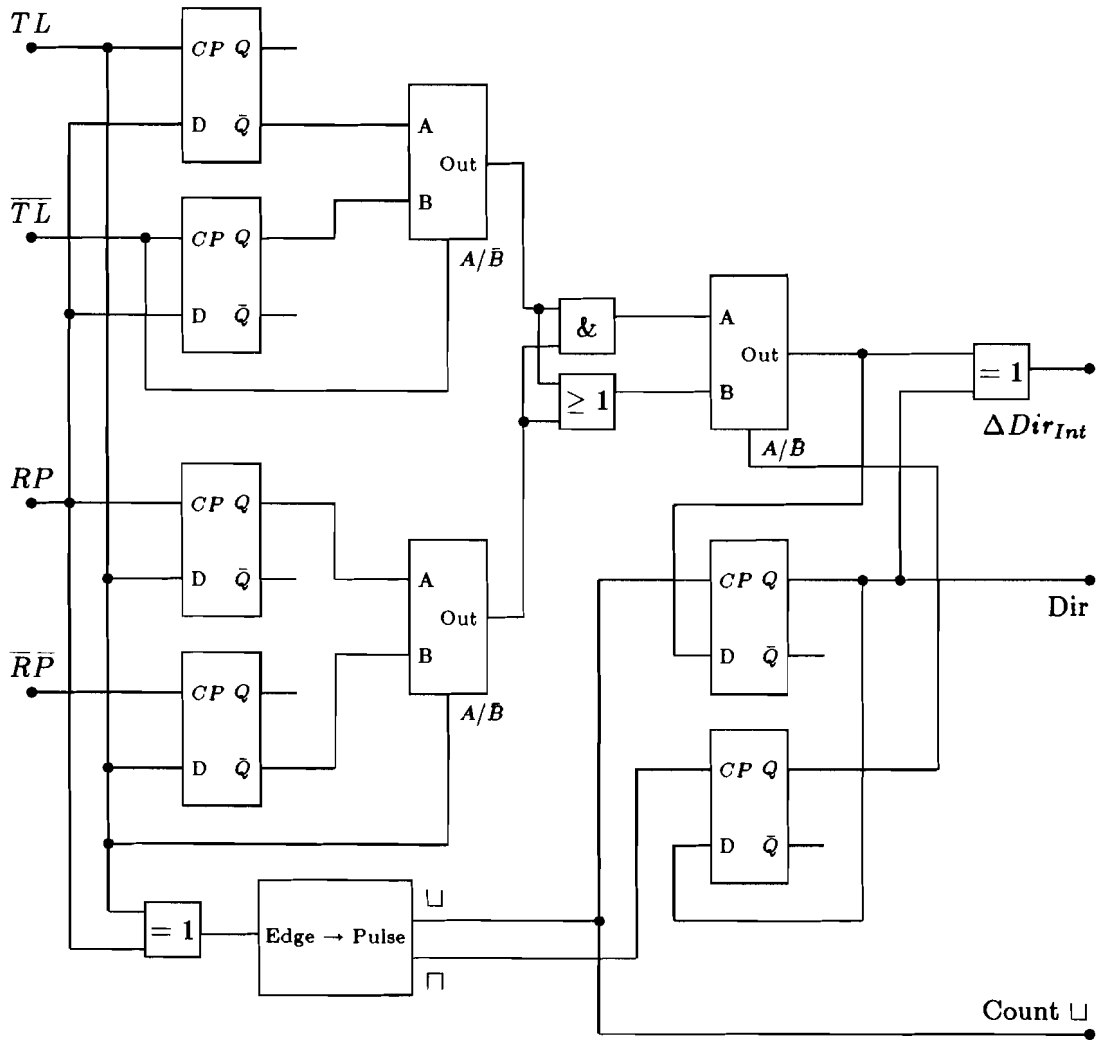
Figure 4.11: *Circuit to perform the RPDIP function (see text)*

60

Transition	Level	Direction
TL ↓	RP = 1	Outwards
TL ↓	RP = 0	Inwards
TL ↑	RP = 1	Inwards
TL ↑	RP = 0	Outwards
RP ↓	TL = 1	Inwards
RP ↓	TL = 0	Outwards
RP ↑	TL = 1	Outwards
RP ↑	TL = 0	Inwards

Table 4.1: *Radial Direction* (↔) *indicated by edge/level combinations of RP and TL*

The 4-bit pattern at the flip-flop outputs (two Q and two $\overline{Q}$) can be reduced to a 2-bit pattern with the help of the 2–1 multiplexers. Both bits being similar in this 2-bit pattern implies a particular direction — unlike bits are only temporarily generated immediately after a direction change before the entire new pattern has been clocked through. The problem is that 8 different 'types' of change in the main bit-pattern can be produced by a direction-reversal, depending upon precisely *where* between two tracks that it occurs. Figure 4.12 indicates the possibilities. In the notation used in the caption, ↩ represents a turn-about from rightwards to leftwards motion, and likewise, ↪ is a change from leftwards to rightwards.

A pattern of 1 1 at the multiplexer-outputs always represents outward-motion, just as 0 0 is always inward. A problem arises, however, when 1 0 and 0 1 are generated. At face value, it is unclear if they represent an intermediate stage between 11 → 10 (01) → 00 or between 00 → 01 (10) → 11. To determine this, a *previous-state* check is necessary, which is performed with the help of an and-gate, or-gate, 2–1 mux, and D flip-flop. This arrangement may seem a little odd, but it integrates very nicely with the rest of the circuitry for producing the ΔDIR_{Int} interrupt and the count-pulse ⊔. A detailed explanation of the circuit-function should not be necessary.
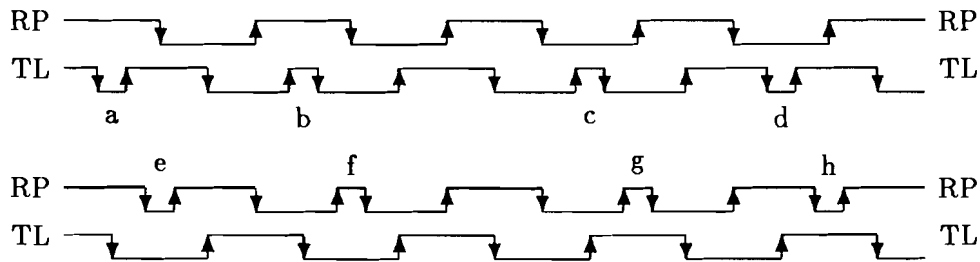
Figure 4.12: *Transition-patterns representative of the 8 possible direction reversals which can occur as seen from a reference track* —

(a) $\hookleftarrow$ @ $\frac{\delta}{4}$ (b) $\hookrightarrow$ @ $\frac{3\delta}{4}$ (c) $\hookleftarrow$ @ $\frac{3\delta}{4}$ (d) $\hookrightarrow$ @ $\frac{\delta}{4}$ (e) $\hookleftarrow$ @ $\frac{\delta}{2}$
(f) $\hookrightarrow$ @ $\frac{\delta}{2}$ (g) $\hookleftarrow$ @ centre-track (h) $\hookrightarrow$ @ centre-track

4.5.6 The software algorithm for the experimental digital-damping-only version of the controller

With the help of the RE_x circuit and $RPDIP$, the software is really quite simple. A parallel arrangement of both the old 8400 and the new 8051 microprocessors was used. The 8400 was used to start-up the player, and then the 8051 was switched in during playback to take over the functions of the trackloss correction routine. Because the 8051 only implemented the trackloss service routine, only a short and simple procedure had to be written in the new processor's code. The parallel arrangement also meant that direct A/B comparisons were possible between the new and old systems.

Trackloss procedure and functions of the software routine —

1. The RE_x signal is used as a quasi-proportional radial-error signal to greatly improve the arm's ability to remain within the catch-in region after a shock to the CD mechanism.

2. If the shock was so great that RE_x could not hold the arm within the capture-range of the track, then at the $3\delta/4$ boundary, the RCO signal is made low to open the control-loop. The μp subsequently instructs the DAC to supply its maximum braking-current to the arm.

3. During the motion of the arm over the tracks (before it can be braked),

the transition-edges on RP and TL are counted to keep account of the position-error relative to the original track.

4. The phase difference between RP and TL is monitored for a sign change which indicates that the constant braking-force has succeeded in stopping the arm's motion. At this point, the velocity goes through zero, and the arm begins to move *backwards* in the direction of the original track.

5. The task now on hand involves dealing with 'known' quantities. On the return journey back to the original track, the quarter-track counter may be decremented instead of incremented. Timing-measurements between the quarter-track edges supply velocity feedback, which allows the μp to vary the amplitude and polarity of the DAC-current to damp the arm's motion. When the quarter-track counter reaches a count of 3, RCO is returned high again, and control is handed back to RE_x. If the μp's velocity calculations were correct, RE_x will guide the arm back onto the track without any overshoot.

Even in its rudimentary form, this primitive realisation of the strategy proved that it works, and can result in tracklosses with inaudible consequences. An average of one trackloss in three produced no audible effects, the system performing rather wildly on the other occasions. It was felt that this resulted only from 'teething-problems' with the experimental setup, and the otherwise encouraging results prompted further development of the system. To this end, it was decided to perform a simulation of the dynamic behaviour of the system, using the Univerity of Delft's PSI Ψ simulation program. It was hoped that this would enable basic improvements and lead to an optimal solution.

Chapter 5

PSI Simulation

PSI is an interactive block-oriented simulation program for studying the behaviour of dynamic continuous and discrete systems. Over 50 block types are available, and the system to be modelled is expressed in terms of simple function-blocks and transfer characteristics in the s-domain. This is quite different from *SPICE*, for example, where the system is specified at electronic-component level. For a more detailed description of the PSI package, consult [PSI].

The great advantage of simulation is that, once a reasonable model of the system is defined and described, it becomes very easy to check new ideas on a 'try-it-and-see' basis. A good simulation will involve the use of a model which is detailed enough to give useful results, but not so cumbersome that it becomes impossible to interpret the output. An ideal situation is reached when a good correlation between simulated and real-life behaviour exists, and where it is possible to logically account for the discrepancies.

The simulation was used in this application for studying the 'trackability' of the radial controller after an external shock. In practice, such external stimulus generates complex sets of *relative* movements between the light-spot and the track. In the interests of simplicity of interpretation of the results, the simulated stimulus involves *only movement of the disc*, and the results therefore reflect the ability of the actuator to track these movements. The disc was modelled as being fixed to the surrounding world via a simple spring and damper, so that it can resonate at a single frequency. While the frequency and damping were constant, it was possible to adjust the *amplitude* of the excitation, thereby simulating varying shock-strengths. This represents quite a reasonable simplification of the real-life situation in a CD player.

The radial control-system was first modelled in its simplest form, and the features of the new trackloss correction strategy were subsequently added one by one. The offset-correction and AGC circuits were omitted for the purposes of simplicity. Initial efforts concentrated on the behaviour of the system *within* the capture-and-hold range bordering the track, and when this was optimised, the μp-supervised functions were modelled. The entire model consists of some 85 blocks, a complete listing of which is given in Appendix B. This listing shows how the system is described to PSI, indicating the block names, types, inputs, and relevant parameters. Only the main points of the model will be discussed here.

5.1   Behaviour within the track-capture range

Initially, a study was made of the track-holding capabilities of the system, with the simple philosophy that if radial tracking is not lost in the first place, then the extended features of the new system are effectively redundant. The effect of the RE_x signal and the $3\sqrt{3}$-times greater phase-plane target were studied using the system model shown in simplified form in figure 5.1. Several of the peripheral PSI blocks used to create the various functions have been omitted for clarity.

The block *optics* represents several sub-blocks which generate the RE and SUM signals, together with their digitised forms RP and TL. The LEAD and LAG networks are both PDC-blocks, of the form

$$\frac{1 + s\tau}{1 + as\tau}$$

and RE_x consists of a weighted-summer and sample/hold blocks. The amplifier block represents the K-factor for setting the loop gain, which may also be used to adjust the bandwidth. The radial actuator is mechanically modelled as a double-integrator, and the current-control model of its electrical behaviour (block 'motor') is shown in figure 5.2. A mathematical treatment and complete block-structure of the radial motor is provided in Appendix C. In this model, a limiter is included to represent the supply-rail voltage of the power amplifier, and L_{self} is an INF block of form

$$\frac{K}{1 + s\tau}$$

The feedback path represents the current-feedback used to combat the self-inductance effects of the coil at higher frequencies. It uses a zero to create

65
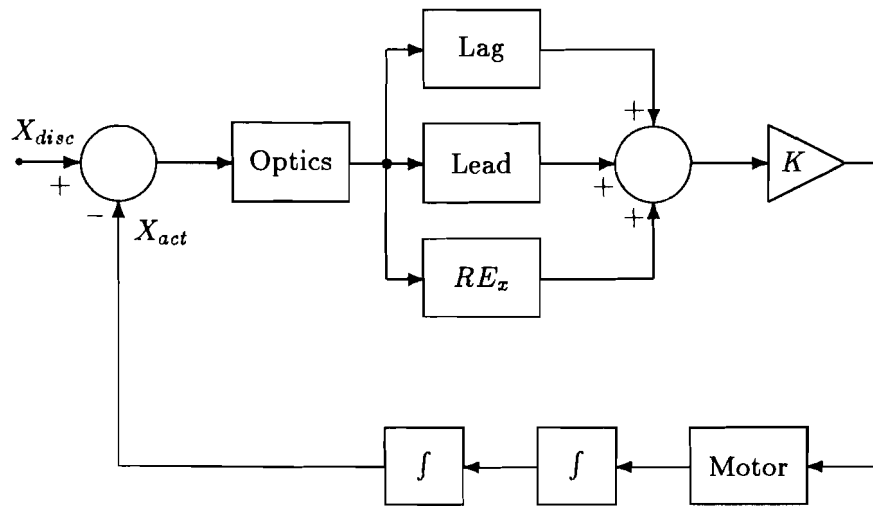
Figure 5.1: *PSI — Simplified block-diagram of radial-loop*
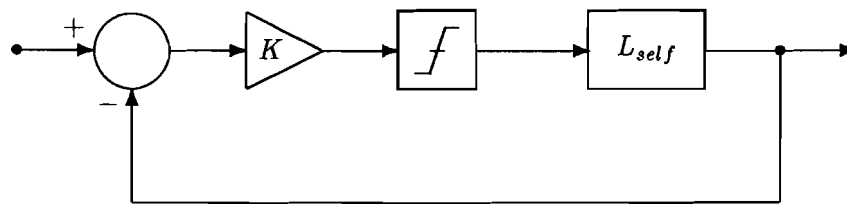
Figure 5.2: *PSI — Block-diagram showing simplified electrical model of the radial-motor*

an effective Q-factor 'hump' in the voltage-transfer characteristic, thereby cancelling the pole due to L_{self}.

The excitation to the system via X_{disc} (X_p in the plots) was produced by a simple second-order system, built using two integrators and gain blocks, enabling easy fixing of ω_n and β. The variable-height–constant-width pulse used to excite the resonance was produced by a BNG bang-bang block.

Figures 5.3 to 5.5 indicate the behaviour of the system for various different amplitudes of simulated shocks. The diagrams use the notation XP in place of X_{disc}. The example showing the system's reaction to the same shock both with and without RE_x indicates the usefulness of a wider quasi-proportional capture-and-hold range surrounding the track. In the plot representing the *old* strategy, the shock results in re-capture of the *neighbour* track, whereas RE_x successfully returns the arm to the *original*.

5.1.1 Increasing the bandwidth during the mirrored-slope of RE$_x$

Under normal circumstances, the maximum-allowable bandwidth BW_{max} of the radial control loop is limited to a value safely under the resonant frequencies of the dynamic system. This ensures sufficient gain and phase margins to guarantee stability. A low radial-bandwidth, however, means sluggish reaction of the controller in tracking fleeting movements of the arm after a shock. A higher bandwidth is desirable, but not permissible. It should be possible, however, to *temporarily* increase the bandwidth above the safe-limit, provided that this is done for only a short period of time in relation to the periodic-time corresponding to the resonant-frequencies. Under normal playing conditions, the controller only 'needs' the normal scope of RE_x, to absorb internal vibrations and follow eccentricity. The extended slope is only used in trackloss correction. It seemed logical, therefore, that increasing the bandwidth of the controller *only during the extended slope of* RE_x could effect a marked improvement in the system's reaction, without seriously compromising stability. Theoretically, the system would be temporarily unstable, but for such a short time-duration that it could not have any detrimental consequences.

In order to check the possible benefits of such an action, the possibility of bandwidth *doubling* to $2 \times BW_{max}$ was examined using the PSI simulation. Increasing the bandwidth simply involved switching between two different loop-gains, as indicated in figure 5.6. Figure 5.7 shows the difference between the behaviour of the system with and without bandwidth-doubling. The
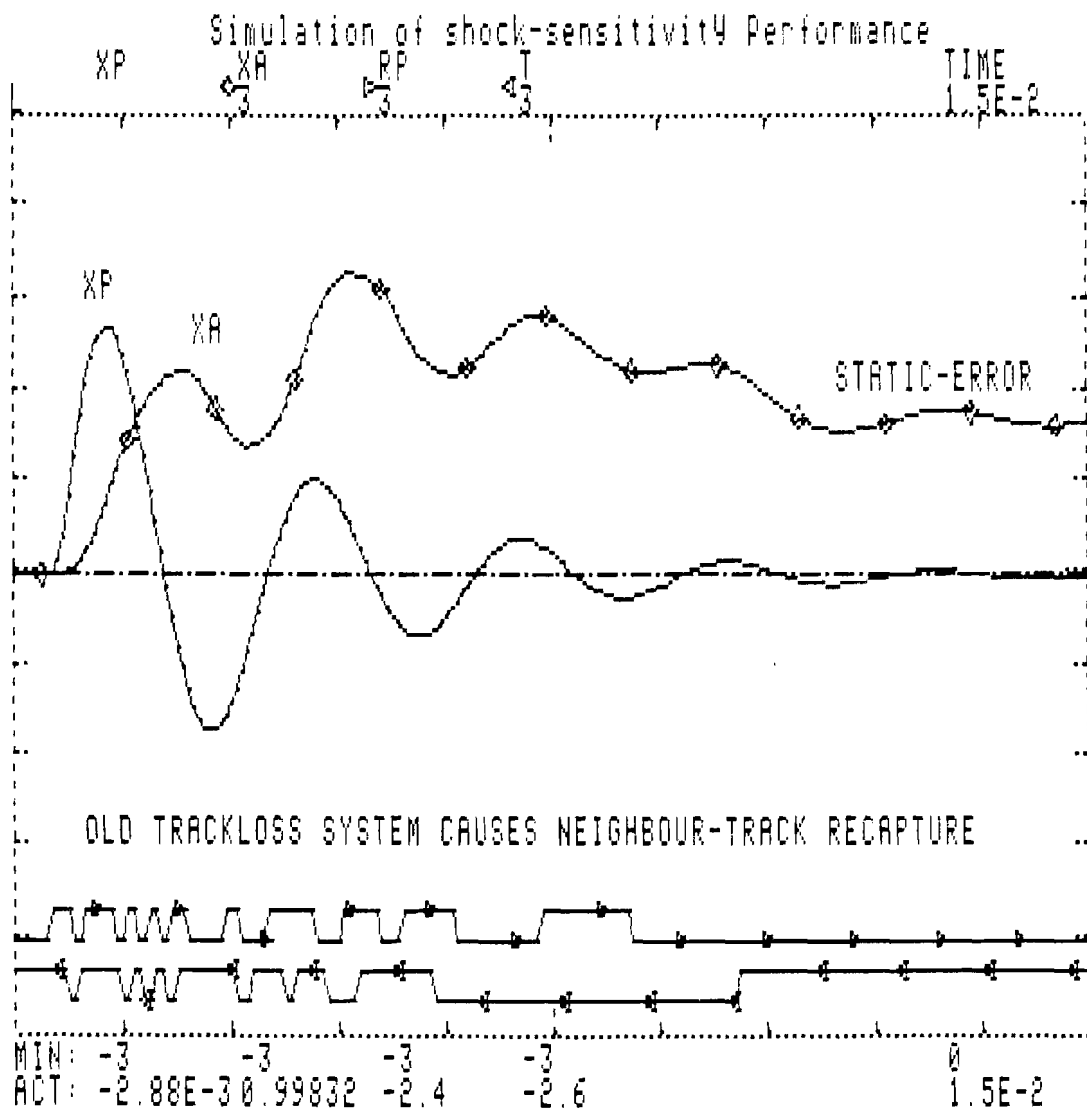
Figure 5.3: *PSI* — *Simulated behaviour* without RE_x-control (old system). The shock results in re-capture of the neighbour track, where RE is also zero. This is evidenced by the static-error between X_p and X_a, which does not reduce to zero.
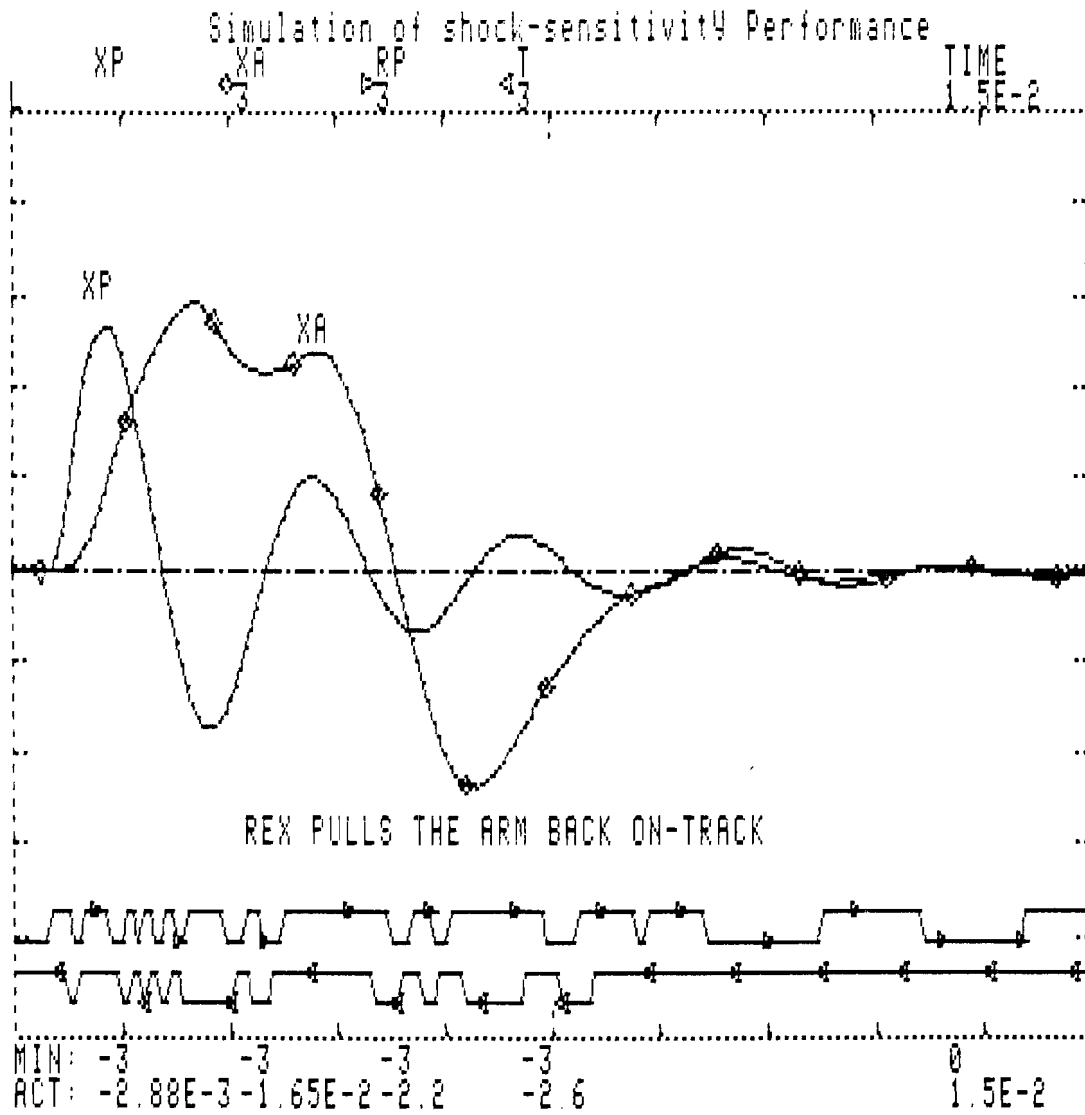
Figure 5.4: *PSI — Simulated behaviour with RE_x-control, for the same applied shock as in figure 5.3. The arm is successfully returned to the original track.*

69

Simulation of shock-sensitivity Performance

XP   XA   REX   TIME
MAX: 1   0 1   0 3   5E-3

XA

XP

REX

MIN: -1   -1   -3   0
ACT: -1.37E-2 0.14364 -0.83511   5E-3
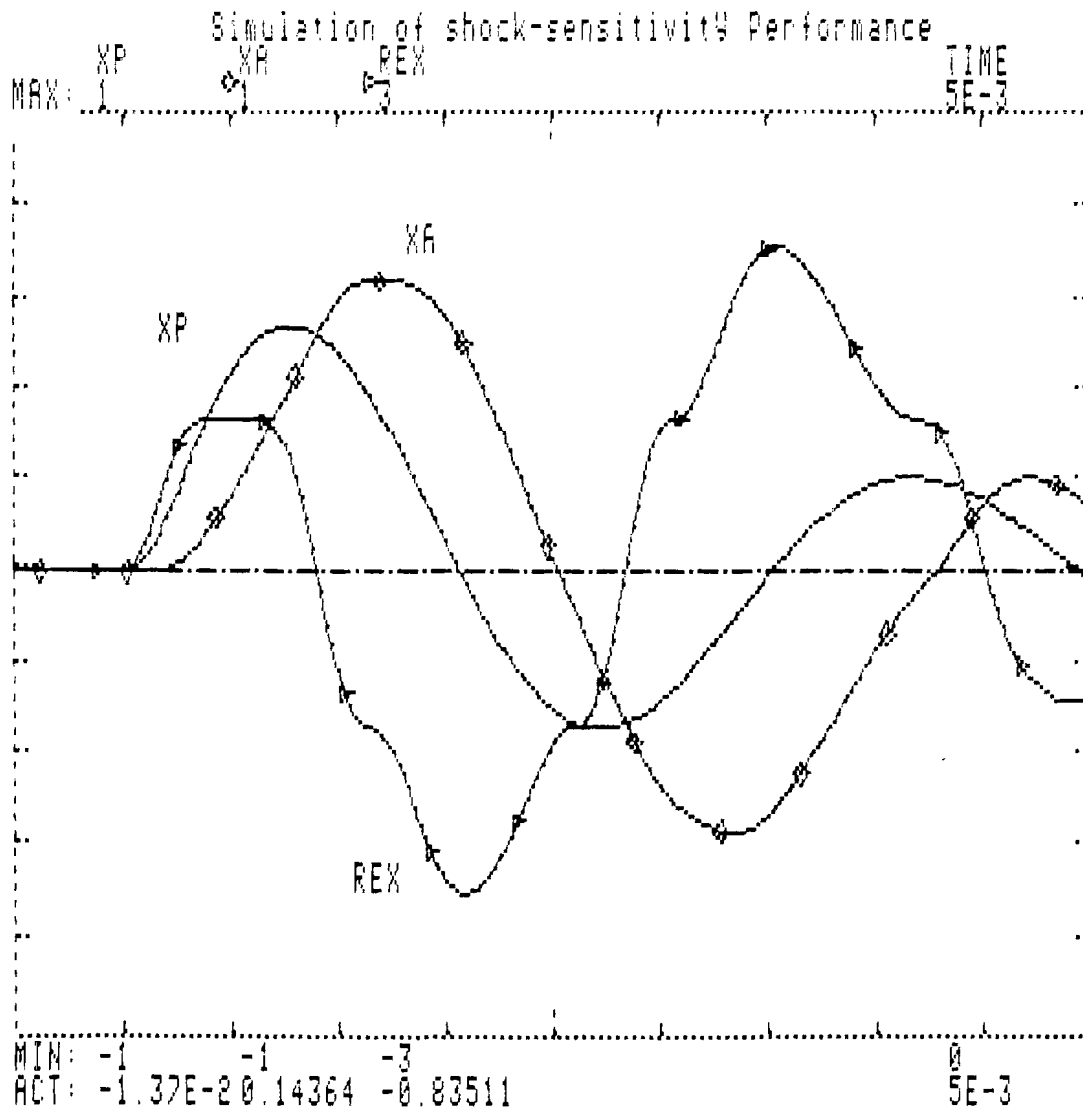
Figure 5.5: *PSI* — *Simulated behaviour under RE_x-control. The need for the extended scope of RE_x is quite evident. The resonant movement of the disc causes some swinging of the arm, but it remains within the capture-and-hold range*

70

differences suggest that it could be worthwhile to implement the idea in the practical circuit.
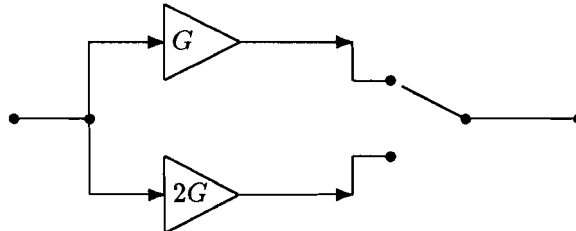
Figure 5.6: *Block-diagram of circuit to allow bandwidth-doubling during the extended scope of RE_x*

5.1.2 Increasing the power-stage supply-rail voltage during the mirrored-slope of RE$_x$

One of the inherent quantities associated with any *CDM* mechanism is the self-inductance of the coil used in the radial-positioning actuator. This impedes rapid changes in the current-flow through the coil, and therefore represents a limitation to system performance. This would not be a problem if higher voltages were available for producing the current, but the limited 12V supply (14.5V max) available in the car does pose a restriction. The inclusion of a switch-mode power supply with a car CD player would solve this problem, but it would not be possible to fit it into the standard DIN [1] enclosure. A possible alternative is the use of a *bootstrapped* power-stage for the radial actuator drive. Bootstrapping involves the use of a charged-up capacitor which can be called upon to effectively double the power-rail voltage for short periods of time. This temporarily-increased V_{cc} would make it easier to change the current flowing in the coil, and hence reduce the electrical 'inertia' of the actuator.

---

[1] DIN stands for *Deutscher Industrie Normen*, or German Industrial Standards. The physical size of components for integration into a standard dashboard enclosure must conform to DIN 75500.

Effect of temporarily-increased Bandwidth

XP   XA   TIME
MAX: 3   3   1E-2

XP

XA

MIN: -3   -3   0
ACT: 0.10304 0.17027   1E-2
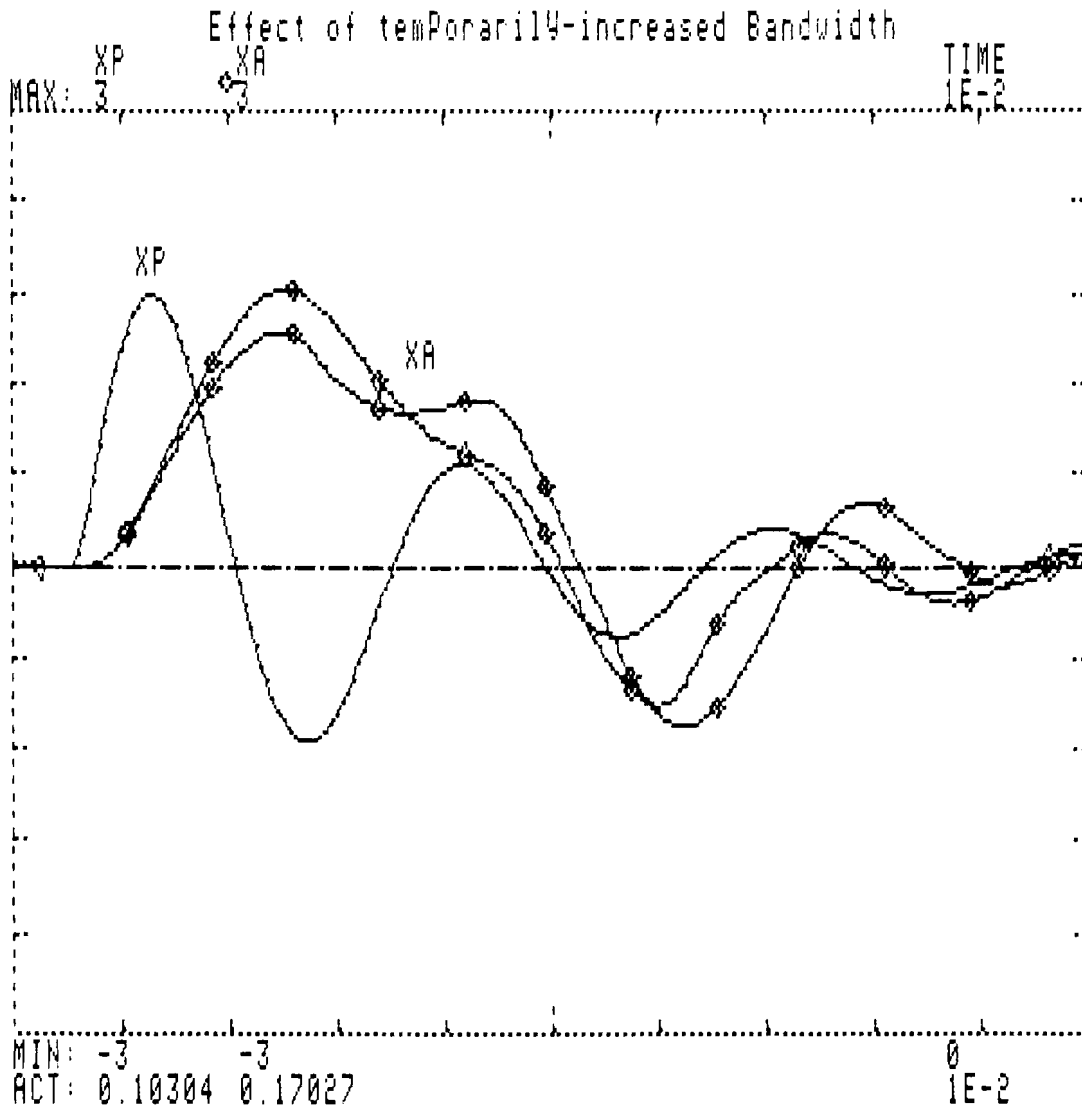
Figure 5.7: *PSI* — *Effect of temporary bandwidth-doubling upon shock-sensitivity. The two curves marked by XA show the differences between the actuator's reaction both with and without the improvement.*

Figure 5.8 shows how this is simulated using selectable limiters in the motor model, and figure 5.9 shows the effect upon system performance. The
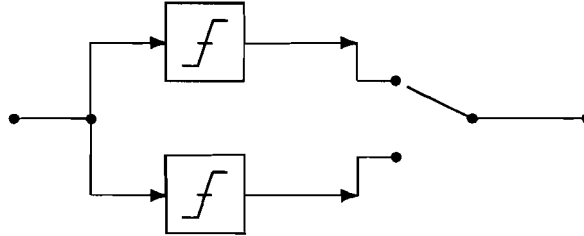
Figure 5.8: *Block-diagram of simulated power-stage bootstrapping, active during the* $\frac{\delta}{4} < |x| < \frac{3\delta}{4}$ *slope of* RE_x.

improvements are quite noticeable, and would suggest that implementation of this idea might also be worthwhile in practice. The main limitation on a practical realisation would be the size of the capacitors used — the bigger they are, the longer the increased voltage can be sustained. A value of at least several tens of μF would be necessary in practice, which represents quite a large physical item to integrate into a portable or CAR player.

5.2 System behaviour when the radial error is $> 3\delta/4$

Having analysed the system's ability to hold the original track, and the benefits inherent to the use of RE_x, a simulation of the *off-track* behaviour was carried out. This enabled, for example, an evaluation of the relative merits and de-merits of both the *SDA* and time-measurement damping methods. For this purpose, the simpilifed block-diagram indicated in figure 5.1 on page 66 was only slightly modified, and several *extra* peripheral functions were added. As it was desired to check the *feasibility* of the strategy and evaluate its performance, and not to determine the merits and de-merits of a particular *means* of implementation, it was chosen to simulate each of the functions by the simplest means possible, rather than by a direct simulation of any possible real-life physical circuit or method.

Effect of bootstraPPed radial Power-stage

XP   XA   TIME
MAX: 3   3   1E-2

XP

XA

MIN: -3   -3   0
ACT: 0.10304 0.10446   1E-2
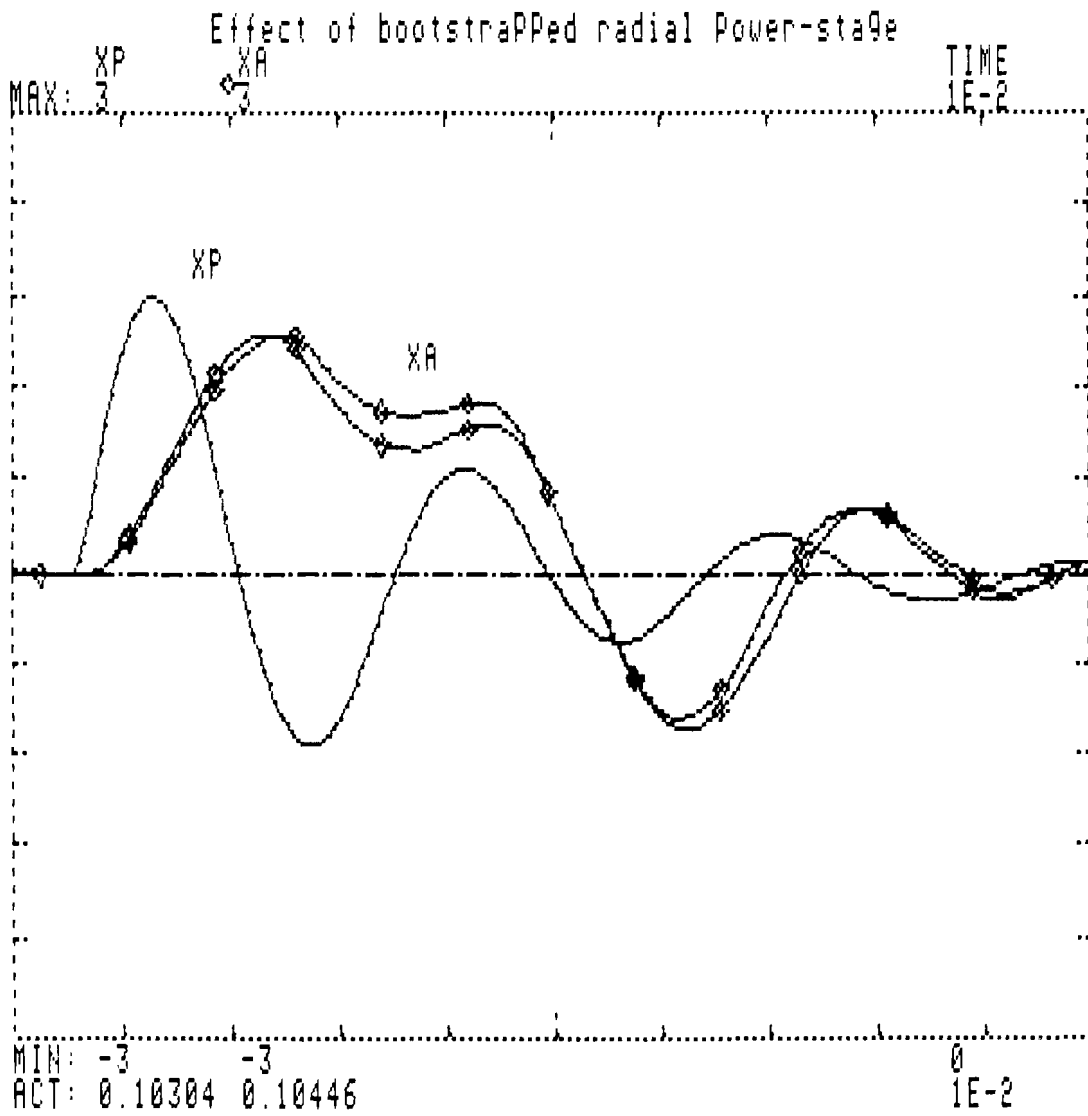
Figure 5.9:   PSI — Effect of power-stage bootstrapping upon
shock-sensitivity. The two curves marked by XA show the differences be-
tween the actuator's reaction both with and without the improvement.

5.2.1 The quarter-track counter

In the simulation model, the push-pull process is not modelled, and the error signals have to be given their sinusoidal form using SIN blocks operating upon 'linear' inputs. The position of the arm X_{act} is therefore directly available in proportional form at the input of the RE block. This is indicated in the main block-diagram, with the relative-error appearing at the output of the subtractor before the *optics* block. To determine this error quantised to $\frac{\delta}{4}$ accuracy (i.e. create an effective *quarter*-track counter), a PSI *FIX* block can be used as a value-quantiser. This is indicated in figure 5.10.
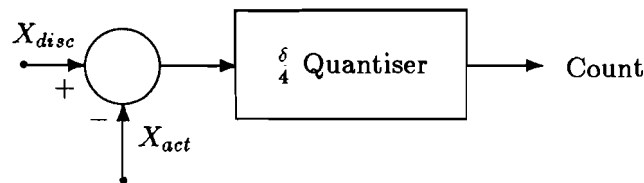
Figure 5.10: *PSI — Radial positional-error quantiser simulates track-counter*

5.2.2 Simulating damping

The simulation of the SDA action is very simple, as it only involves multiplying of the LEAD signal by ± 1 depending upon the logic level of TL. Damping via the time-measurement calculations is slightly more involved, however. It too was simulated in the easiest practical way, and then sampled to provide information at discrete intervals. Figure 5.11 indicates the basic idea.

It was desired to determine the *relative*-velocity between the light-spot and the track, which involves a simple subtraction of the individual absolute velocities. The velocity of the arm $\dot{X}_{act}$ is already 'available' in the model as the output of the first integrator representing the mechanical behaviour of the actuator. The velocity of the disc $\dot{X}_{disc}$ is calculated by differentiating the position value X_{disc}. $\dot{X}_{act}$ is then subtracted from this, and relative-velocity information results. This, however, represents a continuously variable signal, whereas velocity information calculated on the basis
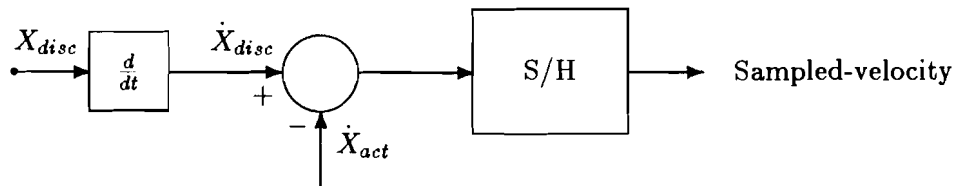
Figure 5.11: *PSI* — *Radial relative-velocity sampler simulates 'digital' damping*

of time/distance measurements would only be available at discrete position (and hence time) points. For this reason, the velocity signal was fed to a sample-and-hold circuit, with momentary sampling occurring at each change of the value of the quarter-track counter. This accurately simulates the real-life system, with the advantage that it allows direct evaluation of the limitations of discrete-time/position velocity information (the continuous signal before the sampler can be easily compared with the discrete output).

The simulation helped to give a first impression of the behaviour of the system after a 'heavy' shock. In the plots shown in figures 5.12 to 5.14, the signal X_p represents the movement X_{disc} of the disc after a shock. This was simulated as an exponentially-decaying sinusoid, whereby initial sweeping displacements of the disc decay to effectively leave it in its original rest position. Coupled with the slow reaction of the arm (resulting from a low radial bandwidth), this results in initial rapidly-changing relative movements between the arm and disc, which decay to leave a simple static-error. The *SDA* and digital damping systems should behave quite differently under these initial post-shock conditions. The continuous nature of the *SDA* system, though comparatively slow, can at least track the relative movements in real-time. The digital damping, on the other hand, though providing an effective higher bandwidth, suffers from the fact that it is a *discrete-position/time* system. In the moments directly after a shock, this could have negative consequences, as it implies working 'blindly' between the sampling instants, and therefore an inability to keep track of changes as easily as a
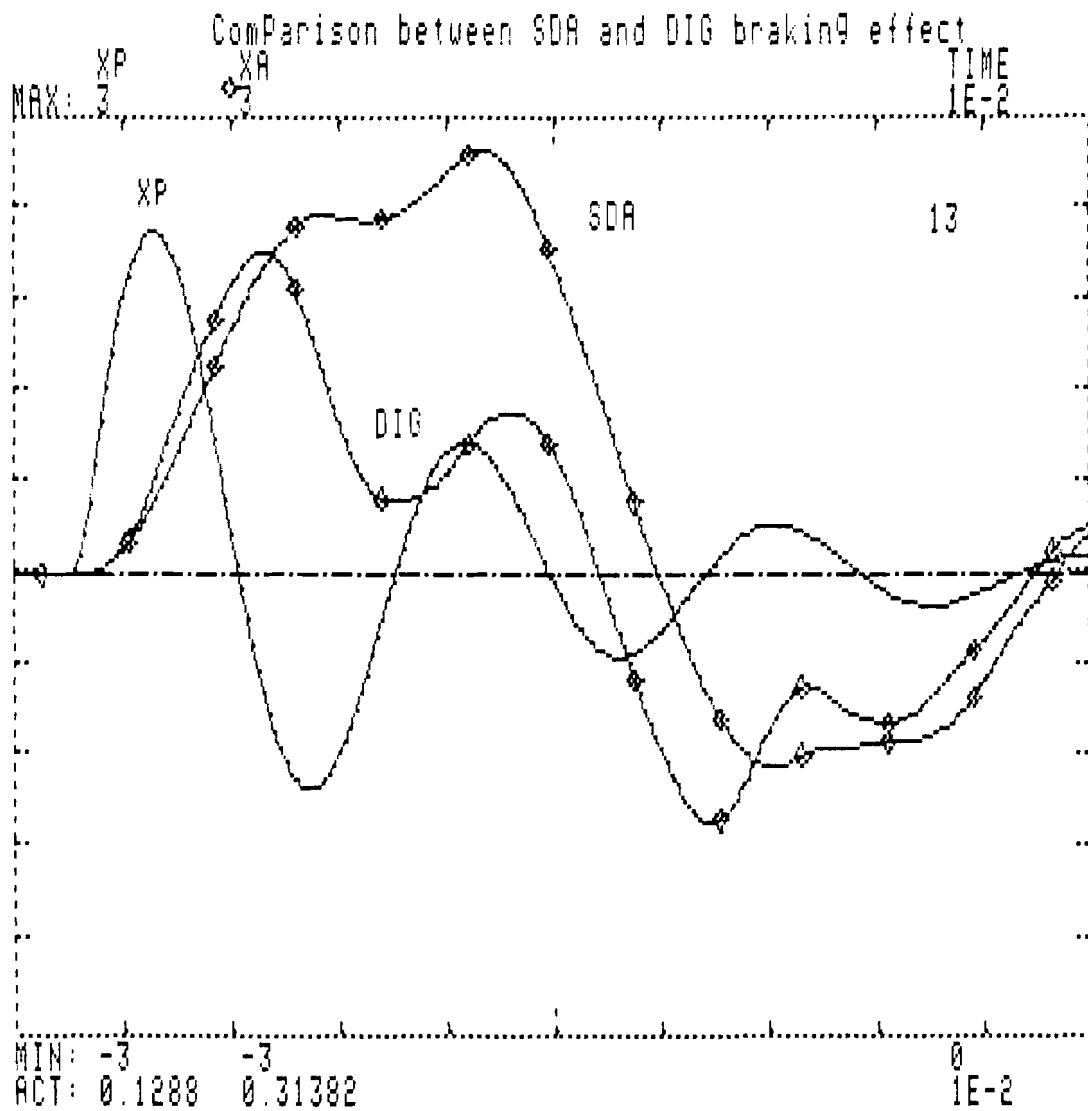
Figure 5.12: *PSI* — *Simulated behaviour outside* 3δ/4 - *Example 1*
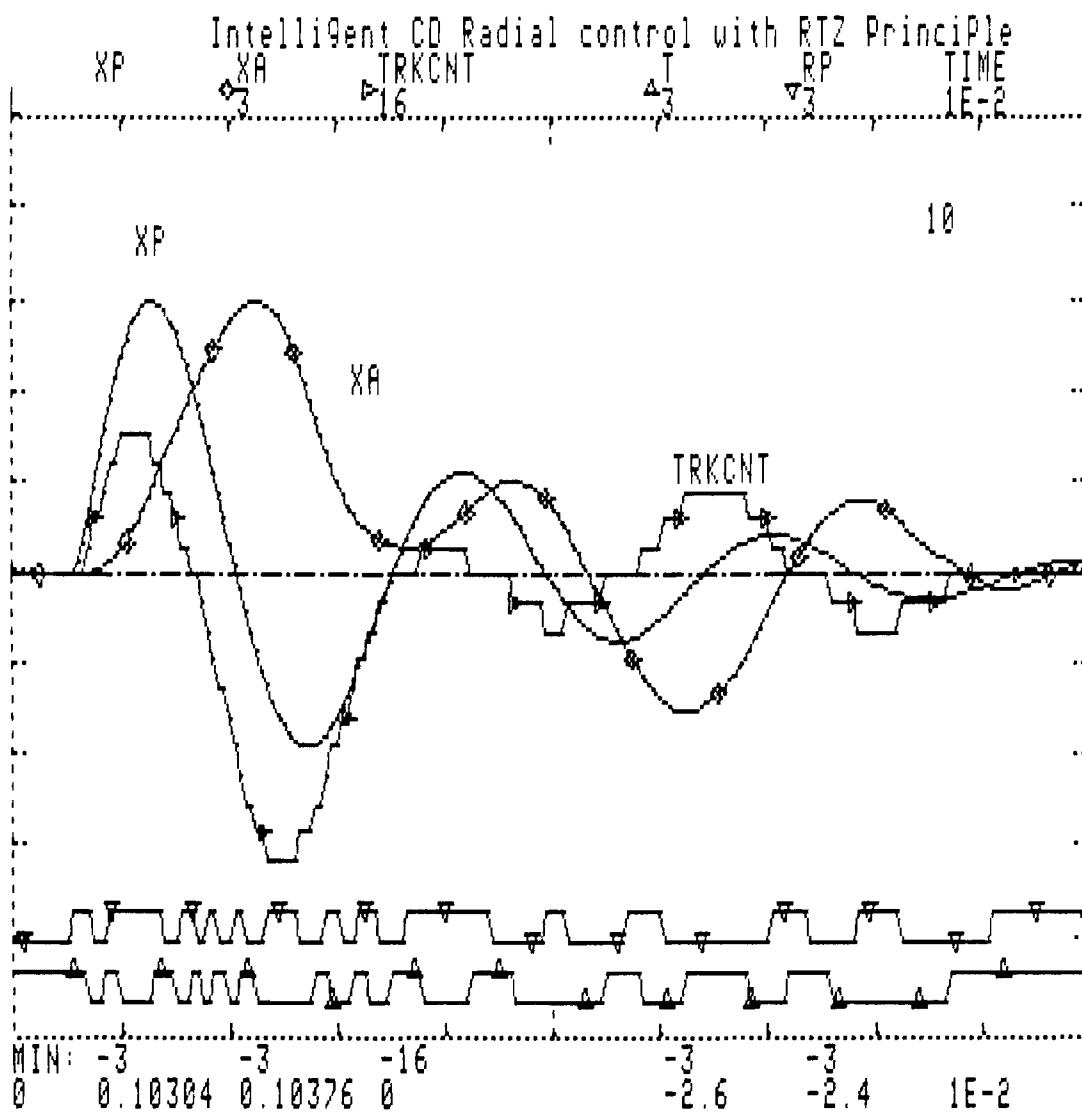
Figure 5.13: *PSI — Simulated behaviour outside 3δ/4 - Example 2*
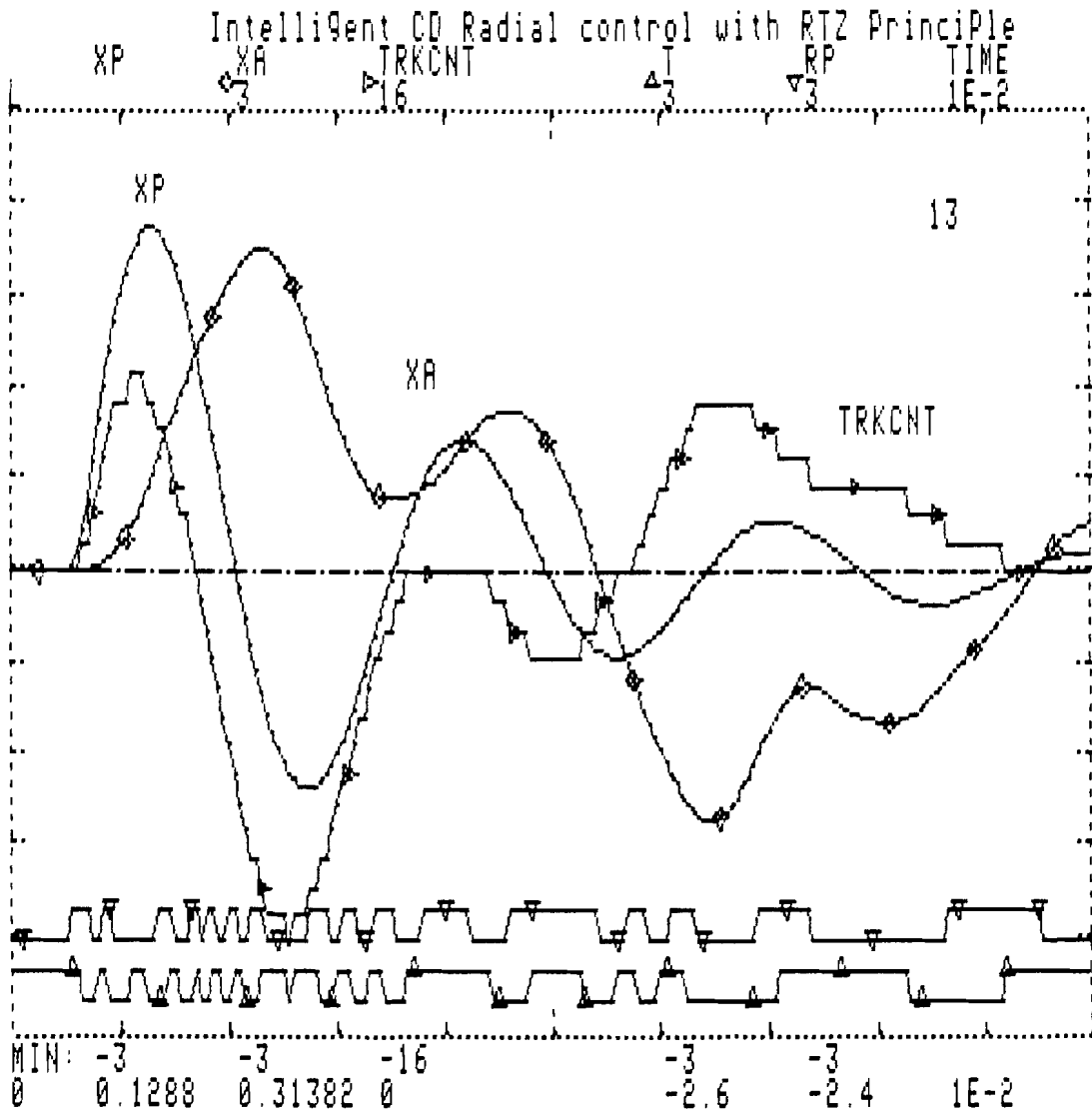
Figure 5.14: *PSI — Simulated behaviour outside 3δ/4 - Example 3*

continuous system. The plots indicate the essential differences in speed between both principles, the greater braking effect of the DAC current being clearly evident.

Based upon the indications provided by the simulation, it was decided that a *hybrid* between the *SDA* and DIG damping would probably provide the best results. The implemented strategy is as follows —

- Initially, the d.c. content of the RE_x signal is used as a *steering* signal to return the arm to the track. The *SDA* principle is used to *brake* the motion of the arm.

- If this is ineffective (high initial-velocity), as soon as the positional error reaches 32 quarter-tracks [2] (8 tracks), the μp switches on the DAC current to hasten the braking process. Based upon the calculated velocity, the μp can regulate the supplementary action appropriately.

- As soon as the arm has 'turned around' and begins to move back towards the track, the velocity signal *SDA* changes polarity ($\dot{x}$ changes sign). RE_x is still used as a steering signal, but *SDA* now creates an effective velocity-loop, and regulates the speed of the arm to a constant value. As on the outward journey, the DAC current is also used to hasten the process while/if the track-counter value is greater than 32.

- When the decrementing track-count reaches 3, the extended slope of RE_x is used to guide the arm to centre-track, and then the sample/hold switch S_1 (figure 4.7, page 55) is permanently closed to remove the mirroring-offset. The read-out process may now recommence, and the trackloss routine can go back to wait for the next interrupt.

Some of the example plots also indicate a signal $TRKCNT$, representing the $\delta/4$-quantised track counter. The fact that this reduces to zero indicates that the return-to-original-track strategy is indeed successfully implemented.

5.2.3 Frequency-dependance of SDA action

The *SDA* principle, shown in figure 4.6 on page 53, has one severe disadvantage — it is frequency-limited due to the use of a non-ideal differentiator, which means that it will not function properly for high arm-velocities. This stems from the fact that the +1 slope of the differentiator does not continue

---

[2]This value is purely empirical, and has been chosen from experimental results

to infinite-frequency because of the presence of higher system poles. There-fore, the +90 deg phase-shift provided by the differential action decreases as a function of frequency. Figure 5.15 indicates the form of the bode-plot (amplitude and phase) for such a non-ideal differentiator. The SUM signal, on the other hand, represents a 'genuine' cosine function, meaning that it (and thus TL) does *not* shift accordingly with frequency. TL was chosen to provide the $\times \pm 1$ multiplication on the LEAD signal because it had the same phase as the differential signal with respect to RE. Because of the phase-shifting, however, this will not be the case at high frequencies, and the switching will occur at the wrong timing instants. This means that more and more negative damping will be created. The main consequence hereof is that, if the arm leaves the track with an initially-high velocity, then the SDA signal, having lost much of its 'rectification', will have a reduced av-erage braking-power. The main braking action must then come from the LAG network, which takes time to charge up, so that large positional-errors can build up before the arm can be reversed towards the direction of the original track.

In this application, the usefulness of the SDA signal becomes question-able above frequencies of about 2KHz. Figures 5.16 and 5.17 show the effect of the $\times \pm 1$ switching at both 200Hz and 2KHz. At the lower frequency, the inversion occurs neatly, but at the higher frequency it is obviously less than ideal. Figure 5.18 shows the effect when the arm accelerates over the tracks — at lower velocities the signal is largely unipolar, but as velocity increases, it becomes more and more bipolar, with a resultant shifting of the average value of the signal towards zero. This may be directly compared with the photograph shown in figure 5.19, which shows the behaviour of a CD player implementing the new trackloss correction strategy. The similar-ities show a clear link between the simulation and the reality in the player.
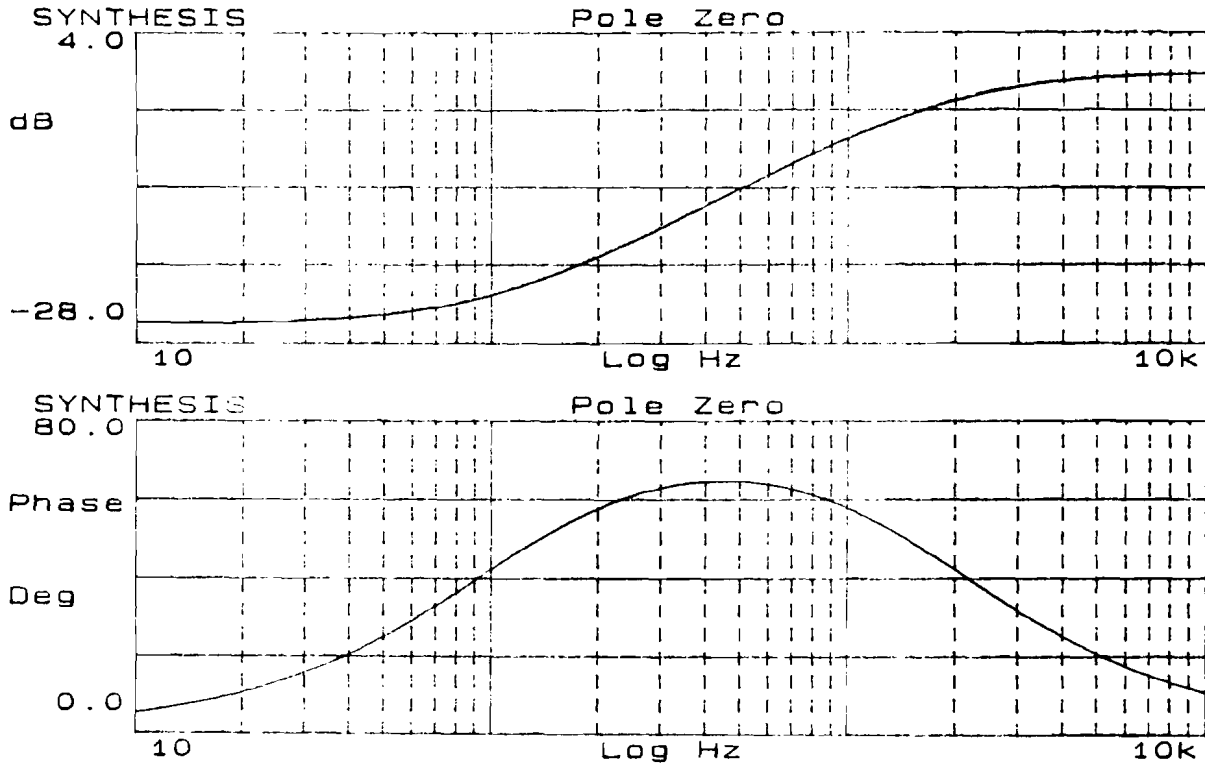
Figure 5.15: *Frequency-dependance of* SDA — *Bode plot of non-ideal differentiator, indicating the loss of the $\frac{\pi}{2}$ phase-shift at higher frequencies*
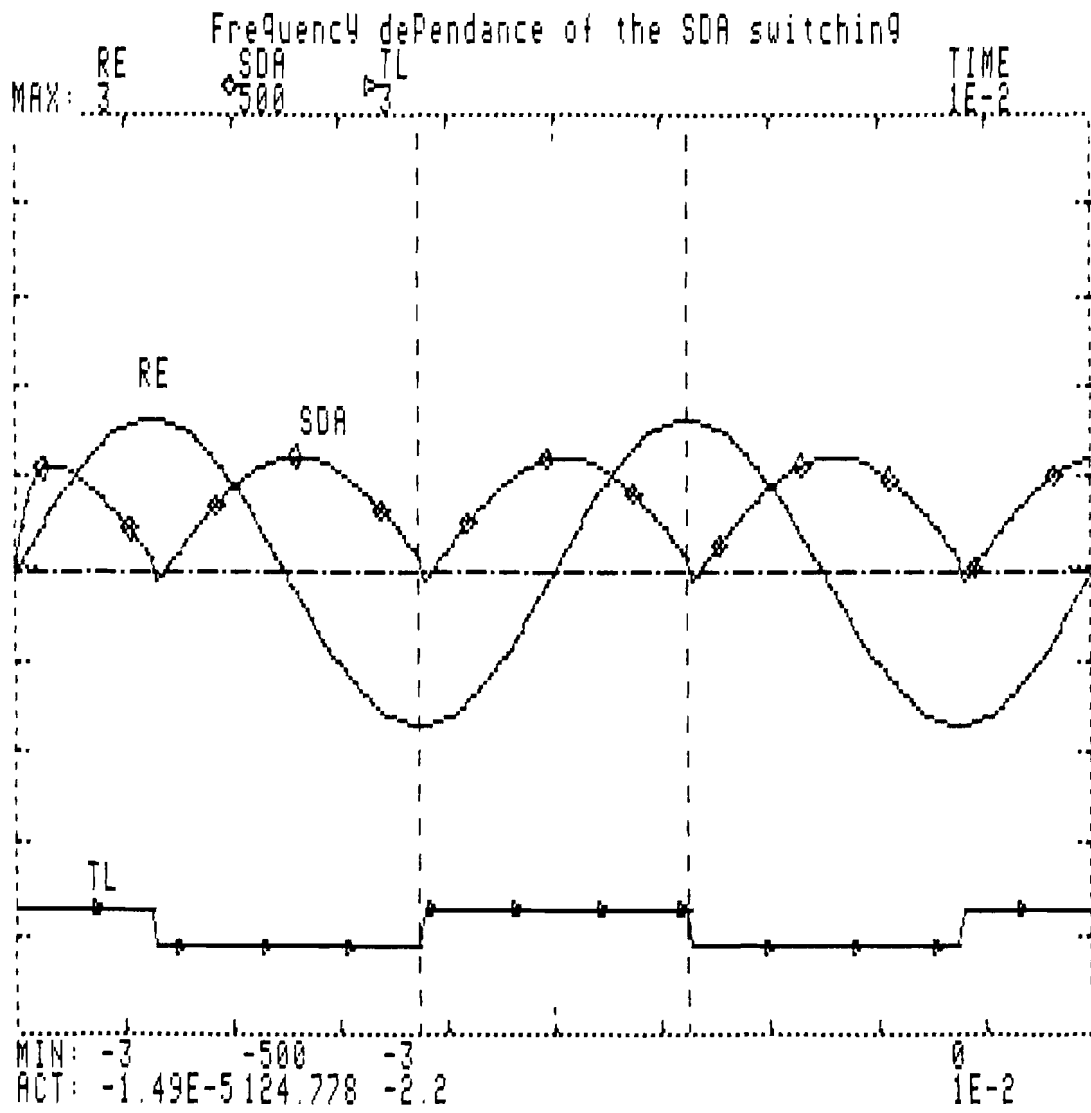
Figure 5.16: *Frequency-dependance of* SDA — *Simulation at* 200Hz
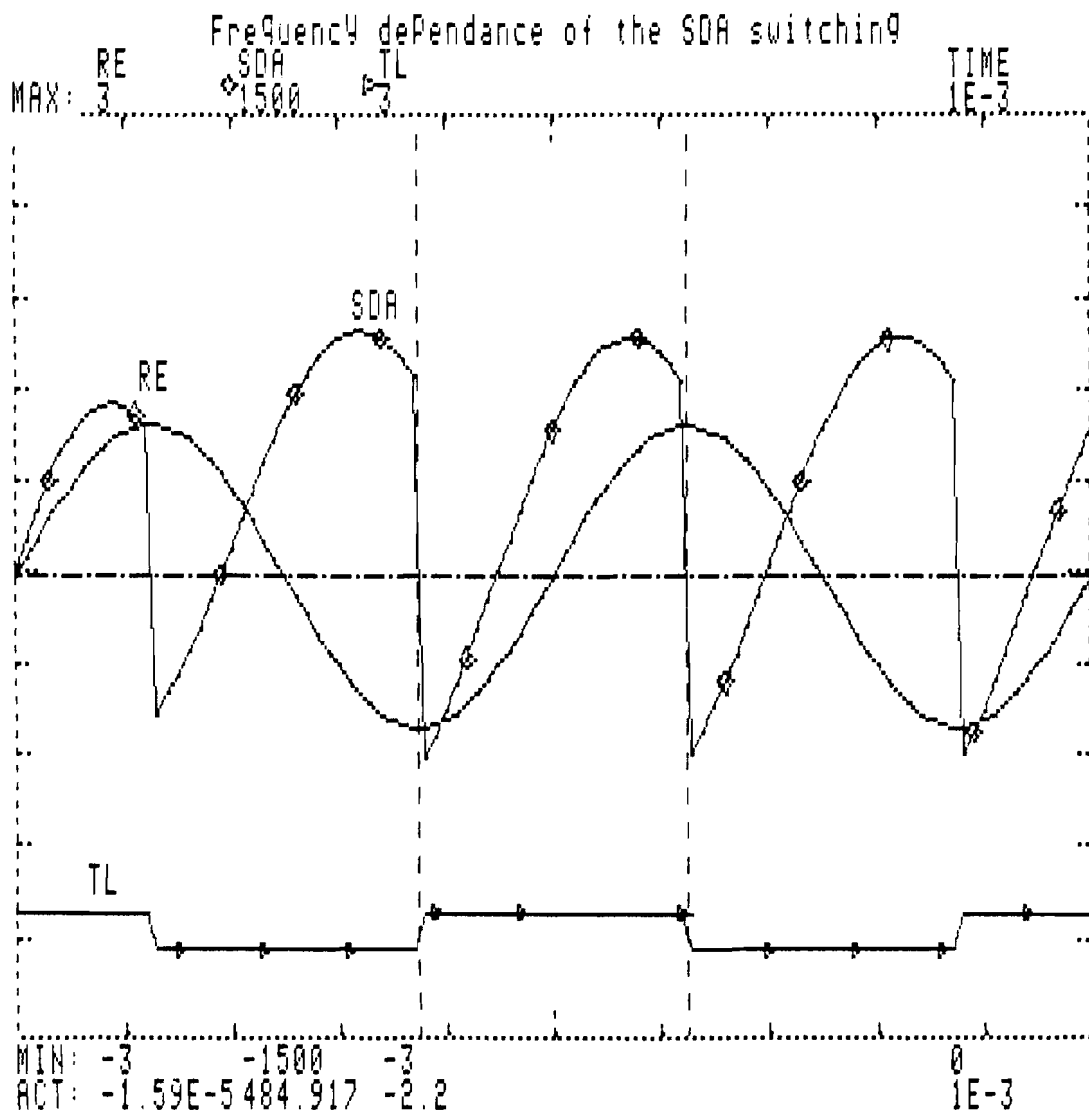
Figure 5.17: *Frequency-dependance of* SDA — *Simulation at 2KHz*
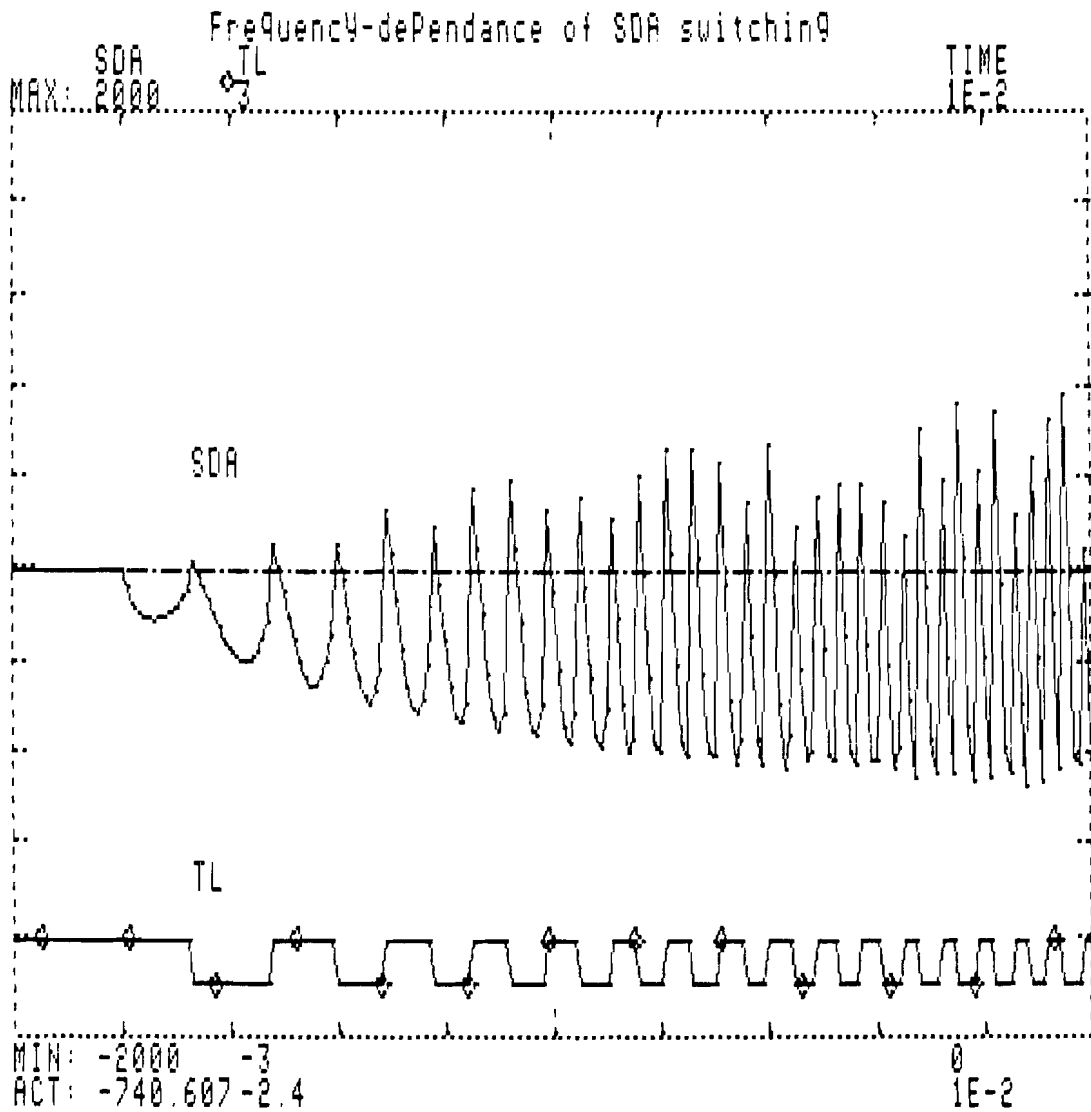
Figure 5.18: *Frequency-dependance of* SDA — *Example shows the case of constant-acceleration of the arm across the disc. This causes an effective frequency-sweep, showing performance deterioration of the* SDA *signal as a function of velocity.*
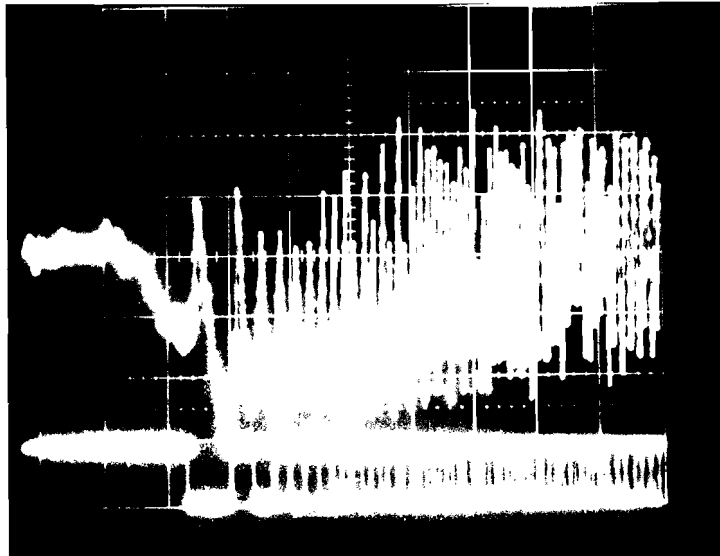
Figure 5.19: *Frequency-dependance of SDA* — *Acceleration of the arm over the tracks. This is a photo showing the real behaviour of a CD player with the new trackloss system implemented. The top signal is the SDA, and the bottom one is TL. The shortening periodic-time of TL indicates the acceleration, and the shifting of the average level of the SDA signal towards zero is clearly visible. This may be directly compared with the simulated situation shown in figure 5.18.*

Chapter 6

Definitive implementation, results and conclusions

The *RTZ* strategy proposed as the optimal means of trackloss correction was, in fact, implemented *twice* during the course of development. The initial implementation was used as a basis for experimentation and verification of feasibility of the idea. For this reason, it was based upon the discrete servo electronics of the CD204 player, where the lack of integration assures accessibility of all relevant signals. When the experiments had been verified, a second implementation based upon the current generation of integrated servo electronics (TDA8808 and TDA8809) was initiated. This represented a prototype form of the DC070 car CD player, which will be introduced on the market at a future date. This was based extensively upon the existing DC085 design, but the servo μp was replaced by the 8051, and the TDA8808 and TDA8809 were used in place of the earlier TDA5708 and TDA5709 designs. The second implementation therefore differed quite extensively from both the first experimental setup and existing player designs. Table 6.1 summarizes the essential differences and features.

The meaning of the various differences is explained in the following list. In the terminology, player 'A' refers to the first experimental implementation, while 'B' refers to the DC070 prototype.

6.1 Configuration

- The CD204 player uses the 'first' generation of servo electronics, which are implemented in discrete form. The DC085 uses the second gen-

87

CD204	DC085	Experimental setup	DC070 prototype
Discrete servo	TDA5708/9	Discrete servo	TDA8808/9
CDM1	CDM3	CDM1/CDM3	CDM3
8400 μp	47C400 μp	8051 μp	8051 μp
		RPDIP in hardware	Software only
		De-spiking hardware	Zig-zag sampling
		RE_x	RE_x
		Loop opened by RCO	Loop always closed
		Digital damping only	Digital + SDA
			CRI switching
			C_{lag} short-circuiting

Table 6.1: *Differences between the various different servo-implemetations explained*

eration custom CD servo IC's TDA5708 and TDA5709. In the *RTZ* prototype, it was chosen to use the improved features of the newer TDA8808 and TDA8809 designs, which had just become available as engineering samples.

- The servo-μp used in both experimental players is the 8051. Player A had the additional possibility of a direct A/B comparison between the old and new trackloss correction systems. In order to implement the track-counter and direction-detection functions, player A used the RPDIP circuit (figure 4.11, page 60) driving the counter input and INT1 lines of the μp. With a reduction in hardware, but at the cost of software overhead, player B omitted the hardware, relying instead on sampling *RP* and *TL* and servicing the counter register after edge detection purely from within software routines.

- Player A used the de-spiking hardware shown in figure 4.9 (page 57) to clean up the *RP* and *TL* signals before they were processed by the RPDIP circuit. Player B performed the entire de-spiking task in software, the μp sampling *RP* and *TL* *alternately*, in a zig-zag fashion. As soon as an edge is detected on one of the signals, sampling is switched to await the next edge on the *other* signal, thereby ignoring the multiple transitions caused by noise. The assumption made here is that one signal is almost always maintains a stable level during any noise on the other. This is because most of the spikes

are caused by the zero-crossing of the relevant analog signal coupled with a comparator that does not have built-in hysteresis. Noise can, however, occur on both RP and TL simultaneously, and this is most likely to happen in the presence of a scratch at the read-out point. The zig-zagging can therefore result in incorrect edge-counting and direction-of-motion measurements. It also makes it impossible to detect a direction-reversal immediately after its occurrence — it will be detected two edges later instead of one — but the μp 'knows' this, and it is a simple housekeeping task to adjust the figure in the track-counter accordingly.

Resistance of the system to false-alarm trackloss indications caused by disc scratches was increased by requiring that the pulse-width of the *first* detected TL interrupt be at least $100\mu s$. The software-implemented system has the advantage that the pulse-width limiting threshold can be adapted to velocity conditions, thereby removing the timing delay for high arm-velocities. Compared to the hardware-assisted solution, it does cost additional software overhead, representing an additional sampling-frequency limitation for the system.

- A disappointing trait in player A was that, despite the greatly-increased track-capture range provided by the use of the RE_x signal, the arm almost always overshot the original track if the magnitude of its excursion was in any way significant. The origin of this was seen to lie in the low-frequency memory of the LAG network which serves as the integral action of the controller. During the journey back towards the correct track after a successful direction-reversal, the capacitor C_{lag} becomes charged up and assists in pushing the arm along. When the destination track is reached, the LAG network takes some time before it 'realises' this, and so it keeps pushing the arm, which can cause it to overshoot the track. A simple short-circuiting of C_{lag} when the quarter-from-original boundary has been reached alleviates this problem. The switch necessary to do this is inherently a part of the TDA8809 radial-error processor I.C.

Short-circuiting of C_{lag} after each direction-reversal of the arm (in the case of multiple direction-changes induced by constant vibration or repeated shocks) is also seen to improve system performance *outside* the track-capture range.

- Initial results from player A showed a marked ability to return ac-

89

curately to the original track, even in the presence of noise and disc scratches. The subjective effects were, however, somewhat disappointing, as the result of even a small excursion of the arm was often quite audible. The only possible explanation for this was that the decoder circuit was incorrectly handling the data spuriously read-in during the motion of the arm over the tracks. The arm moves relatively slowly compared to the 4M bits/s data rate resulting from the rotation of the disc, so the light-spot can actually read pieces of data from each track it passes over. Such random data bursts can cause the synchronising timer within the decoding chip to lose the synchronisation pattern, resulting in audible needle-shaped 'spikes' at the audio output of the player.

In normal user-initiated music-search track-jumping, this problem is also encountered. To solve it, the servo-μp switches the *counter-reset inhibit* CRI line of the decoder chip, allowing free-running of the synchronizing counter during track skips. When this action was taken during the trackloss routine (player B), a very marked subjective improvement in system performance resulted. This meant that the maximum excursion of the arm could amount to *several* tracks without *any* audible consequences for the music.

6.2 Test stimuli

In the test experiments, four different types of artificial mechanical stimuli were used —

1. The player was mounted on a shaker driven by random low-frequency noise, thereby simulating the vibrations encountered in the car environment.

2. The shaker can also be driven by a one-shot pulse, the amplitude and duration of which may be altered to vary the strength of the resulting shock. This is useful in simulating a single hard knock.

3. A one-shot pulse such as described above can be directly applied to a summing-point in the player's radial power-stage. This has the advantage that it is a purely 'electrical' shock, and does not excite a lot of the mechanical resonances of the mechanism. This eases interpretation of the results, and has the advantage that it is very repeatable.

4. The player can also be mounted on a so-called 'shock-table', consisting of a flat surface to which limited-swing shock-inducing hammers are fitted. The angle from which the hammer is allowed to fall determines the strength of the shock, and ensures a high degree of repeatability.

The best stimulus of all is that provided by an actual driving test under strictly-controlled conditions. Figures 3.3 and 3.4 (pages 24 and 25) were plotted using data gathered during such tests. During the driving, disturbances in the audio output are counted using the mute/spike counter described by [McGee], with the aid of a 1KHz-sinewave test-disc. The use of this in place of human judgement has the advantage that it allows measurements to be objective rather than subjective.

6.3 Measured results from the new system

Figures 6.1 to 6.4 show some oscilloscope photos of the typical behaviour of the prototype player. In all four cases, the stimulus used was of the direct-pulse-to-actuator type, discussed above under point (3). The bottom two digital signals are RP and TL, and the centre signal shows the pulse used in the excitation. The uppermost signal is RE_x in the first example, and SDA in the others.

The required action of the system can be summarised as follows —

> *The applied pulse causes the arm to start moving away from the track. The controller should attempt to brake this motion, keeping count of the number of quarter-tracks skipped over until the arm stops. It must detect the reversal of direction and adjust the 'bookkeeping' accordingly (set the counter in decrement mode). The arm must then be steered back to the correct track, in a controlled manner and without incurring overshoot, so that readout can re-commence as quickly as possible.*

The captions under the photographs describe the behaviour in each case.

6.4 Conclusions

Performance Summary As well as using the listed stimuli, the performance of the system was also evaluated using a rather more down-to-earth means — hitting the mechanical suspension directly with the blade of a
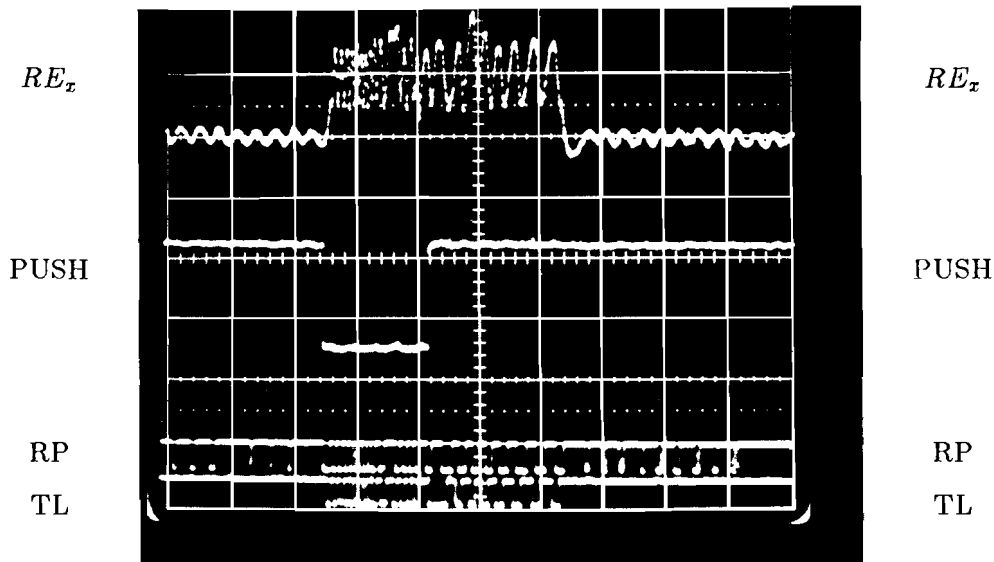
Figure 6.1: *The top signal shows the RE_x waveform, representing the proportional action of the controller. Before the shock, and after complete recovery, the small sinusoidal amplitude indicates the effect of the wobble at 600Hz. After the excitation pulse (centre) is applied, RE_x becomes active as a steering signal, attempting to guide the arm back to the on-track position. The sinusoidal nature, with the $2\hat{RE}$ DC offset, is clearly visible. The turn-around point of the arm is discernible in RP and TL, in the fifth division from left. It is evidenced by the occurrence of both a positive-going and consecutive negative-going edge on RP (upper) while TL (lower) remains low. After reversal, the arm is guided back to the correct track, and at $x = \frac{6}{4}$, the offset is removed again from RE_x. No overshoot whatever occurred, and normal re-tracking is evidenced by the wobble signal. The total excursion was about 7 tracks, or 28 quarter-tracks, the result being totally inaudible. The total off-track time is about 20ms, the time/division setting being 5ms/div.*

92
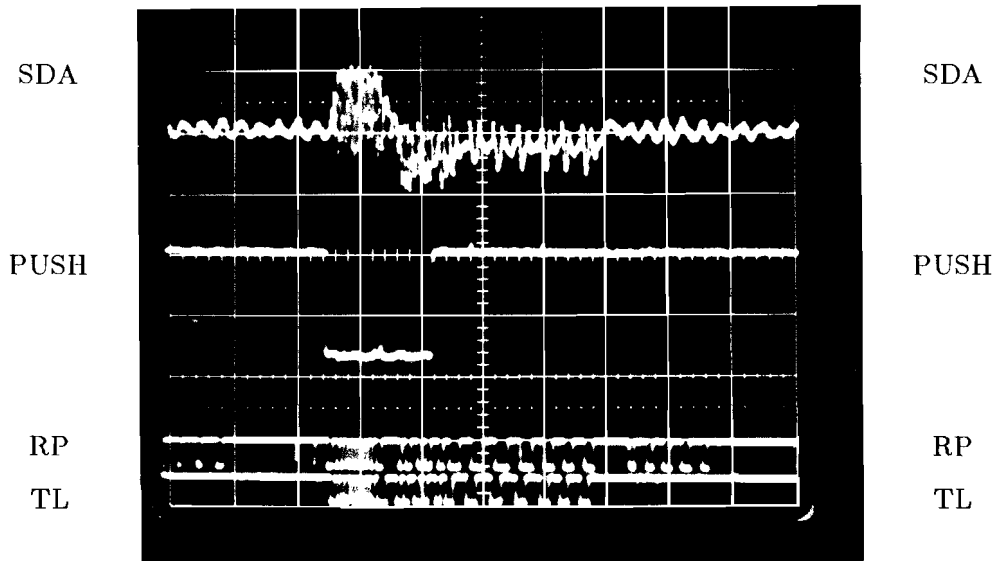
Figure 6.2: *Similar situation to that depicted in the previous figure, but indicating the SDA velocity signal instead of RE_x. At a point $3\frac{1}{2}$ divisions from the left of the scale, the polarity of the SDA signal inverts, the changing sign of the velocity thereby indicating the direction-reversal. After turn around, the RE_x signal (not shown here, but pictured in the previous figure) steers the arm back, and the SDA is now used to regulate the return-velocity to a constant value (velocity loop). After about $4\frac{1}{2}$ divisions, it is evident that the periodic-time of the signal has decreased to a constant, longer, value. This is also evidenced in RP and TL. Again, no overshoot of any form occurs, and this shock also had no audible consequences.*

SDA

PUSH

RP
TL

SDA

PUSH

RP
TL
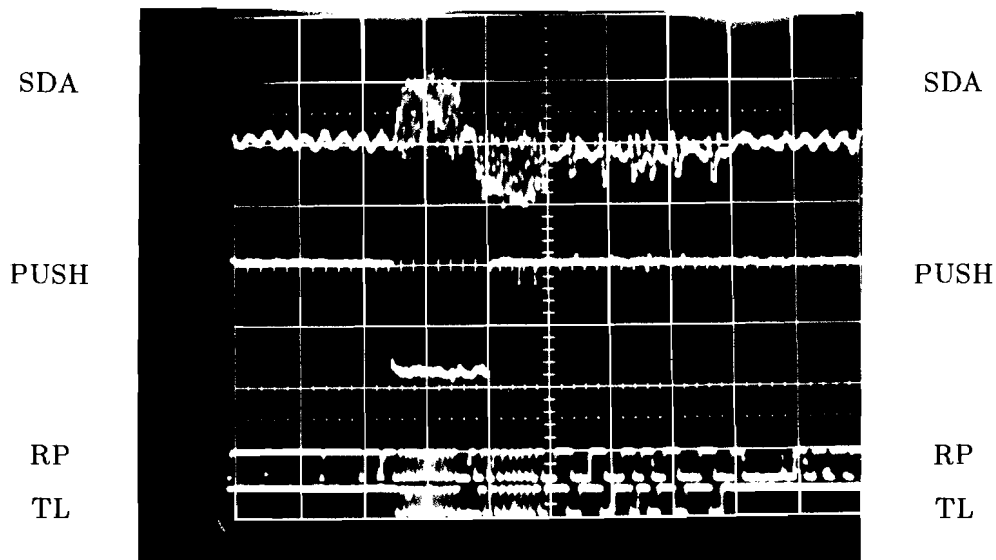
Figure 6.3: *This situation is exactly similar to example 2, and indicates the repeatability of the system's functioning. The same applied pulse-width was used, but the amplitude was increased slightly compared to the last case. The result is that the off-track time is some 5 ms longer. Increasing the width of the pulse has little effect, because once it lies above a certain threshold, the LAG capacitor has sufficient charge-up time to apply a counter-force against it. A comparison with the previous photograph verifies that turn-around took place somewhat later in this case, and therefore the maximum excursion is somewhat larger. Return to original track still occurred without overshoot, however, and the consequences of the trackloss were again imperceptible.*

SDA

PUSH

RP

TL

SDA

PUSH

RP

TL
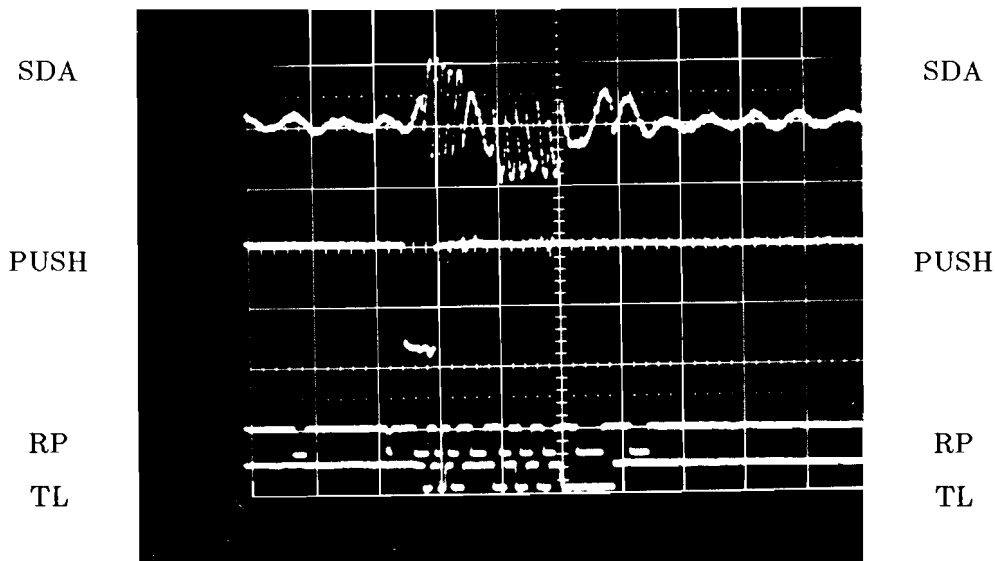
Figure 6.4: *This example shows the system reaction to a very small shock, and the time/div has been shortened to facilitate easier examination of the activity on RP and TL. The turn-around is clearly visible on the digital signals, and occurs 3.6 divisions from left. The arm also quite clearly overshoots the correct track by $\frac{5}{2}$, visible in the centre of the sixth division, but does return correctly. This behaviour was measured in the player before the lag short-circuiting explained in the text was implemented, and is indicative of the typical small overshoots encountered. Such small disturbance-pulses could be repeated in bursts with an almost alarming frequency without audible consequences. The total excursion represents approximately 5 tracks (20 quarter-tracks), and the 'absence' time is only several milliseconds.*

screwdriver. The results were very impressive indeed (compared to the older trackloss correction system), and *no* disturbances whatsoever were audible for excursions up to about $16 \times \frac{\delta}{4}$ in magnitude. Up to a limit of about $40 \times \frac{\delta}{4}$, the audibility depended upon the music material, and whether the μp made any incorrect decisions due to disc flaws/software bugs. In any case, the audible 'tick' resulting from an error was much less evident and disturbing than the rhythm-distortions produced by the workings of the original trackloss system. The following conclusions have been drawn —

- Use of the RE_x signal as a tracking-error signal in the region immediately adjacent to a track increases the track-hold capability of the system after a shock, and makes re-capture significantly easier in the RTZ system.

- The *coherent* nature of the strategy and its in-phase operation results in a large net braking effect, limiting the typical post-shock excursion of the arm compared to the older system.

- Assured return to the original track either greatly reduces or totally eliminates the audible effects of trackloss, provided that it occurs quickly and accurately. The data-loss due to the intermediate rotation of the disc is insignificant, and causes no perceivable disturbance in the audio. Switching of the CRI line to the decoder electronics greatly reduces the number of audible 'spikes' produced in the audio output.

- Position and direction information to quite a high degree of accuracy may be decoded from the periodicity of the error-signals. This is, however, sensitive to disc-flaws, and represents perhaps the most serious limitation to the performance of the system — reliability.

- Use of subcode information to return to the original track is indeed considerably inferior to the proposed method. Results from a competitor 'walkman' player implementing a subcode-based RTZ system show that up to *two seconds* can be necessary to return to track even after a light shock. The subjective effect of this is, in fact, just as irritating as a considerable rhythm-distortion.

- The repetition-rate of small-excursion tracklosses can be surprisingly high without any audible consequences.

As yet, the system has not been evaluated under actual driving conditions in a car. While the laboratory results look promising enough to predict

that the performance will be adequate, it is nevertheless wise not to make any sweeping predictions, and cautious optimism is to be advised. There is quite a fundamental difference between the type of stimulus generated by the 'electrical' means and the vibration produced in a car. The implementation for in-car use has been attempted with a minimum of hardware, and relying upon the TDA880x I.C.'s for most of the electronics. These i.c.'s have not been purposely designed with this application in mind, and have some inherent shortcomings. The most notable of these is perhaps the AGC circuit used on the HF audio signal. It's function is to keep the amplitude of the HF signal at a constant level for the PLL stage in the decoder electronics. In order to achieve good playability results, the bandwidth of the AGC has been chosen to effect masking of fingerprints on the disc. In this application, however, a much lower bandwidth is desired. If the arm moves away *slowly* from the track, the pinching-off of the HF signal is similar to that produced by a fingerprint, and the AGC increases the gain to null the effect. Because the TL signal is dependant upon the level of the HF signal, it may not be produced in such circumstances. The system can then behave in an unpredictable manner, and the μp can make an incorrect direction or counting decision because the offset correction can drift. It is as yet unknown if the vibration patterns in a car can excite this behaviour. Another severe restriction is that imposed by the DIN enclosure, the small size of which limits the amount of free physical headroom around the suspended CD mechanism. If vibration in a car results in the mechanism's coming in contact with its surroundings, then all the electronic trickery imaginable can do precious little to help the situation, and this represents an effective upper-limit on the performance of the system.

6.5 Possibilities for future development

The work presented in this thesis represents the conception and initial development phases of the project. Much work has yet to be done on refinements and improved *implementation*. As is the case with any project, many new ideas occur during the course of experimentation, and it is now possible to present a list of just some of the points to be considered for future developments.

- Perhaps most important is the issue of *reliability* of the system. Improvement in the software and/or the use of additional signal-processing hardware should reduce the likelihood of false-count or

97

direction-decision errors in the face of disc-imperfections.

- Shifting the pole of the differentiating network which produces the *SDA* action to a higher frequency should increase the high-velocity performance of the system. An additional integrator can be added to the loop at another point to keep it stable.

- The practical benefits of the power-stage bootstrapping and temporary bandwidth-hikes as simulated with *PSI* should be investigated to examine the real effects on system performance.

- The 'hybrid' between the DAC and *SDA* damping action can be better refined, and perhaps even be made *adaptive* to velocity conditions.

- The *μp* software must be extended to include the possibility of using subcode as an 'if all else fails' measure. Abnormally severe shocks (dropping a walkman player, for example) could cause such large-scale excursions of the arm that the ensuing velocity would lie above the limitations of the system performance. Loss of focus would be almost certain to occur in such a situation. Since the periodicity-based position determination cannot function under such circumstances, the only alternative is to use the subcode information.

- The application of the velocity-loops and extended track-capture range system to music-search routines should be investigated. It is theoretically possible to effect a substantial decrease in searching-time by such means.

- The degree of usefulness of the system in other members of the compact disc generic family must be investigated.

- A full study of the effects of the system upon *playability* has yet to be performed.

Most of these points, however, represent means of fine-tuning the performance of the system, and the progress to date has already laid the foundation in proving both the feasibility and desirability of the chosen solution.

Acknowledgements

The project work involved a period of approximately one year, from January 1986 to January 1987, with the involvement of the Technische Universiteit Eindhoven commencing in June 1986. In September 1986, the promising results of the work up to that point prompted the formation of a special project group, with the goal of speeding the project towards completion. Up to that point in time, the project had remained the sole work of the author. The formation of the team occurred shortly after work on the PSI simulation commenced, with the author reporting on the findings of the simulation results to the main group. Their task was to implement the new trackloss recovery system in a car CD player, and the time and effort invested by these people helped immensely in accelerating the pace of the project. The author wishes to express his sincere gratitude to all mentioned for their assistance, suggestions, and cooperation.

Bibliography

[PTR]   Philips Technical Review, Volume 40, 1982, No. 6.

[McGee]   McGee, P.J.L. 'An audio mute/spike counter for CD',
          Philips internal report nr. AR59-CD-1610, June 1986.

[PSI]   PSI Manual, Department of Electrical Engineering,
          Laboratory for Control Engineering,
          Delft University of Technology, May 1984

[ODS]   Bouwhuis et al., 'Principles of Optical Disc systems',
          Adam Hilger Ltd., 1985.

Glossary

CIRC The *cross-interleave reed-solomon* coding scheme used in encoding the digital data on a compact disc. Through the use of redundant bits, it makes possible the correction of data errors due to disc imperfections.

'Digital' damping Term referring to the means of velocity determination based upon measurement of the time between successive edges on RP and TL. Each edge marks the passing of a distance of one-quarter of the track-pitch, and the average-velocity is easily calculated from knowledge of the time taken to cover a fixed distance.

EFM The *eight-to-fourteen modulation* scheme used in creating the channel bits for CD. Groups of 8 bits are converted to groups of 14, with special restrictions on the number of consecutive zeros allowable. The net result is to create a high information packing-density on the disc.

FE The *focus error* signal, which is used by the focus servosystem to keep the laser spot correctly focused on the disc.

MUTE Term referring to a deliberately induced short-duration silence in the audio output. Muting is used to mask the 'ticks' and 'pops' which could otherwise be audible as a result of uncorrectable data errors.

Playability Term used to refer to the ability of a CD player to play a damaged disc without audible consequences.

PP The *push-pull* technique of radial error signal generation. It involves comparing the difference in light flux between the 0 and ± 1 diffracted orders in the light reflected back from the disc. In the case of CD, with a track pitch of $1.6\mu m$, this generates a sinusoidal RE signal with a period of one track pitch.

RE The *periodic* sinusoidal *radial error* signal generated by the push-pull technique and used by the radial servo system to maintain radial tracking.

RE$_x$ (Extended S-curve). A processed form of RE obtained by mirroring the sinusoid about its peak value. The result is to increase the usefulness of RE by a factor of three, which widens the capture-and-hold range in the immediate vicinity of a track.

RP A digitised version of the RE signal. Its polarity (high or low) at the moment of a trackloss signal can be used to indicate the direction of

radial movement of the arm. RP is also called RE_{dig}.

RCO The radial-control on/off line from the servo μp. It switches the two-pole *loop-switch* to select either RE or the DAC current as the controller of the radial arm.

RTZ Return-to-zero. In this context, it refers to the return-to-original-track strategy, which implies that the controller will always steer the scanning laser beam back to the track it was reading before the disturbance.

SDA Term referring to the *switched differential action* method of controlling the velocity of the radial actuator. Differentiation of the RE positional-error signal produces velocity information, but the resultant cosine function provides alternate positive and negative damping. Negative damping is effectively positive-feedback of velocity information, and must be avoided. The SDA principle involves a level-of-*TL*-dependant multiplication of the cosine term by ± 1, which provides an effective inversion of the signal during the periods of negative damping, thus creating a unipolar velocity signal.

SUM The sum of the four photodiode currents, from which the audio

HF signal is generated for decoding, and from which the trackloss signal can be derived. Optically, this is referred to as the *central aperture* signal, CA.

TL A digitised version of the SUM signal, which is at a logical high if the radial positional error x is such that $|x| < \frac{\delta}{4}$ and at a logical low if $\frac{\delta}{4} < |x| < \frac{3\delta}{4}$ A logic low on this signal indicates that the level of the HF signal is too low for decoding of the audio content, and also that the unstable control slope of RE has been reached.

Trackability Term used to refer to the ability of a CD player to correctly track a disc in the presence of external stimuli and/or disc flaws.

Wobble The 650 Hz sinusoidal signal which is deliberately injected into the radial control loop with the purpose of enabling offset correction and an AGC function to maintain a constant loop bandwidth.

Appendix A

Derivation of radial-velocity under SDA control

Proportional

$$
\begin{aligned}
PD &= RE \quad \text{if on-track} \\
\overline{PD} &= 2\hat{RE} \quad \text{if off-track} \\
\overline{H}_p &= 2
\end{aligned}
$$

Differential

$$
RC = \tau = \frac{1}{\omega_p}
$$
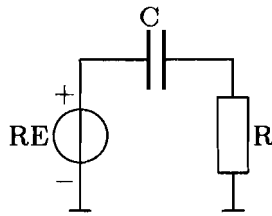
$$
\frac{U_{RE}}{U_R} = H_d(s) = \frac{\frac{s}{\omega_p}}{1 + \frac{s}{\omega_p}}
$$

Steady state

$$
H_D(\omega) = \frac{j\frac{\omega}{\omega_p}}{1 + j\frac{\omega}{\omega_p}}
$$

Imaginary part

$$H_{DI}(\omega) = \frac{\frac{\omega}{\omega_p}}{1 + (\frac{\omega}{\omega_p})^2}$$

The TL-dependant multiplication by ± 1 has the same effect as full-wave rectification of the differential action. The average value hereof is therefore

$$\sigma = 2 \int_0^\pi \sin x \, dx$$

$$= 2 \left[-\cos x \right] \begin{matrix} \pi \\ 0 \end{matrix}$$

$$= 4$$

$$\Rightarrow \quad Average = \frac{4}{2\pi} = \frac{2}{\pi}$$

The ratio between the gains of the proportional and differential parts is 1:10

$$\overline{H}_p = 10 \ \overline{H}_{DI}$$

Using the notation

$$x = \frac{\omega}{\omega_p}$$

The relationship becomes

$$2 = 10 \ \frac{2}{\pi} \ \frac{x}{1 + x^2}$$

Solving for the root x, we get

$$X_1 = 0.35$$
$$X_2 = 2.83$$

Since $x < 1$, the root X_1 is valid, and therefore

$$\frac{\omega}{\omega_p} = 0.35 = \frac{f}{f_p}$$

The variable f_p represents the corner-frequency of the pole which 'flattens' the +1 slope of the differentiator by cancelling its zero. In this application, $f_p \approx 2\text{KHz}$.

$$\Rightarrow \quad f \approx 750Hz \quad \rightarrow \quad T \approx 1.4 \ ms/track$$

Appendix B

Listing of the PSI model of the new radial controller

Block	Type	Input1	Input2	Input3	Par1	Par2	Par3
SAMPLE	ABS	IMPULSE			1		
$|OPTICS|$	ABS	OPTICS			1		
$|TRKCNT|$	ABS	TRKCNT			1		
ADIR	BLN	OPTICS	+1		2		
RCO	BLN	CAPTURE			1		
XOR	BLN	TL-DIG	RP-DIG		6		
SHOCK	BNG	TIME			0	2	5×10^{-4}
+1	CON				1		
−1	CON				−1		
0	CON				0		
2π	CON				2π		
3	CON				3		
FREQ	CON				10		
FULLPWR	CON				10		
NORMPWR	CON				−1		
REFTIME	CON				7.5×10^{-4}		
RPHI	CON				−2.2		
RPLO	CON				−2.4		
TLHI	CON				−2.6		
TLLO	CON				−2.8		
TCOUNT	DPY	MAXX			0.85	0.88	1
TRKCNT	FIX	OPTICS			4	0	1
$-RE$	GAI	RE			−1		
$-\Sigma$	GAI	Σ			−1		
D/DT2	GAI	D/DT1			1×10^{6}		
EXTRAK	GAI	PREGAIN			1		
GAINADJ	GAI	PREGAIN			1		
KMOTOR	GAI	MOTOR			583		
POSTGAIN	GAI	LSELF			5.25×10^{6}		
PREGAIN	GAI	LAGSUM			0.1155		
RELVEL	GAI	D/DT2			1		
D/DT3	INT	D/DT2			0	1	
DISC1	INT	PULSE	DISC2		0	1×10^{7}	-4.8361×10^{6}
DISC2	INT	DISC1	DISC2		0	1	−659.7
DISC3	INT	PULSE	DISC4		0	1×10^{7}	-4.7769×10^{5}
DISC4	INT	DISC3	DISC4		0	1	−138.2

Block	Type	Input1	Input2	Input3	Par1	Par2	Par3
LAG	INT	PARALLEL			0	503	
LPF	INF	POSTGAIN			0	1	5×10^{-6}
LSELF	INF	CLASSG			0	0.148	5.11×10^{-4}
RADSPEED	INT	LPF			0	1	
XA	INT	RADSPEED			0	1	
VCC-1	LIM	KMOTOR			-12	12	1
VCC-2	LIM	KMOTOR			-12	12	1
MAXX	MAX	$+1$	$|TRKCNT|$		0		
FULL	MUL	IN-OUT	FULLPWR				
MLEAD	MUL	LEAD	SIGN				
NORMAL	MUL	IN-OUT	NORMPWR				
OMEGAT	MUL	2π	FREQ	TIME			
NOISE	NOI				-0.10	0.10	1
LEAD	PDC	RE			0	1×10^{-3}	0.1010
APP	REL	APPROACH	RPLO	RPHI			
APPROACH	REL	RELVEL	0	$+1$			
CLASSG	REL	Σ	VCC-1	VCC-2			
DAC	REL	APPROACH	NORMAL	FULL			
DIRSIGN	REL	DIGVEL	$+1$	-1			
HIGHERBW	REL	Σ	GAINADJ	EXTRAK			
INOUT	REL	IN-OUT	TLLO	TLHI			
IN-OUT	REL	OPTICS	-1	$+1$			
LOOPSWCH	REL	RCO	DAC	HIGHERBW			
PULSE	REL	TIMER	SHOCK	0			
RP	REL	RE	RPLO	RPHI			
RP-DIG	REL	RE	0	$+1$			
SIGN	REL	Σ	$+1$	-1			
TL	REL	Σ	TLHI	TLLO			
TL-DIG	REL	Σ	$+1$	0			
ECCENTR	SIN	OMEGAT			1	0	1
RE	SIN	OPTICS			2π	0	1
Σ	SIN	OPTICS			2π	$-\frac{\pi}{2}$	1
DIGVEL	SPL	SAMPLE	RELVEL		-1		
EXTEND	SPL	SDA	RE		1×10^{-6}		
LAGHOLD	SPL	$-\Sigma$	LAG		1×10^{-6}		
CAPTURE	SUB	$|TRKCNT|$	3				
D/DT1	SUB	$|OPTICS|$	D/DT3				
IMPULSE	SUB	XOR	DXOR				
LAGSUM	SUM	LAG	LAGHOLD	PARALLEL	0	1	1
MOTOR	SUB	LOOPSWCH	LSELF				
OPTICS	SUB	XP	XA				

Block	Type	Input1	Input2	Input3	Par1	Par2	Par3
PARALLEL	SUM	MLEAD	RE-X		1×10^{-2}	1	
RESONATE	SUM	DISC2	DISC4		1	0	
RE-X	SUM	RE	EXTEND		-1	2	
SDA	SUM	$|TRKCNT|$	$+1$		-1	1	
TIMER	SUB	TIME	REFTIME				
XP	SUM	RESONATE	ECCENTR	NOISE	1	0	0
DXOR	TDE	XOR			0	1×10^{-6}	5×10^{-7}
PRE-TRIG	TDE	TIME			0	5×10^{-4}	5×10^{-6}

Appendix C

PSI simulation of the radial-motor

In the simulation of the *CDM3* radial motor and power-stage, the following circuit is assumed —
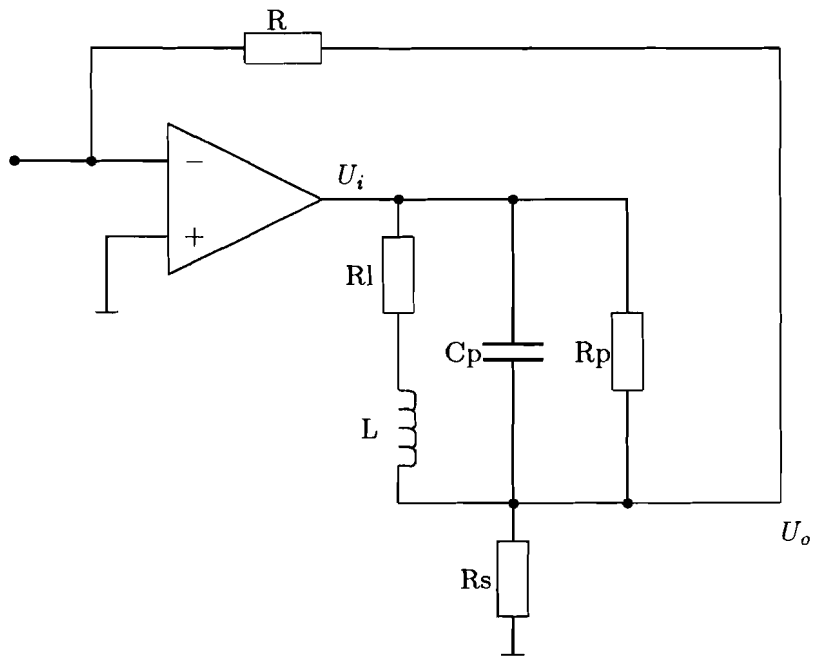
The six passive components indicated are:

R_l The series resistance of the coil
L The inductance of the coil
C_p The parallel capacitor used for damping
R_p The total parallel resistance $R_{damp} \| R_{loss}$
R_s The current-sensing resistor
R The opamp feedback resistor

The following mathematical relationships are easily determined

$$\frac{U_o}{U_i} = \frac{R_s}{R_s + \frac{1}{\frac{1}{R_p} + sC_p + \frac{1}{sL + R_l}}}$$

$$= \frac{R_s}{R_s + \frac{sL + R_l}{1 + (sL + R_l)(\frac{1}{R_p} + sC_p)}}$$

$$= \frac{R_s + R_s(\frac{1}{R_p} + sC_p)(sL + R_l)}{(sL + R_l) + R_s + R_s(\frac{1}{R_p} + sC_p)(sL + R_l)}$$

$$= \frac{R_s + R_s(\frac{1}{R_p} sL + \frac{1}{R_p} R_l + s^2 C_p L + sC_p R_l)}{sL + R_l + R_s + R_s(\frac{1}{R_p} sL + \frac{1}{R_p} R_l + s^2 C_p L + sC_p R_l)}$$

$$= \frac{s^2 [R_s C_p L] + s [R_s \frac{1}{R_p} L + R_s C_p R_l] + [R_s + R_s \frac{1}{R_p} R_l]}{s^2 [R_s C_p L] + s [R_s \frac{1}{R_p} L + R_s C_p R_l + L] + [2R_s + R_s \frac{1}{R_p} R_l + R_l]}$$

This has the general form

$$\frac{U_o}{U_i} = \frac{as^2 + bs + c}{as^2 + ds + e}$$

Rewriting as a difference-equation

$$\Rightarrow \quad U_i [as^2 + bs + c] = U_o [as^2 + ds + e]$$

$$\Rightarrow \quad U_i [a + \frac{b}{s} + \frac{c}{s^2}] = U_o [a + \frac{d}{s} + \frac{e}{s^2}]$$

$$\Rightarrow \quad U_o a = U_i [a + \frac{b}{s} + \frac{c}{s^2}] - U_o [\frac{d}{s} + \frac{e}{s^2}]$$

$$= U_i a + \frac{1}{s} \left[U_i b + U_i \frac{c}{s} - U_o \left(d + \frac{e}{s} \right) \right]$$

$$= U_i a + \frac{1}{s} \left[\frac{1}{s} \left(U_i c - U_o e \right) + \left(U_i b - U_o d \right) \right]$$

$$\Rightarrow \quad U_o = U_i + \frac{1}{a} \frac{1}{s} \left[\frac{1}{s} \left(U_i c - U_o e \right) + \left(U_i b - U_o d \right) \right]$$

It is now possible to draw a block diagram based on the above difference equation, as indicated in figure C.1.
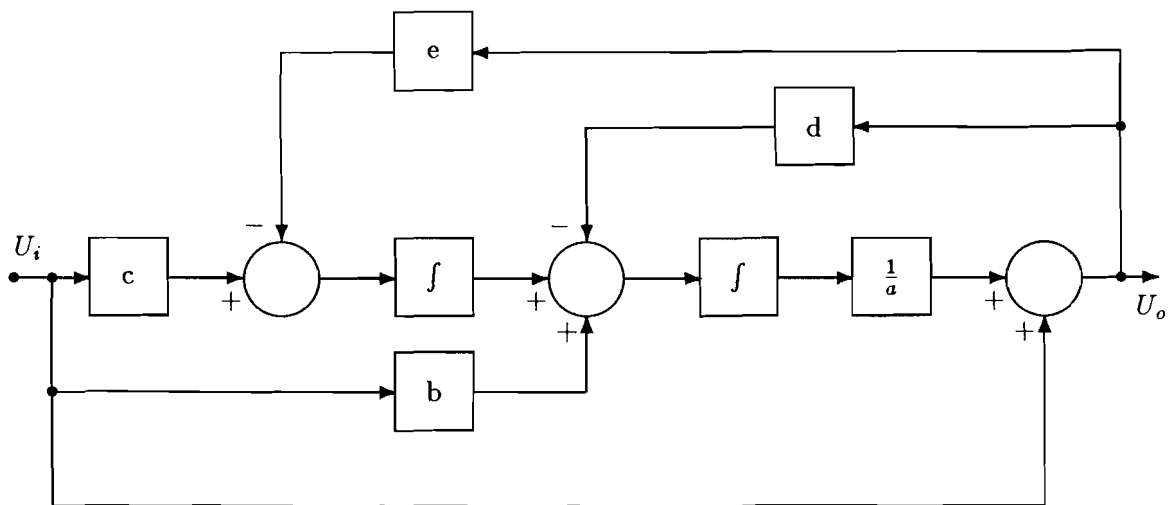
Figure C.1: *Block diagram form of radial motor difference-equation*

The gain factors a,b,c,d,e,f indicated in the figure are given by the following equations —

$$a = R_s C_p R_l$$

$$b = R_s \left(\frac{L}{R_p} + C_p R_l \right)$$

$$c = R_s \left(1 + \frac{R_l}{R_p} \right)$$

$$d = L + R_s \left(\frac{L}{R_p} + C_p R_l \right)$$

$$e = R_s \left(2 + \frac{R_l}{R_p} \right) + R_l$$

Including the current sensing and feedback, the limiting provided by the V_{cc} and V_{ss} rails of the opamp, and the mechanical $1/s^2$ due to the mass of the arm, the entire model becomes as indicated in figure C.2.
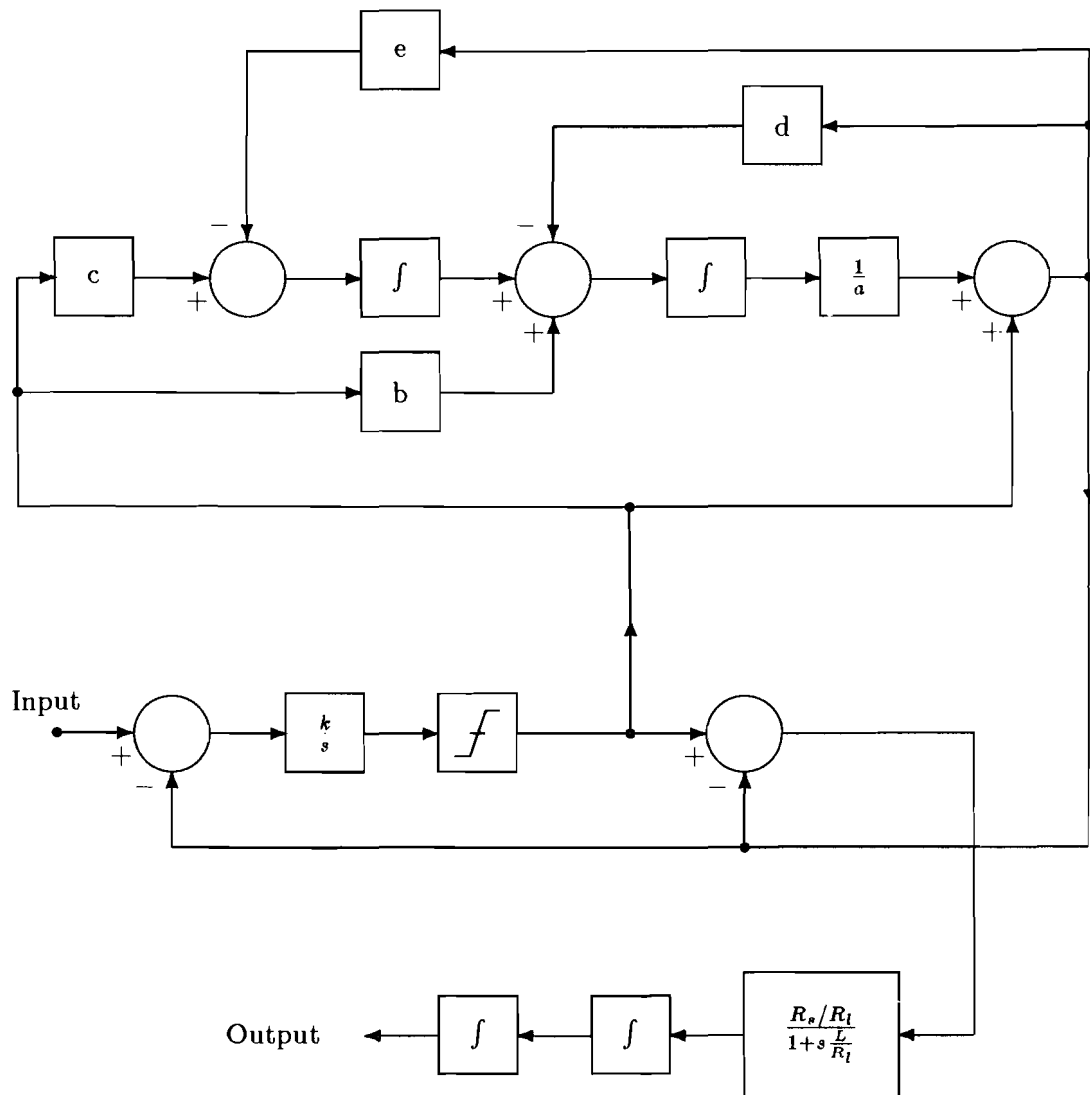
Figure C.2: *Block diagram showing the entire current-control model*

113